*Physics – Uspekhi* **60** (4) 345 – 384 (2017) 

*REVIEWS OF TOPICAL PROBLEMS* PACS numbers: **32.50.+d**, 32.80.Qk, 42.50.Nn, **42.55.–f**

# Superradiance: the principles of generation and implementation in lasers*

Vl V Kocharovsky, V V Zheleznyakov, E R Kocharovskaya, V V Kocharovsky

DOI: https://doi.org/10.3367/UFNe.2017.03.038098

## Contents



**Abstract. The electrodynamics of active continuous media is applied to theoretically examine collective spontaneous emission regimes of dipole oscillator ensembles. Recent experiments in which the superfluorescence phenomenon has been observed are reviewed. The focus is on propagation and interaction effects experienced by the inhomogeneous waves of active center polarization and electromagnetic fields. The superradiant laser dynamics is examined and prospects for the realization of superradiant lasers using low-$Q$ cavities are discussed.**

**Keywords:** collective spontaneous emission, Dicke superradiance, coherent processes, mode selection, multimode lasers

**Vl V Kocharovsky, V V Zheleznyakov, E R Kocharovskaya**
Institute of Applied Physics, Russian Academy of Sciences,
ul. Ul'yanova 46, 603950 Nizhny Novgorod, Russian Federation
E-mail: kochar@appl.sci-nnov.ru, zhelez@appl.sci-nnov.ru, katya@appl.sci-nnov.ru
**V V Kocharovsky** Institute of Applied Physics,
Russian Academy of Sciences,
ul. Ul'yanova 46, 603950 Nizhny Novgorod, Russian Federation;
Department of Physics and Astronomy, Texas A&M University,
College Station, Texas 77843, USA
E-mail: vkochar@physics.tamu.edu

Received 3 March 2017
*Uspekhi Fizicheskikh Nauk* **187** (4) 367 – 410 (2017)
DOI: https://doi.org/10.3367/UFNr.2017.03.038098
Translated by M Sapozhnikov; edited by A Radzig

## 1. Introduction. From the quantum Dicke superradiance problem to the classical dissipative instability problem

### 1.1 Various aspects of the superradiance concept

Quite a spectacular term 'superradiance', initially proposed by Dicke [1] to describe a well-manifested phenomenon of collective spontaneous emission of a lumped ensemble of dipole oscillators, is applied in many contemporary studies for a considerably more diverse class of problems, has a

* The review presents in the extended form the report by the authors at the scientific session of the Physical Sciences Division, Russian Academy of Sciences, dedicated to the centenary of Vitaly Lazarevich Ginzburg's birth, which was held on 5 October 2016 (see *Usp. Fiz. Nauk* **187** 443 (2017) [*Phys. Usp.* **60** 412 (2017)]). (*Editor's note.*)

variety of shades, and as a whole carries a broader and, hence, a less specific implication. The only thing that remains invariable in different contexts is its meaning characterizing the phasing of emission from elements of some systems: nuclear spins or atoms, simple or organic molecules, impurity centers in glasses or quantum dots in semiconductor crystals, Josephson junctions or microlaser chips, nano- or macroelements of aerial arrays, etc.

The coherent emission mechanism based on the phasing of elements of different microwave arrays or generators was extensively used and studied in the middle of the 20th century even before the appearance of Dicke's paper. A well-known example is radar, where the directivity diagram of a phased array is controlled by changing the amplitude–phase distribution of excitation currents in emitting elements.

In this review, we will use both the broad and the specialized meaning of the term 'superradiance', separating problems in which the coherent dynamics of dipole oscillators interacting via their own radiation field is fundamentally important (various aspects of terminology are discussed in Refs [2–5]). Moreover, we will assume that the radiative interaction dominates in transitions of separate active centers between energy levels and, in particular, determines the spontaneous transition time both for an isolated excited center($T_1$) and for an ensemble of excited centers as a whole ($T_{1c} < T_1$). In the case of spontaneous emission, the superradiant behavior appears in a quite dense ensemble of excited active centers with close or equal transition frequencies under conditions when quantum oscillations of emitting dipole moments of active centers acquire a cooperative nature also affecting quantum oscillations of the total electromagnetic field (see Section 2).

Under these conditions, it is impossible to calculate the spontaneous transition time based on Fermi's golden rule and to interpret spontaneous transitions in active centers from high-energy levels to lower levels by the action of some combination of independent vacuum (quantum) fluctuations of their dipole moments and the surrounding electromagnetic field. Notice, however, that, as in the case of spontaneous emission of an isolated dipole oscillator (cf., for example, Refs [6–9]), such an interpretation is unnecessary, because the nature of spontaneous emission, including collective emission, can be readily explained classically [3, 10–15]. As was done 30 years ago [16], we will use below namely this circumstance, which was often emphasized in our conversations with V L Ginzburg, to whom this review is devoted on the 100th anniversary of his birth.

### 1.2 Method of the electrodynamics of continuous media

The nature of any, in particular, spontaneous emission of an individual active center in a dense ensemble significantly differs from that in a vacuum, i.e. in the limit of a strongly rarefied ensemble when active centers are in fact isolated. It happens so because the structure, dispersion, and decay or growth rate (decrement or increment) of self-consistent natural oscillations or waves of dipole oscillations and the electromagnetic field in dense ensembles considerably differ from those in rarefied ensembles. Such a significant change in natural electromagnetic excitations appears, of course, not only when a dense ensemble is placed in a vacuum but also when it is placed into a medium or an electrodynamic system (waveguide, cavity) where waves and oscillations are also modified by the self-consistent oscillations of active-center dipoles. Such an 'outside medium' in superradiance problems can usually be considered passive (like a vacuum) and characterized by the positive permittivity $\varepsilon_0$ and the nonnegative ohmic conductivity $\sigma_0$.[1] It is assumed in this case that external electromagnetic waves are absent, i.e., the emission field is spontaneously produced by active centers excited at the initial instant and (or) upon continuous incoherent (nonresonant) pumping.

Under these conditions, collective spontaneous emission with the characteristic lifetime $T_{1c}$ considerably shorter than $T_1$ takes place when the self-consistent oscillations and waves mentioned above have growth rates ($\sim T_{1c}^{-1}$) considerably exceeding the incoherent relaxation rate $T_2^{-1}$ of free (partial) oscillations of the dipole moment of an individual active center determined by the phase decay time of these oscillations, $T_2 \lesssim T_1$. It is critical that collective spontaneous emission can originate from the quantum or thermal noise level, and then in the absence of continuous (CW) pumping it is called *superfluorescence*. In general, when there exist initial, even small, phased oscillations of dipole moments of active centers produced, for example, by a trigger pulse from an external resonance electromagnetic field, such a process is called *superradiance*. Finally, in the case of continuous pumping, *superradiant lasing* takes place. It is important that in all these situations the nature of the process is the same and can be related from the quantum point of view to the induced emission of quanta of self-consistent oscillations or waves by active centers. From the classical point of view, the process is reduced to a well-known multifaceted problem of either *active quasistatic systems* (lumped generators) in the case of a localized cluster or a small number of active centers occupying a region smaller in size than the emission wavelength $\lambda_0$ or the *electrodynamics of continuous active media* (distributed amplifiers and generators) in the case of many active centers occupying an extended region of size $B \gtrsim \lambda_0$ [3, 7, 18–20].

The classical approach based on the electrodynamics of continuous active media applied to the superradiance phenomenon was developed in the 1980s. It was first presented in review [3], although its efficacy could hardly be doubted even in the 1970s after the quantum analysis of both single-pulse superfluorescence in a lumped model and oscillating superfluorescence in a distributed sample performed in these years (see, for example, papers [10, 11, 21]). In the 1950s–1960s, the possibility of spontaneous phasing of dipole oscillators in a dense ensemble did not receive proper attention, and the theoretical analysis of superradiant processes, following Dicke's work [1], predominantly concerned the features of collective spontaneous emission of one or another system of two-level active centers prepared in phased states by a pulse from an external electromagnetic field. Notice that this situation, applied to collective spontaneous radio emission of a lumped spin ensemble, first of all nuclear spins, was well known for a long time and was qualitatively discussed even before Dicke's work (see Refs [22–26], although the first distinct experiments [27–34] in this field were performed after the first reliable optical experiments on superfluorescence of atoms and molecules [35–42]).

[1] If an active 'outside medium' amplifying the electromagnetic field at oscillator frequencies is located at the sites or near dipole oscillators (so that $\sigma_0 < 0$), near-field effects can cause the instability of the ground state of active centers even in the absence of amplifiable electromagnetic waves, thereby making impossible the standard formulation of the spontaneous emission problem [17].

Most of these experiments, like Dicke's initial problem, concerned ensembles with weakly inhomogeneously broadened transition frequencies of active centers and were described in the mean-field model or unidirectional superradiance model (see, for example, reviews and books [12, 14, 43–47] and also Sections 2 and 3). In all such cases, as shown in Refs [3, 16, 48], collective spontaneous emission is based on the dissipative (radiative) instability of self-consistent polarization oscillations or polarization waves having negative energy and inducing the accelerated synchronous emission of the internal energy of dipole oscillators. We will demonstrate in Section 2 that this approach allows us not only to study the semiclassical dynamics of collective spontaneous emission but also to construct the efficient quantum description of many classically formulated problems on superradiance, initiated by Dicke's quantum calculations in 1954 and by the work of his followers in the 1960s–1970s [21, 49–55].

The developed approach provides a qualitative interpretation of recent experimental studies of collective spontaneous emission in various ensembles of dipole oscillators (see, for example, Refs [56–68, 315*]. Some of these experiments will be considered in Section 4. Of special interest are experimental studies of phase transitions in systems of radiatively interacting dipoles, including nonequilibrium dipoles, but not necessarily possessing an inverse population of energy levels [69–73].

The example of an open system demonstrating the nonequilibrium phase transition is presented in Ref. [74]. The system is composed by an ensemble of multilevel atoms placed into an optical cavity and involved in Raman transitions in the presence of an external controling laser field. The presence of the latter is crucial for the existence of the Dicke phase transition to a state with a nonzero intensity of the optical emission of atoms.[2] Recently, various analogs of this open system allowing phase transitions were also studied, and the first experimental proof of their existence is presented in Refs [70, 71]. Such phase transitions, including the hypothetical Dicke quantum phase transition [15, 83–86], are not related to the collective generation of radiation pulses discussed in our review, and therefore relevant recent investigations will only be mentioned in the conclusions.

### 1.3 Some challenging problems

In this review, we will consider experimental attempts to obtain superradiance (or superfluorescence) in dipole ensembles with strongly inhomogeneously broadened spectral lines and theoretical concepts about the conditions required for obtaining superradiance, when collective spontaneous emission is impossible without the selection of emitted electromagnetic modes or modification of the energy eigenstates of dipoles and their distribution over these states. These attempts are related to promising applications and the expected rich generation dynamics of various superradiant modes, both in the initial formulation of the problem about the emission of preliminarily excited dipoles and in the presence of continuous pumping. In the latter case, we are dealing with superradiant lasers which can be created based on recently developed active media and can open new prospects not only for spectacular fundamental experiments on the border of quantum and classical physics of many-particle systems but also for the development of important applications, for example, in information technologies and spectroscopy.

It should be noted that various manifestations of collective spontaneous emission for ensembles of dipole oscillators with inhomogeneously broadened spectral lines may not be confined to the generation of polarization waves or polariton modes with negative energy, or may not include them at all. They can be described by the excitation and nonlinear interaction of a broader set of electromagnetic modes or waves related to oscillations of dipole oscillators in some parts of a spectral line and having positive energy. Nevertheless, superradiance is always characterized by the presence of rather fast transient or correlation effects to which a spectral band corresponds. This band covers the natural frequencies of dipole oscillators forming the corresponding electromagnetic waves or modes, which predetermines the radiation-induced self-phasing of dipole oscillations and therefore the collective effects of their behavior.

The review outline is as follows. Section 2 is devoted to the description of collective spontaneous emission in the simplest mean field models. In Section 3, we consider the more advanced models of distributed systems with homogeneously broadened spectral lines for simplicity. In Section 4, we discuss observations of the superfluorescence of waves in a continuous spectrum in various nonequilibrium media, the main attention being paid to collective electron–hole recombination in semiconductors. Section 5 considers the dynamics of discrete modes and describes the expected superfluorescence regimes upon pulsed pumping and superradiant lasing upon continuous (CW) pumping of active media in combined low-$Q$ cavities. Final Section 6 contains general conclusions and concerns problems of superradiant lasers and collective states in many-particle systems with radiative and nonradiative interactions.

## 2. Mean field model, quantum fluctuations, and classical analogs of superfluorescence

### 2.1 Semiclassical two-level model equations

For definiteness, we will use, unless otherwise stated, the efficient two-level approximation of point active centers in the form of dipole oscillators at frequency $\omega_{21}$ with the dipole transition moment $\mathbf{d}$ (possible level degeneracy is ignored for simplicity). Then, in our approach based on the electrodynamics of continuous active media [3, 20, 53, 87–89], the main properties of collective quantum-electrodynamic phenomena, including Dicke superradiance, are described by Maxwell's equations for electric and magnetic fields $\boldsymbol{\mathcal{E}}$ and $\boldsymbol{\mathcal{B}}$ and semiclassical equations for polarization $\boldsymbol{\mathcal{P}}$ (the dipole moment of a unit volume), and the population difference $N = N_2 - N_1$ of the upper and lower energy levels of active centers in a unit volume:

$$\operatorname{rot}\boldsymbol{\mathcal{E}} = -\frac{1}{c}\frac{\partial\boldsymbol{\mathcal{B}}}{\partial t}\,, \quad \operatorname{rot}\boldsymbol{\mathcal{B}} = -\frac{1}{c}\frac{\partial(\varepsilon_0\boldsymbol{\mathcal{E}} + 4\pi\boldsymbol{\mathcal{P}})}{\partial t} + \frac{4\pi\sigma_0}{c}\boldsymbol{\mathcal{E}}\,, \quad (1)$$

$$\frac{\partial^2\boldsymbol{\mathcal{P}}}{\partial t^2} + \frac{2}{T_2}\frac{\partial\boldsymbol{\mathcal{P}}}{\partial t} + (\omega_{21}^2 + T_2^{-2})\boldsymbol{\mathcal{P}} = -\frac{\omega_c^2}{\pi}\boldsymbol{\mathcal{E}}\,, \quad (2)$$

$$\frac{\partial N}{\partial t} + \frac{N - N_p}{T_1} = \frac{2}{\hbar\omega_{21}}\boldsymbol{\mathcal{E}}\frac{\partial\boldsymbol{\mathcal{P}}}{\partial t}\,, \quad (3)$$

* Paper [315] is added in proof reading. (*Editor's note*.)

[2] Note that such a Dicke phase transition in a closed atomic system predicted in Refs [75–77] is impossible because the Hamiltonian contains a term proportional to the vector field potential squared (see Refs [78–82]).

where $c$ is the speed of light in a vacuum. In general, it is assumed that active centers are located with density $N_0(\mathbf{r})$ in an isotropic matrix with the real permittivity $\varepsilon_0(\mathbf{r})$ and ohmic conductivity $\sigma_0(\mathbf{r})$ and are nonresonantly pumped. The pumping produces the population inversion $D_\mathrm{p} = N_\mathrm{p}(\mathbf{r}, t)/N_0(\mathbf{r})$ in each active center with the rate $T_1^{-1}$ also taking into account the contribution of its individual spontaneous relaxation (both nonradiative and radiative with the rate $T_{01}^{-1} = 4d^2\omega_{21}^3\sqrt{\varepsilon_0}/(3\hbar c^3)$ for an isolated center).

Equations (1)–(3) should be supplemented with initial conditions and boundary conditions at the boundaries of the active medium, the matrix, and additional electrodynamic constructions, for example, the waveguide and cavity walls. Formally, the inhomogeneous distribution $N_0(\mathbf{r})$ of active centers is taken into account by the coefficient of the electric field in Eqn (2) — the square of the 'cooperative frequency' depending on the population inversion:

$$\omega_\mathrm{c}^2 = \frac{2\pi d^2 \omega_{21} N_0 D}{\hbar}\,, \tag{4}$$

which is positive for the positive inversion $D = N(\mathbf{r}, t)/N_0(\mathbf{r})$ ($|D| \leqslant 1$). For simplicity, here and in many cases below we ignore possible differences between frequencies of active centers, i.e., the inhomogeneous broadening of their spectral line, and omit in the cooperative frequency the factor $\sim 1/3$ related to averaging over the orientation of active dipoles, thus assuming that $\mathbf{d} \parallel \boldsymbol{\mathcal{E}}$ for all them. Thus, Eqns (2) and (3) are in fact written for quantum-mechanical averages of the dipole moment and the inversion of one immobile active center $\langle \mathbf{d} \rangle = \boldsymbol{\mathcal{P}}/N_0$ and $\langle D \rangle$, respectively (here, angle brackets denote quantum-mechanical averaging rather than spatial averaging, as everywhere below). Of course, Eqns (1)–(3) do not carry information on quantum self- or cross-correlations in the behavior of individual active centers or on nonclassical quantum properties of the electromagnetic field, which are also of interest and have recently been studied in Refs [15, 90–96].

If the characteristic size $B$ of a total system is small compared to the so-called cooperative length $c/\omega_\mathrm{c}$ (usually determined for $D = 1$ and independent of $\varepsilon_0$), the delay effects for collective spontaneous emission and the distribution inhomogeneity of active centers can usually be disregarded and the mean field model can be applied. This model is equivalent in many respects to the Dicke grain model[3] [47, 106–110].

[3] It is well known [3, 89, 97] that the random motion of atoms (molecules) in a gas inevitably interacting with each other as two dipoles (in Weisskopf collisions) leads to a strong relaxation of polarization. Thus, the dipole moment of a unit volume in the medium relaxes with the rate $T_2^{-1} \simeq N_0 d^2/\hbar$, making impossible superradiance in grains (samples with volume $V < \lambda_0^3$) predicted by Dicke, where $\lambda_0 = 2\pi c_0/\omega_{21}$ is the emission wavelength and $c_0 = c/\sqrt{\varepsilon_0}$ is the speed of light in the matrix. According to experimental facts and theoretical considerations [20, 98–104], the superradiance of an ensemble of active centers in such a grain is possible only in the case of their certain spatial and orientational ordering, which weakens the incoherent polarization relaxation caused by the interaction of dipoles and makes accounting for differences between the acting and mean fields important, which we ignore here for simplicity. The important role of these differences is illustrated by the model of the antiferroelectric Dicke phase transition predicting the possibility of spontaneous formation of a quasistatic polarization structure in the thermodynamically equilibrium gas of interacting two-level dipole molecules [105].

### 2.2 Spatial averaging of fields

There are two main variants of moving to the mean field model. The first one is the averaging of the field amplitudes in Eqns (1)–(3) over the volume $V$ occupied by the ensemble and the exclusion of spatial derivatives from Eqn (1) taking into account radiative losses, i.e., by replacing ohmic losses $\sigma_0$ by the effective quantity $\sigma = \sigma_0 + \sigma_\mathrm{rad}$, including radiative losses $\sigma_\mathrm{rad}$ through all facets of the sample. The second variant considers only one certain spatial mode of the electrodynamic system under study with frequency $\tilde{\omega}$ close to $\omega_{21}$, and the finite photon lifetime $T_\mathrm{E} = (2\pi\sigma)^{-1}$ in the mode. This also allows us to ignore spatial derivatives and restrict ourselves to the analysis of only the time dynamics of the field amplitudes of the chosen mode with the field-matched polarization and inversion. In the latter case, to take into account only partial possible occupation of the mode volume by the active medium and the difference between its profile and the density profile $N_0(\mathbf{r})$ of active centers, the averaged occupation factor $\tilde{\Gamma} \leqslant 1$ is usually introduced [5, 111, 112]. Along with the homogeneous permittivity $\varepsilon_0$ of the matrix, this factor can be readily excluded from the initial system of Eqns (1)–(4) by making the substitution

$$\begin{gathered}\tilde{\boldsymbol{\mathcal{B}}} = \frac{\boldsymbol{\mathcal{B}}}{\sqrt{\tilde{\Gamma}}}\,, \quad \tilde{\boldsymbol{\mathcal{E}}} = \boldsymbol{\mathcal{E}}\sqrt{\frac{\varepsilon_0}{\tilde{\Gamma}}}\,, \quad \tilde{\boldsymbol{\mathcal{P}}} = \boldsymbol{\mathcal{P}}\sqrt{\frac{\tilde{\Gamma}}{\varepsilon_0}}\,, \\ c_0 = \frac{c}{\sqrt{\varepsilon_0}}\,, \quad \tilde{\sigma}_0 = \frac{\sigma_0\tilde{\Gamma}}{\varepsilon_0}\,, \quad \tilde{\omega}_\mathrm{c}^2 = \frac{\omega_\mathrm{c}^2\tilde{\Gamma}}{\varepsilon_0}\,,\end{gathered} \tag{5}$$

which leads to Eqns (1)–(3) for the mode with the chosen profile with $\varepsilon_0 = 1, \tilde{\Gamma} = 1$ and the renormalized speed of light, ohmic losses, and cooperative frequency.

The mean field model qualitatively correctly describes many properties of collective spontaneous emission and their physical meaning for most of the experiments and theoretical problems considered (see, for example, Refs [4, 5, 14, 47, 113, 114]). (The mean field model also explains many features of the superradiant dynamics of ensembles of other dipole oscillators, for example, three-level or quasiclassical oscillators [58, 60, 110, 115–125, 315] for which cascade superfluorescence involving two or more transitions between active-center levels is possible.) We will not repeat here the known particular conclusions, especially since we return to some of them in Sections 3–5. The general conclusion mentioned in the Introduction is that collective spontaneous emission (both superfluorescence and initiated superradiance) having a classical nature, in the case of negligible inhomogeneous broadening of spectral lines, is caused by the instability of the so-called hot polariton modes (or polarization waves) possessing negative energy and growing due to superradiant emission with the growth rate exceeding the relaxation rate of dipole oscillations of an individual active center: $\mathrm{Im}\,\omega > T_2^{-1}$ [3, 48]. This inequality serves as a criterion for collective spontaneous emission and can be fulfilled for a quite high cooperative frequency (4): $\omega_\mathrm{c}(\tilde{\Gamma}/\varepsilon_0)^{1/2} > T_2^{-1}$. The additional condition is that the photon lifetime for corresponding so-called cold modes (or electromagnetic waves) for the zero inversion $N = 0$ must not greatly exceed the time of dipole oscillations of individual active centers, $T_\mathrm{E} \lesssim T_2$, to avoid the transformation of superfluorescence or superradiance to the quasiperiodic energy exchange between active centers and field modes, i.e., optical nutation of each active center under the action of the field of other active centers.

It should be noted that in a sample with well-reflecting faces or in a closed circular optical fiber, where the spatial mode structure is uniform enough and radiation escape is strongly hindered, the fast collective relaxation of inverted active centers caused by dissipative instability is possible in the presence of ohmic or diffraction losses of the field. Its oscillogram, as in the case of superfluorescence, demonstrates either a single-pulse process of superabsorption with a duration of $\sim \pi\sigma/\omega_c^2(t=0)$ (for $\pi\sigma \gtrsim \omega_c(t=0) \gg T_2^{-1}$) or a slowly relaxing oscillatory process of optical nutation of the Bloch vector in a self-consistent field with period $\omega_c^{-1}(t=0)$ (for $\omega_c(t=0) \gg \pi\sigma, T_2^{-1}$) [126]. The oscillatory type of this process, as with collective spontaneous emission in the mean field model [4, 14, 112, 114, 127–129], is caused by the nonadiabatic interaction of polariton and electromagnetic modes in a sample with the rapidly changing inversion $N(t)$. If active centers are located in a plasma (for example, atoms in a partially ionized gas or impurity centers in a semiconductor) and a plasma-dipole resonance takes place, $\omega_{21} \simeq 4\pi e^2 N_e/(m_e\sqrt{\varepsilon_0})$, where $e$, $m_e$, and $N_e$ are the electron charge, mass, and density, respectively, then, along with the ohmic *superabsorption* of the stored inversion energy, the collective spontaneous transfer of this energy to long-wavelength quasihomogeneous electron oscillations is possible due to the absolute dissipative instability of polarization waves with negative energy and their connection with plasma waves carrying positive energy. The maximum growth rate of this instability has the form [4]

$$\max \operatorname{Im}\omega = \left[\frac{\omega_c^2}{\varepsilon_0} + \left(\frac{\pi\sigma_0}{\varepsilon_0} - \frac{1}{2T_2}\right)^2\right]^{1/2} - \frac{\pi\sigma_0}{\varepsilon_0} - \frac{1}{2T_2}\,.$$

A similar nonlinear process, both single-pulse and oscillatory, is considered in work [131], where the possibility of its realization in partially ionized gases and semiconductors is discussed in the mean field model, which is natural in this case. Such problems dealing with the superradiance of plasmons, which are excited, for example, in a metal nanoparticle under the action of inverted active centers (organic molecules or quantum dots), by phasing their dipole oscillations and rapidly transferring the inversion energy stored in them to heat and partially to electromagnetic radiation, were considered in papers [64, 132–137]. In addition, the authors of these papers also considered the superradiance of two-dimensional gratings of such nanoparticles with active centers (so-called spasers from the first letters of words surface plasmon amplification by stimulated emission of radiation). Such questions have recently come to the fore in connection with rapid progress in nanoplasmonics.

In this case, several polariton modes (or polarization wave packets) can be self-excited during the same process and all of them will be 'hot', i.e., different from cold modes (or electromagnetic wave packets) due to inclusion of the nonzero inversion, $N \neq 0$, and the dispersion of the active medium of dipole oscillators according to Eqns (1)–(3). The linear stage of the development of all such hot polariton modes having different frequencies, growth rates, profiles, and occupation factors can be adequately described in the mean field model. However, a description of the nonlinear stage of the process and the interaction between these modes often requires going beyond the framework of this model, because the structure of hot modes depends on the spatial distribution of the active center inversion. The inversion rapidly changes at the nonlinear stage and, as a rule, does not allow the application of the adiabatic approximation of slowly varying noninteracting hot modes, which is implied in fact in the mean field model for each individual mode. In this respect, superfluorescence and superradiance differ qualitatively from the known superluminescence phenomenon which usually concerns the boundary stationary problem of amplification of intrinsic incoherent emission (luminescence) of noninteracting active centers in the medium formed by them. From the point of view of an individual isolated active center, superluminescence constitutes the quasistationary emission of a 'partial' photon induced by an incoherent wave field independently produced and amplified by other active centers in the absence of external radiation sources, exclusively due to vacuum fluctuations of the electromagnetic field and the dipole moment of an individual active center.

### 2.3 Quantization of modes with negative energy and superfluorescence fluctuations

The quantum properties of collective spontaneous emission, for example, the statistics of delay times of emitted pulses, their propagation directions, and electric field polarization in them, are in fact predetermined by quantum fluctuations of hot modes (or waves) at the linear stage of their growth. They begin to dominate at that time in quantum-correlation characteristics of particle states, whereas initial quantum correlations in a many-particle ensemble are 'forgotten', and effective 'quantum-mechanical' fluctuation forces in semiclassical equations prove to be insignificant [3, 13, 15, 16, 21, 53, 126, 138–140]. These properties can be elucidated with the help of the mean field model adapted to describe all $m = 1, \ldots, M$ of hot modes involved in the superradiance process and having growth rates $\operatorname{Im}\omega_m \equiv \omega_m''$ on the order of the maximum $T_{1c}^{-1}$. In the quantization of this model and more general equations like (1)–(3), the dissipative character of the instability governing superfluorescence as a result of interaction between quantum oscillators (modes or waves) with opposite energy signs is the most important. This feature in the dynamics of developing fluctuations of collective excitations from the micro- to macrolevel is expressed in the use of the Hermitian Hamiltonian operator $\hat{H}$ in the quantum theory, which is not positively defined (in the linear approximation). Such an approach allows us to take into account the frequency and spatial dispersions, nonlinearity and inhomogeneity, anisotropy, and sources in the active medium.

The simplest variant is illustrated by progressing the dynamic dissipative instability of two coherently interacting oscillators with different quantum energy signs — partial polarization oscillations of active centers ($\omega_1^{(0)} = \omega_{21}$), and the electromagnetic field in a vacuum ($\omega_2^{(0)} = ck$) in the single-mode superradiance model ignoring relaxation:

$$\hat{H} = -\hbar\omega_1^{(0)}\hat{a}_1^+\hat{a}_1 + \hbar\omega_2^{(0)}\hat{a}_2^+\hat{a}_2 + \frac{1}{2}\,\hbar\omega_c(\hat{a}_1\hat{a}_2 + \hat{a}_2^+\hat{a}_1^+)\,, \tag{6}$$

$$\frac{\mathrm{d}\hat{a}_j}{\mathrm{d}t} = -\mathrm{i}\hbar^{-1}[\hat{a}_j, \hat{H}]\,, \quad [\hat{a}_j, \hat{a}_{j'}^+] = \delta_{jj'}\,, \quad [\hat{a}_j^+, \hat{a}_{j'}^+] = [\hat{a}_j, \hat{a}_{j'}] = 0\,.$$

The Hamiltonian of interest providing the law of conservation $\mathrm{d}(\hat{n}_1 - \hat{n}_2)/\mathrm{d}t = 0$ for the difference in the numbers of quanta $\hat{n}_j = \hat{a}_j^+\hat{a}_j$ of partial oscillators is reduced to the

[4] Hereinafter, the dispersion of the permittivity $\varepsilon_0$ and conductivity $\sigma_0$ of the matrix itself containing active centers is disregarded, although it can be significant for a number of analogs of the Dicke superradiance (see, for example, Refs [3, 20, 130]).

diagonal form

$$\hat{H} = \hbar\omega_1 \hat{\tilde{a}}_2^+ \hat{\tilde{a}}_1^+ + \hbar\omega_2 \hat{\tilde{a}}_1 \hat{\tilde{a}}_2 + \hbar\omega_1^{(0)}\,,$$
$$\omega_{1,2} = \frac{1}{2}\left\{\omega_1^{(0)} + \omega_2^{(0)} \pm \mathrm{i}\left[|\omega_c|^2 - (\omega_1^{(0)} - \omega_2^{(0)})^2\right]^{1/2}\right\}, \tag{7}$$

by going from the indicated partial creation $\hat{a}_j^+$ and annihilation $\hat{a}_j$ operators ($j = 1, 2$) to the noncommuting normal operators

$$\hat{\tilde{a}}_1^+ = \hat{a}_1^+ - \hat{a}_2 \omega_c \left[2(\omega_1 - \omega_2^{(0)})\right]^{-1},$$
$$\hat{\tilde{a}}_2 = -\mathrm{i}\omega_c \left\{\hat{a}_1^+ \omega_c \left[2(\omega_1 - \omega_2^{(0)})\right]^{-1} - \hat{a}_2\right\} \times \left\{2\left[|\omega_c|^2 - (\omega_1^{(0)} - \omega_2^{(0)})^2\right]^{1/2}\right\}^{-1}. \tag{8}$$

These evolve independently of each other and satisfy cross commutative relations [141–143]

$$\frac{\mathrm{d}\hat{\tilde{a}}_j^+}{\mathrm{d}t} = -\mathrm{i}\omega_j \hat{\tilde{a}}_j^+\,, \quad \left[\hat{\tilde{a}}_1^+, \hat{\tilde{a}}_2^+\right] = 1\,, \quad \left[\hat{\tilde{a}}_j^+, \hat{\tilde{a}}_{j'}^+\right] = 0\,. \tag{9}$$

From this, we can readily obtain the main quantum effect of the oscillation excitation of even initially unexcited coupled oscillators, i.e., the spontaneous creation of quantum pairs from the vacuum state when the average number of quanta increases from the zero initial value: $\bar{n}(t) = |\omega_c/2\omega_1''|^2 \sinh^2(\omega_1'' t)$. Here, we assume for definiteness that $\omega_1'' \equiv \mathrm{Im}\,\omega_1 > 0$. In the $t \to \infty$ asymptotics, the statistical distribution of the number $n$ of quanta proves to be exponential, $\rho(n, t) = \bar{n}^{-1} \exp(-n/\bar{n})$, which corresponds to the Gaussian statistics of the field amplitude fluctuations. For a 'start' from thermal fluctuations with temperature $T$, the asymptotic form of $\rho(n, t)$ is the same, but with a greater mean number of quanta:

$$\bar{n}(t) = \left|\frac{\omega_c}{4\omega_1''}\right|^2 \left(\frac{1}{2}\coth\frac{\hbar\omega_1^{(0)}}{2k_B T} + \frac{1}{2}\coth\frac{\hbar\omega_2^{(0)}}{2k_B T}\right)\exp(2\omega_1'' t)\,, \tag{10}$$

where $k_B$ is the Boltzmann constant.

The inclusion of relaxation leads to a different variant of the dissipative instability realized in the interaction of a dynamic subsystem having negative energy (of the quantum oscillator $\hat{a}_1$) with a thermostat consisting of a continuum of uncoupled oscillators $\hat{b}_k$ with positive energy:

$$\hat{H} = -\hbar\omega_1^{(0)} \hat{a}_1^+ \hat{a}_1 + \sum_k \hbar\omega_k \hat{b}_k^+ \hat{b}_k + \frac{1}{2}\sum_k \hbar(\beta_k \hat{a}_1 \hat{b}_k + \beta_k^* \hat{b}_k^+ \hat{a}_1^+)\,. \tag{11}$$

The correctness of applying this model to quantization of the initial classical dynamic system [144] is justified by the independence of macroscopically observed results from the choice of microscopic parameters $\beta_k = \beta(\omega)$ and $g(\omega)$ within the continuous spectrum of frequencies $\omega_k$, when $\sum_k \ldots \simeq \int \mathrm{d}\omega\, g(\omega) \ldots$. In this limit, the Weisskopf–Wigner approximation allows us to find analytically the (observable) complex frequency $\omega_1 = \omega_1^{(0)} + \Delta\omega_1' + \mathrm{i}\omega_1''$ of a dynamic oscillator changed by the thermostat (see Ref. [3]) and to show that the dissipative instability has an irreversible character and spontaneously develops even from the unexcited vacuum state, giving an exponential law of increasing the average number of quanta: $\bar{n}(t) = \exp(2\omega_1'' t) - 1$ ($t \geqslant 0$). Generally, for a 'start' from spontaneous and/or thermal fluctuations, the asymptotic form like (10) is again valid:

$$\bar{n}_1(t) = \coth\frac{\hbar\omega_1^{(0)}}{2k_B T}\exp(2\omega_1'' t)\,, \quad t \to \infty\,. \tag{12}$$

The quantization variants presented above were generalized in Refs [3, 139] and combined into a closed scheme of the phenomenological quantum electrodynamics of active media (PQEDAM). This scheme includes both the coherent interaction of dynamic oscillators (modes or waves) with energies of different signs and the irreversible relaxation or incoherent excitation of these oscillators coupled with a thermostat consisting of a continuum of oscillators with energies of both signs. Such approach was used for the systematic analysis of macroscopic manifestations of quantum fluctuations in superradiance studied earlier experimentally [40, 52, 59, 62, 63, 100, 103, 145, 146] and theoretically [49, 50, 91, 113, 147, 148] for different concrete cases with the help of special particular methods.

As an example of such analysis, consider the statistics of the delay time $t_d$ of superradiance of discrete hot modes with growth rates $\omega''$ and numbers of quanta $n_m$ ($m = 1, \ldots, M$), which are independent random quantities with the same asymptotic probability distribution and the average $\bar{n}(t) = n_{\mathrm{eff}} \exp(2\omega'' t)$ like Eqns (10), (12). By writing the probability distributions of the total number of quanta, i.e.

$$n_\Sigma = \sum_{m=1}^{M} n_m\,, \quad \rho(n_\Sigma) = \left(\frac{n_\Sigma}{\bar{n}}\right)^{M-1}\left[(M-1)!\bar{n}\right]^{-1}\exp\left(-\frac{n_\Sigma}{\bar{n}}\right), \tag{13}$$

we will use the known criterion for finding the maximum of a superradiance pulse [12, 51, 149–152]. According to this critertion, the probability of emitting a superradiance pulse in the time interval $0 < t < t_d$ is equal to the probability that the total number of quanta by the time $t_d$ will exceed half the number $N_0 V/2$ of inverted active centers. By differentiating this condition with respect to $t_d$ and assuming $\omega'' \approx \max(\omega'') = T_{1c}^{-1}$, we obtain the required distribution of the normalized delay time [138]:

$$f\left(\frac{2t_d}{T_{1c}}\right) = \frac{u^M}{(M-1)!}\exp\left[-M^2\frac{2t_d}{T_{1c}} - u\exp\left(-\frac{2t_d}{T_{1c}}\right)\right], \quad u \equiv \frac{N_0 V}{2n_{\mathrm{eff}}} \gg 1\,. \tag{14}$$

Thus, the statistics of the superradiance delay time depend on the sample shape via the number of unstable polariton modes. Therefore, for a cylinder with the cross section $S$, length $B$, and Fresnel number $F = S/(\lambda_0 B)$, it follows according to estimates [12] that $M \sim (F^2 + 1 + 1/F)/3$, and for a sphere with radius $r_0 \gg \lambda_0$, the number of modes is $M \sim (2\pi r_0/\lambda_0)^2$. For an arbitrary three-dimensional sample with a large Fresnel number and not too strong reflections from the boundaries, superradiance is formed by statistically independent filaments (cf. the Van Cittert–Zernike theorem) and the number of 'diffraction' modes formed by them is $M \sim F^2$ (such modes are discussed in Refs [152–156]). The greater the number $M$ of modes, the smaller the mean delay time $\bar{t}_d = T_{1c}\ln\sqrt{u/M}$ and the

smaller its fluctuations:

$$\sigma^2(M) \equiv \frac{\overline{t_d^2} - (\bar{t}_d)^2}{(\bar{t}_d)^2} = \left(\frac{\pi^2}{6} - \sum_{m=1}^{M-1} \frac{1}{m^2}\right)\left(\ln \frac{u}{M}\right)^{-2} \approx M^{-1}\left(\ln \frac{u}{M}\right)^{-2}. \quad (15)$$

This result, consistent with the results of known experiments [157, 158], is applied to active samples both with partially reflecting boundaries ensuring the existence of discrete hot modes and in the absence of noticeable reflections when the unidirectional superradiance of the continuous-spectrum waves forming these 'diffraction modes' appears.

A similar quantum analysis based in fact on the linear stage of the superradiant instability of modes in a short enough active-medium sample with length $B \ll c/\omega_c$ allows determining the statistics of various parameters of collective spontaneous emission pulses, for example, the propagation directions or orientations of the polarization ellipse and the degree of radiation field ellipticity. However, for samples with lengths on the order of the cooperative length $c/\omega_c$ or more, when collective spontaneous emission is reabsorbed and the nonlinear interaction between spatially inhomogeneous modes makes them poorly defined and considerably affects the parameters of output pulses, the calculation and investigation of quantum-statistical properties of the generated field are fraught with difficulties. For such distributed samples, as we will show in Section 5, the use of modes with a fixed spatial structure of the field is severely restricted and the description of even semiclassical (nonquantum) dynamics of superradiant pulses proves to be far from trivial, often requiring intricate numerical simulations.

### 2.4 Classical analogs of collective spontaneous emission

The quantum analysis of the superradiance of modes discussed above also concerns ensembles of more complicated oscillators, in particular, quasiclassical ones, in which several (or many) energy levels are involved in the formation of collective spontaneous emission and nonlinearity differs from the saturating two-level nonlinearity. We have no way to discuss here such ensembles in detail and will only mention some of them discussed in the literature theoretically and/or studied experimentally.

The best known examples of weakly anharmonic oscillators with almost equidistant energy levels are highly excited oscillating molecules, Rydberg atoms, and cyclotron electron oscillators both in a vacuum (where the nonequidistance of Landau energy levels is caused by the velocity dependence of the relativistic mass) and in crystals (where the nonequidistance of energy levels is mainly caused by band nonparabolicity, i.e., the dependence of the quasiparticle mass on the wave vector of a state in the Brillouin zone). The simplest effect in a dense ensemble of such 'classical' oscillators coherently excited by a pulse of an external resonance field and oscillating in phase is the collective superradiant decay of their oscillations (see, for example, Refs [125, 159–161]), similar to the radiative decay of phased spins and the Dicke superradiance of synchronously oscillating two-level atoms mentioned in Section 1.2. However, of most interest is the possibility of superfluorescence or initiated superradiance (i.e., an exponential growth in the collective emission of an ensemble of such oscillators due to self-phasing under the action of their own field) beginning with quantum or thermal noise or a very weak (triggering) resonance signal, respectively. It is important that, due to the difference between the nonlinearity of weakly anharmonic oscillators and the saturation nonlinearity of two-level oscillators, the superradiance dynamics and the superfluorescence pulse shape in these two case are considerably different.

Such classical analogs of the Dicke superradiance have been theoretically studied for more than a quarter of a century [118, 119, 122, 125, 130, 162] (mainly qualitatively but also quantitatively in the mean field model). Experimental studies of the superradiance of highly excited oscillating molecules or Rydberg atoms still lie ahead (this is favored by large dipole moments of resonance transitions and the possibility of populating an individual high-energy level, as already demonstrated in experiments [38, 39, 163–168]). Successful experiments and detailed numerical calculations of different variants of collective spontaneous emission have been performed in vacuum electronics for bunches of weakly anharmonic electron oscillators, where, depending on the properties of the waveguides and the driving magnetic field used in experiments, superfluorescence is provided by the bremsstrahlung, Cherenkov, or cyclotron radiation mechanism [169–175]. The regime of amplified spontaneous emission in a free-electron laser with a considerable electron velocity dispersion, which is close to superradiance, was considered and compared with superfluorescence in Refs [19, 117, 120, 176–181].

The first proposed classical analog of Dicke superradiance was collective spontaneous emission in a 'superluminal' flow (bunch) of cyclotron electron oscillators moving along a magnetic-field vector in a decelerating electromagnetic system (waveguide) or a medium with $\varepsilon_0 > 1$ at a velocity exceeding $c_0 = c/\sqrt{\varepsilon_0}$ [130, 182, 183]. In this case, superfluorescence in an ensemble of initially nonrotating electrons originates due to the radiative (dissipative) instability of slow cyclotron waves (modes) possessing negative energy. The transverse velocity of the self-consistent (cyclotron) rotation of electrons appears and increases due to a decrease in their kinetic energy and the longitudinal (translational) velocity. Due to such a cooperative transition to higher Landau levels, a considerable part, say, a few percent of the electron kinetic energy can transform into a runaway coherent emission pulse. (The relation of superradiance to the dissipative instability of waves with negative energy in plasma beam systems is discussed, for example, in Refs [3, 20, 184].) A similar effect is possible for any electromagnetically active oscillators with a quasiequidistant energy spectrum bounded from below.

In a superluminal sample which comprises two-level active centers and is elongated in the direction of their motion, two counter running trains of superfluorescence pulses with different frequencies can be spontaneously generated [130]. In this case, for inverted active centers, a so-called fast polarization wave with the phase velocity exceeding $c_0$ (normal Doppler effect) has negative energy and can experience dissipative instability, whereas for noninverted centers, a slow polarization wave with the phase velocity smaller than $c_0$ (anomalous Doppler effect) possesses these properties. Therefore, the unidirectional superradiance process can alternately repeat many times involving fast and slow polarization waves due to the change in the sign of the population difference $N_2 - N_1$, taking place each time after the emission of a next superfluorescence pulse due.

Notice that for all classical analogs of the Dicke superradiance considered above, the introduction and quantiza-

tion of hot modes or normal waves within the framework of the PQEDAM taking into account the nonequilibrium character of active oscillators allow us to effectively study the quantum-statistical properties of collective spontaneous emission and to assign a close analogy with an ensemble of two-level oscillators considered in this review.

## 3. Features of cooperative emission in distributed systems

### 3.1 Grounds for the one-dimensional approximation

Experiments and numerical simulations of collective spontaneous emission [36, 56, 59, 111, 112, 115, 116, 140, 157, 158, 185–193] show that, in an extended active sample with the characteristic length $B \gtrsim c/\omega_c$ and the large Fresnel number $F = S/(B\lambda_0) \gtrsim 1$ specified by the characteristic cross section $S$ of the sample, a strongly inhomogeneous anisotropic stochastic field is produced. Its structure considerably changes with each new pumping 'shot' due to quantum or thermal fluctuations of the effective initial conditions, determining in which directions the waves will grow most of all, thereby removing the pumping-driven population inversion of energy levels of active centers. As a rule, upon uniform pumping, highest-power pulses are emitted along the longest paths in a sample and can be qualitatively described in the one-dimensional approximation taking into account cooperative emission only from active centers falling within a cylinder with the cross section $S_1 \sim B\lambda_0$ surrounding the given path of length $B$, i.e., with the Fresnel number $S_1/(B\lambda_0) \sim 1$. This gives the limiting superradiance intensity (for any, not necessarily two-level active centers) $I_{SR} \sim cg\hbar\omega_{21}N_0/(4\sqrt{\varepsilon_0})$, where $g$ is the quantum yield. Thus, for optical superradiance in rarefied gases and activated crystals, for example, at $N_0 \sim 10^{11}$ cm$^{-3}$, typical pulse durations are about a few nanoseconds, and pulse intensities are about 10 W cm$^{-2}$, with $g \simeq 1$ for two-level active centers.

The one-dimensional approximation is quite rigorously substantiated for an oblong cylindrical sample with the Fresnel number $\sim 1$ or for the case of excitation of only one transverse mode in the presence of special waveguides, for example, in single-mode fiber amplifiers and lasers or semiconductor heterolasers. This approximation can be applied for the quantitative analysis of experiments.

Based on this approximation, we will consider in Sections 3.2–3.5 some features of superradiance in extended systems and various factors affecting formation of the radiation field, in particular, the possibility of attaining the oscillatory superradiance regime in the conditions of rather weak polarization and field relaxations, when complicated nonlinear oscillatory energy exchange occurs between the medium and field. This process can proceed both locally (according to the mean field model, in particular, due to the interaction of counterpropagating waves) and with a spatial transfer (propagation effects) or frequency transfer (beats of hot modes with different frequencies).

### 3.2 Semiclassical one-dimensional equations

The corresponding semiclassical Maxwell–Bloch equations can be obtained from system (1)–(4). We represent them in the so-called truncated form, assuming that $B \gg \lambda_0$ and all the dipole moments of active centers have the same orientation, and using the complex amplitudes of counterpropagating waves of the field $A_\pm$ and of polarization spectral densities $P_\pm$ in expansions [13, 46, 192, 194–200]:

$$\mathcal{E} = \sqrt{\frac{\tilde{\Gamma}}{\varepsilon_0}}\,\mathrm{Re}\left\{\left[A_+(z,t)\exp(\mathrm{i}k_0 z) + A_-(z,t)\exp(-\mathrm{i}k_0 z)\right]\exp(-\mathrm{i}\omega_0 t)\right\},$$
$$\mathcal{P}(\Delta) = \sqrt{\frac{\varepsilon_0}{\tilde{\Gamma}}}\,\mathrm{Re}\left\{\left[P_+(z,t,\Delta)\exp(\mathrm{i}k_0 z) + P_-(z,t,\Delta)\exp(-\mathrm{i}k_0 z)\right]\exp(-\mathrm{i}\omega_0 t)\right\} f_L(\Delta), \quad (16)$$

and two components of the population inversion density related to them:

$$N(\Delta) = N_0\left\{n(z,t,\Delta) + \mathrm{Im}\left[n_z(z,t,\Delta)\exp(\mathrm{i}2k_0 z)\right]\right\} f_L(\Delta). \quad (17)$$

We will take into account the inhomogeneous broadening of the spectral line, describing its normalized profile with a Lorentzian $f_L(\Delta) = \Delta_0[\pi(\Delta^2 + \Delta_0^2)]^{-1}$, where $\Delta = (\omega - \bar{\omega}_{21})/v_c$ is the normalized detuning of the transition frequency $\omega$ of the active center from the central line frequency $\bar{\omega}_{21}$, and $\Delta_0 = (T_2^* v_c)^{-1}$ is the normalized line half-width. Here, the cooperative frequency

$$v_c = \sqrt{\frac{2\pi d^2 \bar{\omega}_{21} N_0 \tilde{\Gamma}}{\varepsilon_0 \hbar}}, \quad (18)$$

independent of inversion, was introduced, which differs from $\omega_c$ used earlier in Eqn (4) by the absence of the factor $D$ and the presence of the factor $\tilde{\Gamma}/\varepsilon_0$ taking into account redefinition of quantities (5). We will often use it below. Both inversion components $n(\Delta)$ and $n_z(\Delta)$ and the dipole moment $d(\Delta) = \mathcal{P}(\Delta)/(N_0 f_L)$ are related to active centers located in the spectral line at the frequency $\Delta$. Notice that $\max d(\Delta) = d$, $\min d(\Delta) = -d$, $\max n(\Delta) = 1$, and $\min n(\Delta) = -1$ (at $n_z = 0$). For simplicity, we will assume that the matrix, sample, and occupation of the transverse mode with active centers are homogeneous ($\varepsilon_0$, $\sigma_0$, $N_0$, $\tilde{\Gamma} = \mathrm{const}$), and diffraction or waveguide radiation losses along the sample ($-B/2 \leqslant z \leqslant B/2$) include local ohmic losses $\sigma_0$.

We will analyze the selection of longitudinal electromagnetic modes, which is essential, for example, for attaining superradiance in ensembles of active centers with inhomogeneously broadened spectral lines, assuming the presence of the distributed feedback (DFB) of waves due to the weak (with the amplitude $\bar{\beta} \ll 1$) harmonic modulation (with the period $\pi/k_0$) of the real part of the matrix permittivity $\varepsilon_M = \varepsilon_0\,\mathrm{Re}\,[1 + 4\bar{\beta}\exp(2\mathrm{i}k_0 z)]$. The same effect gives the modulation of the waveguide walls (the DFB in lasers is discussed, for example, in Refs [201–207]). Finally, we introduce the normalized detuning $\Phi = (\omega_0 - \bar{\omega}_{21})/v_c$ of the spectral line center $\bar{\omega}_{21}$ from the Bragg resonance frequency $\omega_0 = k_0 c/\sqrt{\varepsilon_0}$ used in expression (16) for moving to complex wave amplitudes. Then, one-dimensional integro-differential equations of the spatio-temporal dynamics of superradiance may be written out in the form

$$\left[\frac{\partial}{\partial\tau} + \Sigma_0 \pm \frac{\partial}{\partial\zeta}\right] a_\pm = \mathrm{i}\beta^{(*)} a_\mp + \mathrm{i}\int \frac{p_\pm(\Delta) f_L(\Delta)}{\sqrt{I}}\, d\Delta,$$
$$\left[\frac{\partial}{\partial\tau} + \Gamma_2 + \mathrm{i}(\Delta - \Phi)\right] p_\pm(\Delta) = -\sqrt{I}\left(\mathrm{i}n(\Delta) a_\pm \pm n_z^{(*)}(\Delta)\frac{a_\mp}{2}\right),$$

$$\left[\frac{\partial}{\partial\tau}+\Gamma_1\right]\left(n(\Delta)-n_\mathrm{p}(\Delta)\right)=-\sqrt{I}\,\mathrm{Im}\left(a_+p_+^*(\Delta)+a_-p_-^*(\Delta)\right),$$
$$\left[\frac{\partial}{\partial\tau}+\Gamma_{1z}\right]n_z=\sqrt{I}\left(a_-^*\,p_+(\Delta)-a_+\,p_-^*(\Delta)\right), \qquad (19)$$

where $*$ denotes complex conjugation and a superscript $(*)$ means no superscript for the upper sign and complex conjugation for the lower sign in the terms with $a_{\mp}$ factors. Here, the following dimensionless quantities were introduced: $I=v_\mathrm{c}^2/\bar{\omega}_{21}^2\ll 1$, $\Sigma_0=2\pi\sigma_0/v_\mathrm{c}$, $\beta=\bar{\beta}/\sqrt{I}$ is the normalized amplitude of the Bragg modulation of the matrix permittivity (determining the ratio of the half-width of the photonic bandgap [201, 202, 204, 206] to the cooperative frequency); $\tau=tv_\mathrm{c}$ and $\zeta=z/B_\mathrm{c}$ are the time (normalized to the cooperative frequency) and the longitudinal coordinate (normalized to the cooperative length $B_\mathrm{c}=c/(v_\mathrm{c}\sqrt{\varepsilon_0})\equiv\lambda_0/(2\pi\sqrt{I})$); $\Gamma_{1,1z,2}=1/(v_\mathrm{c}T_{1,1z,2})$ are the normalized rates of inversion and polarization relaxation, $p_\pm=P_\pm(\Delta)/(dN_0)$ and $a_\pm=A_\pm/(2\pi dN_0)$ are the normalized amplitudes of the spectral density of polarization and the field of counterpropagating waves; $L=B/B_\mathrm{c}$ is the normalized length of the sample, and $n_\mathrm{p}(\Delta)$ is the inversion of an individual two-level active center with the transition frequency $\bar{\omega}_{21}+v_\mathrm{c}\Delta$ produced by continuous pumping ($n_\mathrm{p}=-1$ in the absence of pumping, $\max|n_\mathrm{p}|=1$). For definiteness, we assume that pumping is incoherent because, in the opposite case of coherent laser pumping, its properties will considerably govern the coherent properties of superradiance (as was pointed out in Refs [208–210]).

We make no distinction between frequencies $\omega_0$ and $\bar{\omega}_{21}$ in normalization coefficients and use the wavelength $\lambda_0=2\pi c/(\bar{\omega}_{21}\sqrt{\varepsilon_0})\simeq 2\pi/k_0$, which is twice the Bragg structure period in the matrix or waveguide. The inversion modulation with the period $\lambda_0/2$ caused by the self-consistent beats of counterpropagating waves can reach $\max|n_z(\zeta,\tau,\Delta)|=1$ (at $n(\Delta)=0$), considerably affecting the Bragg selection of hot modes or waves and their nonlinear evolution by implicitly adding complex dynamic quantities $\mp n_z^{(*)}(\tilde{\omega})/\Delta_0$ to the specified quantities $\beta^{(*)}$ in the first equation of system (19). The complex dynamic quantities are determined by the local value of $n_z$ at the frequency $\tilde{\omega}$ of the mode or wave under study.

The estimate of the dynamic coupling of counterpropagating waves presented above corresponds in fact to a *spatial amplification grating* [201, 204, 206, 211–213], i.e., to the modulation of the imaginary part of the active medium permittivity rather than a Bragg grating related to the refractive index modulation, i.e., to the real part of the permittivity, as the coupling coefficient $\beta$ of counterpropagating waves. This estimate is written for wave frequencies $\tilde{\omega}$ at the spectral line center $|\tilde{\omega}-\bar{\omega}_{21}|\ll 1/T_2^*$ in the case of large inhomogeneous broadening ($\Delta_0\gg 1\gtrsim\Gamma_2$), the most important for superradiant selection, and the spectrally broad modulation of inversion $n_z(\Delta)$ with the characteristic width $\Delta_z$ within the limits $\Gamma_2,|\Phi|\ll\Delta_z\ll\Delta_0$ (we assume that $n_z(\Delta)\simeq 0$ in the line wings). In the case of homogeneous broadening, when $1/T_2>1/T_2^*$, the corresponding dynamic coupling coefficients on the amplification grating for frequencies in the central part of the line $|\tilde{\omega}-\omega_{21}|\ll 1/T_2$ will be $\mp n_z^{(*)}/(2\Gamma_2)$. Outside the spectral line for $|\tilde{\omega}-\omega_{21}|\gg 1/T_2$, counterpropagating waves are coupled on the refraction index grating in the active medium and this coupling is characterized by the coefficient $\beta_z=-\mathrm{i}n_zv_\mathrm{c}/[2(\tilde{\omega}-\omega_{21})]$, which in fact is added to the coefficient $\beta$ in the first equation of system (19).

These coupling coefficients implicitly contained in system (19) and caused by the active medium, are consistent with the mode dynamics and depend on the coordinate $\zeta$ and time $\tau$, whereas the coupling coefficient $\beta$ of counterpropagating waves specified by the matrix does not evolve in time, and for simplicity we assume that $\beta=\mathrm{const}$ in space. (In general, it is complex, $\beta=|\beta|\exp(\mathrm{i}\varphi)$, where the phase $\varphi=-2k_0\delta z$ reflects the displacement $-\delta z$ of the symmetry point of the Bragg structure with respect to the sample center at $z=0$.) The distributed reflection and selective amplification of counterpropagating waves affect the mode dispersion and growth rates in the frequency band $|\Delta_\mathrm{E}|\equiv|\tilde{\omega}-\omega_0|/v_\mathrm{c}\lesssim|\beta|+|n_z|/(\Delta_0+2\Gamma_2)$. Notice that in the case of the refractive index grating for $|\beta+\beta_z|L\gtrsim 1$, a 'forbidden' photon frequency bandgap $|\Delta_E|\lesssim|\beta+\beta_z|$ appears in which waves do not propagate in fact.

### 3.3 Dispersion of waves and modes

Generally, the development of superradiance depends on the dispersion of the permittivity of the active medium:

$$\varepsilon(\tilde{\omega})=\varepsilon_0+\frac{\mathrm{i}4\pi\sigma_0}{\tilde{\omega}}-\frac{4\pi d^2N_0}{\hbar}\int\frac{n(\omega-\bar{\omega}_{21})f_\mathrm{L}(\omega-\bar{\omega}_{21})}{\omega-\tilde{\omega}-\mathrm{i}T_2}\,\mathrm{d}\omega, \qquad (20)$$

i.e., on the dependence of the real part of the permittivity $\mathrm{Re}\,\varepsilon$ on the monochromatic field frequency $\tilde{\omega}$, and takes into account the self-consistent spectral profile of the smoothly inhomogeneous inversion component $n(\zeta,\tau,\Delta)$. This dispersion is interrelated with the imaginary part of expression (20), which directly determines the growth rate (or the gain) of the field. If spectral dips in the inversion component $n(\omega-\bar{\omega}_{21})$ are smooth, at least on the $T_2^{-1}$ scale, then, for $1/T_2^*\gg v_\mathrm{c}\gg 1/T_2$ dispersion proves to be weak at the spectral line center, and we can routinely assume that $\mathrm{Re}\,\varepsilon\simeq\varepsilon_0$ and

$$\mathrm{Im}\,\varepsilon(\tilde{\omega})\approx\frac{4\pi\sigma_0}{\bar{\omega}_{21}}+\frac{4\pi d^2N_0T_2^*\left(\bar{D}-2n|_{\omega\approx\tilde{\omega}}\right)}{\hbar},$$
$$|\tilde{\omega}-\bar{\omega}_{21}|\ll\frac{1}{T_2^*}, \qquad (21)$$

according to the Sokhotski formula and ignoring the poles of a smooth function $n(\omega-\bar{\omega}_{21})$. In this approximation, the field instability (amplification) at frequency $\tilde{\omega}$ is possible if $\mathrm{Im}\,\varepsilon<0$, i.e., only if the population inversion of the levels of active centers at this frequency $\omega=\tilde{\omega}$ is decreased by less than half compared to the mean spectral line inversion $\bar{D}=\int(N(\Delta)/N_0)\,\mathrm{d}\Delta$ specified by the initial pumping pulse (for superfluorescence) or maintained by continuous pumping (for a superradiant laser). Numerical simulations often demonstrate a considerable irregularity of the spectral inversion profile $n(\Delta)$ at the nonlinear stage, which complicates analysis of the instability or amplification of monochromatic waves. The latter, linearized analysis, however, is not very relevant due to the nonlinearity of the superradiance process.

It should be noted that both the instability (amplification) of waves or modes and their nonlinear dynamics considerably depend on the field decay rate $\Gamma_\mathrm{E}=1/(v_\mathrm{c}T_\mathrm{E})$ in a cold cavity (i.e., at the zero inversion $N(\Delta)=0$). The corresponding lifetime $T_\mathrm{E}$ is not explicitly present in equations (19) but is determined (as in Eqns (20) and (21)) by both ohmic and

diffraction (waveguide) losses $\sigma_0$ and Bragg distributed reflections $\beta$ of waves and boundary conditions. For the one-dimensional problem under study in the general case of a sample with differently reflecting facets (or in a nonsymmetric Fabry–Perot cavity), the boundary conditions at its ends, $\zeta = \pm L/2$, correspond to the ratio between amplitudes of counterpropagating waves equal to the reflection coefficients $R_{1,2}$ of the facets. In the limit of a purely Bragg cavity ($R_{1,2} = 0$) and, in particular, in the nonreflection limit ($\beta = 0$), the boundary conditions correspond to the free field emission: $a_+(-L/2) = 0$ and $a_-(L/2) = 0$. If $\sigma_0$ is small enough, then for open samples or samples in low-$Q$ cavities with small DFB parameters ($\beta L \lesssim 1$) and/or reflection coefficients of faces, say, $R \lesssim 1/2$, the time $T_E$ is determined, accurate to a logarithmic factor of about unity, by the travel time of light in the sample[5]: $T_E \sim B\sqrt{\varepsilon_0}/c$.

It is known [3, 214, 215] (see also Section 5) that in low-$Q$ cavities with $T_E \lesssim T_2$ the superradiance of discrete modes dominating over continuous-spectrum waves is possible if the condition

$$v_c^2 T_E \gtrsim \frac{1}{T_2} + \frac{1}{T_2^*} \tag{22}$$

is fulfilled, whereas the unidirectional superradiance and superfluorescence of continuous-spectrum waves and also the oscillatory superradiance of discrete modes in higher-$Q$ systems with $T_E \gg T_2$ are possible when the milder condition

$$v_c^2 T_2 \gtrsim \frac{1}{T_2} + \frac{1}{T_2^*}\,, \tag{23}$$

independent of the field decay, is fulfilled.

These and more detailed conditions for the emergence of mode superradiance, as well as the characteristic spectra and growth rates of hot modes (presented in Fig. 1 for homogeneous and inhomogeneous broadenings) are obtained from linearized equations (19) for the specified inversion $n = \text{const}$ of the active medium (spatially and spectrally homogeneous). The mode spectrum is determined by the well-known dispersion equation for the medium and the characteristic cavity equation [197, 198] following from the system of equations (19):

$$\kappa^2 + |\beta|^2 = \left(\Omega + \frac{n}{\Omega + \Phi + \mathrm{i}(\Delta_0 + \Gamma_2)}\right)^2, \tag{24}$$

$$\Omega + \frac{n}{\Omega + \Phi + \mathrm{i}(\Delta_0 + \Gamma_2)} = \frac{R_1\beta + R_2\beta^*}{1 + R_1R_2} + \frac{\kappa(1 - R_1R_2)}{1 + R_1R_2}\,\frac{1 + \exp(2\mathrm{i}\kappa L)}{1 - \exp(2\mathrm{i}\kappa L)}\,. \tag{25}$$

The dispersion relation is local and link the complex frequency detuning $\Omega = (\tilde{\omega} - \omega_0)/v_c$ and the wave-vector detuning $\kappa = (k - k_0)B_c$ of the mode in the presence of Bragg wave rescattering. The characteristic cavity equation is dictated by boundary conditions and singles out the discrete wave numbers $\kappa$ of counterpropagating waves. The left-hand side of Eqn (25) contains, in fact, the quantity $\pm(\kappa^2 + |\beta|^2)^{1/2}$ with signs chosen according to the solution of equations (24) and (25), so as to exclude redundant nonphysical roots for which a wave having an increment (decrement) decays (grows) in its propagation direction.

[5] In the mean field model for a sample in the Fabry–Perot cavity at $\beta = 0$, as follows from the first equation of system (19), $T_E = [2\pi(\tilde{\sigma}_0 + \tilde{\sigma}_{rad})]^{-1}$, where $2\pi\tilde{\sigma}_{rad} = (c/B\sqrt{\varepsilon_0})\ln|R_1R_2|^{-1/2}$.

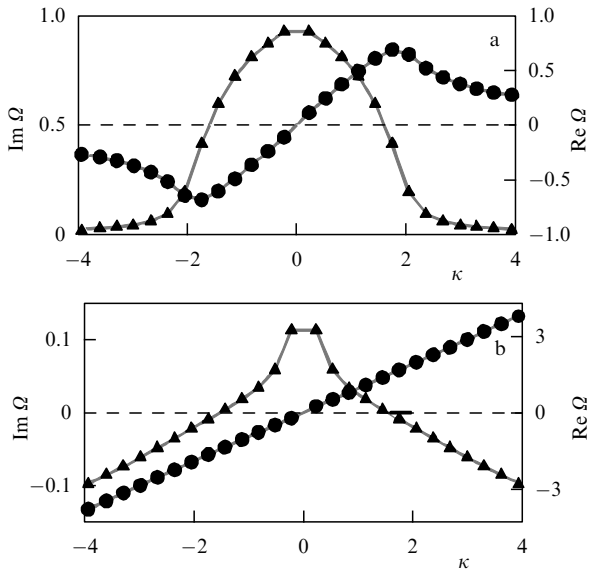


**Figure 1.** Typical dependences of growth rates $\mathrm{Im}\,\Omega$ (triangles) and frequency shifts $\mathrm{Re}\,\Omega$ (circles) on the shift of the wave number $\kappa$ for the branch of unstable polariton modes in an inverted medium with the homogeneous line broadening $\Gamma_2 = 0.02$ (a) and the branch of unstable electromagnetic modes in an inverted medium with large inhomogeneous broadening $\Delta_0 = 4$ (b) for the same combined Fabry–Perot resonator with the DFB ($L = 10$, $\beta = 0.1$, $R_{1,2} = 0.1\exp(-\mathrm{i}\pi/2)$, $\Phi = 0$).

If the polarization relaxation rate $1/T_2$ proves to be smaller than the mode growth rate $\tilde{\omega}'' \equiv \mathrm{Im}\,\tilde{\omega}$, the active centers related to this mode are inevitably phased during the development of the instability. Therefore, they emit collectively or, in other words, emit superradiance, so that the intensity of their combined emission exceeds by many times the sum of emission intensities of each of them.

In the case of a homogeneously broadened spectral line, when $v_c > 1/T_2 > 1/T_2^*$, active centers qualitatively change the dispersion properties of unstable (amplifiable) electromagnetic waves and modes, which transform into polarization waves and polariton modes [3, 16, 48, 88, 139]. According to Eqns (1)–(4) or (19), the permittivity (20) determining them has the form

$$\varepsilon(\tilde{\omega}) = \varepsilon_0 + \mathrm{i}\,\frac{4\pi\sigma_0}{\tilde{\omega}} - \frac{4\pi d^2 N_0 D}{\hbar(\tilde{\omega} - \omega_{21} + \mathrm{i}T_2^{-1})} \tag{26}$$

near the resonance ($\tilde{\omega} \approx \omega_{21}$) and, in a medium with inversion $D > 0$, leads to initiation of unstable polarization waves with dispersion properties considerably different from conventional polaritons in a noninverted medium [216–219]. They produce collective spontaneous emission possessing a growth rate up to $\sqrt{D}v_c$. If the inhomogeneous broadening dominates, when $1/T_2^* > v_c > 1/T_2$, as follows from formulas (20) and (21), the dispersion of electromagnetic waves or modes is weakly changed by active centers, while the maximum growth rate decreases to the so-called *effective cooperative frequency* [215, 220–223]

$$\bar{v}_c = v_c^2 T_2^* \equiv \frac{v_c}{\Delta_0}\,, \tag{27}$$

determined by the cooperative frequency of not all but only a part of the active centers with close frequencies occupying a spectral band with width $2\bar{v}_c$ and having no time to dephase during the formation time of a superradiant pulse $\delta t \sim \bar{v}_c^{-1}$, i.e., $\delta\tau \sim \Delta_0$. This minimal duration of expected field pulses can be achieved due to a special mode selection and is almost

independent of the coupling parameter $\beta$ of counterpropagating waves and relaxation times $T_{1,2}$ until $\delta t \lesssim T_2$, i.e., for $\Delta_0 \lesssim \Gamma_2^{-1}$ (see Section 5).

It is obvious that for obtaining collective spontaneous emission with the highest-power pulses without strong oscillations the active samples are needed with length $L \equiv B/B_c$ on the order of the *optimal* length $L \sim 2$ and $L \sim 2\Delta_0 \gg 1$ determined in the cases of homogeneous and strongly inhomogeneous broadenings by the respective cooperative length $B_c$ and the effective cooperative length $\bar{B}_c = B_c\Delta_0$ (determined by effective cooperative frequency (27)). In the estimates and calculations presented below, we assume that the inversion given initially or specified by pumping ($n_p(\Delta)$ or $D_p$) is on the order of unity. Otherwise, it is necessary to take into account that maximal growth rates are obtained by the multiplication of $\bar{\nu}_c$ by $\nu_c$, and the cooperative lengths by the division of $\bar{B}_c$ and $B_c$ by the inversion and the root from it, respectively.

### 3.4 Nonlinear wave interactions

Let us illustrate the influence of some of the factors pointed out above by the results of numerical simulations mainly performed for samples with optimal dimensions. In the examples presented below, equations (19) were solved, as a rule, under the following initial conditions [incoherent simultaneous (transverse) pumping of all active centers]: $n = 1$, $n_z = 0$, $a_\pm = 0$, $|p_\pm| \sim 10^{-3}$. Polarization was taken in the form of a strongly inhomogeneous function of the coordinate $\zeta$ and frequency $\Delta$. Numerous verifying calculations showed that superfluorescence pulses obtained in the absence of continuous pumping are almost independent of variations in small initial wave amplitudes $|p_\pm|$, $|a_\pm| \lesssim 10^{-3}$, while the characteristics of stable lasing in the presence of continuous pumping are, as a rule, insensitive to the initial conditions, remaining the same for other initial conditions, for example, with zero inversion or in the presence of small 'external' noise of the electromagnetic field (cf. Ref. [224]).

At the same time, a spontaneously appearing standing inversion grating $n_z(\zeta, \tau, \Delta)$ with the wave number $2k \approx 2\bar{\omega}_{21}\sqrt{\varepsilon_0}/c$ causes in a number of cases considerable distributed reflections and discrimination in the amplification of counterpropagating waves with the wave numbers $\pm k$ [197, 198, 200, 213, 225–227]. This grating may be metastable, retaining the initially specified or sporadically established profile for long times. Its relaxation rate $\Gamma_{1z}$ in gas and especially in a condensed medium can noticeably differ from the inversion production rate $\Gamma_1$ upon quasiuniform pumping, for example, due to the spread of small-scale structures of active centers in their thermal motion or diffusion in a matrix (below, we assume for definiteness that $\Gamma_{1z} = \Gamma_1$).

Strictly speaking, there is also a similar polarization grating of active centers with wave numbers $\pm 3k$, oscillating at the field frequency $\tilde{\omega} \simeq \bar{\omega}_{21}$, which is caused by the nonlinear scattering of electromagnetic waves on a standing inversion grating. However, the lifetime $T_{2z}$ of this polarization grating is, as a rule, shorter than the lifetime $T_2$ of dipole oscillations of an individual active center because of various dephasing factors, which are especially significant for inhomogeneously broadened spectral lines, and $T_{2z}$ can be small compared to the lifetime $T_{1z}$ of the inversion grating. In addition, the large amplitude of the polarization grating can be achieved only for short time intervals under the action of superradiant pulses in the conditions when their Rabi frequencies exceed the inverse lifetime $T_{2z}^{-1}$, which is difficult to achieve. Finally, the polarization grating is not directly involved in the formation of the polarization and electromagnetic wave fields but only strains the inversion grating due to nonlinear backscattering of electromagnetic radiation. Therefore, the polarization grating usually plays a secondary role, and we will ignore it below for simplicity. (The possible case of its influence on the instability of some multimode lasing regimes in quantum-cascade lasers in the presence of collective spontaneous emission was recently indicated in work [228].)

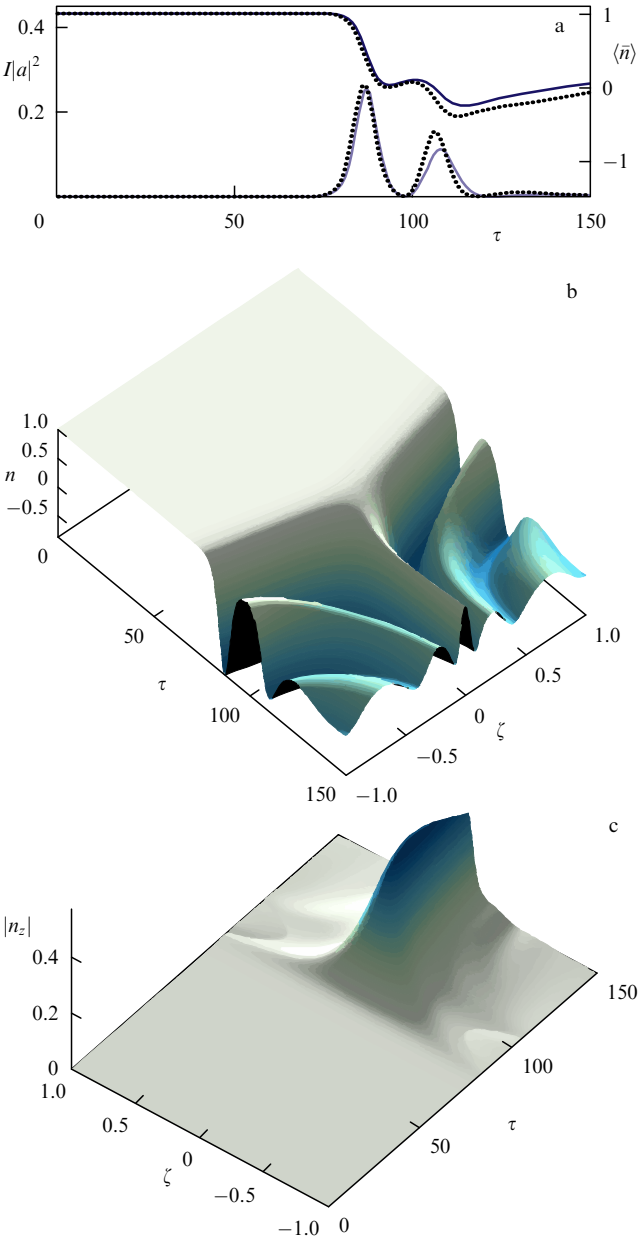


**Figure 2.** Superfluorescence of a sample of length $L = 2$ with negligibly small reflections at the ends ($R = 10^{-3}$) in the case of weak continuous pumping ($n_p = 1$) and almost homogeneous spectral line broadening: $\Gamma_2 = 2\Gamma_1 = 0.02 \gg \Delta_0 = 0.002$. (a) Oscillograms of the normalized output radiation intensity $I|a|^2$ and the mean (over the sample) inversion $\langle\bar{n}\rangle$ taking into account (solid curves) and neglecting (dotted curves) the self-consistent inversion gratings $n_z$. (b, c) Spatio-temporal evolutions of the inversion $n(\zeta, \tau)$ and the inversion grating amplitude $|n_z(\zeta, \tau)|$.

The propagation effects and a possible role of self-consistent distributed reflection and selective amplification of waves are illustrated in Figs 2 and 3 presenting the results

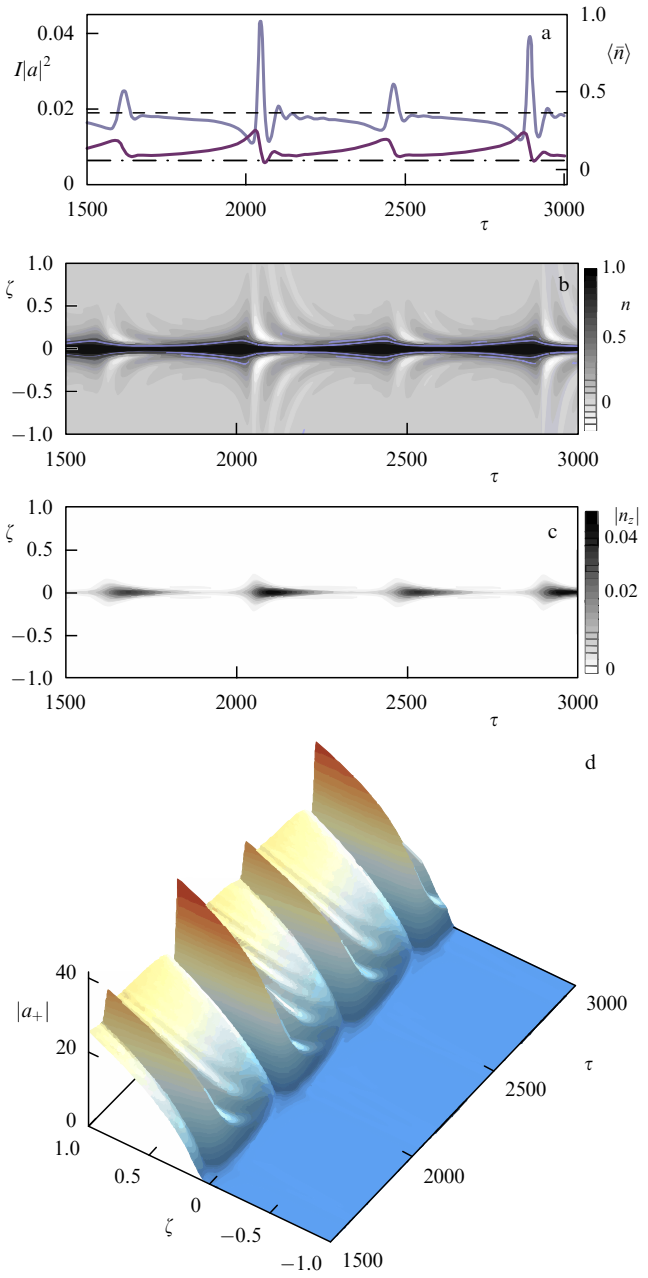


**Figure 3.** Typical view of superradiant lasing upon continuous pumping of the same distributed sample as in Fig. 2. (a) Oscillograms of the normalized output radiation intensity $I|a|^2$ and the mean (over the sample) inversion $\langle\bar{n}\rangle$ taking into account (light and dark solid curves) and ignoring (dashed and dashed-dotted lines) the self-consistent inversion grating $n_z$. (b, c) Quasiperiodic evolutions of the spatial distributions of the inversion $n(\zeta,\tau)$ and the inversion grating amplitude $|n_z(\zeta,\tau)|$. (d) Spatio-temporal evolution of the amplitude profile $|a_+(\zeta,\tau)|$ of the wave running to the right.

of the solution of the system of equations (19) for a distributed sample with optimal length $L = 2$ without the DFB ($\beta = 0$) and the negligibly small reflection coefficient at facets ($R = 10^{-3}$) for a continuously pumped ($n_p = 1$) virtually homogeneous spectral line: $\Delta_0 = 0.002 \ll \Gamma_2 = 2\Gamma_1 = 0.02$. For convenience, the output emission intensity in these and following figures is represented by the dimensionless quantity $I|a_\pm|^2 = (\omega_{R\pm}/\nu_c)^2$ equal to the square of the normalized amplitude of the Rabi frequency $\omega_{R\pm} = d|A_\pm|/\hbar$ in the field of the corresponding wave $A_\pm$ of this emission.

At the initial stage of superfluorescence, continuous pumping does not play any important role, and collective spontaneous emission pulses (in fact identical at both ends of the sample) (Fig. 2a) are formed in the course of developing radiative instability of polarization waves and removal of the initially stored inversion by the wave's field (Fig. 2b). The propagation effects of coherent emission increase the duration of the main unidirectional superradiance pulse to a few inverse cooperative frequencies, and its reabsorption leads to the emission of a repeat, weaker pulse. The inversion grating $n_z(\zeta,\tau)$ appears only in the central part of the sample (Fig. 2c) where counterpropagating waves with comparable amplitudes at the saturation stage of the main pulse exist. The grating has no time to strongly affect the main pulse; however, it noticeably (by approximately 10%) changes the parameters of the repeated pulse (Fig. 2a).

Figure 3 displays a typical episode of the established quasi-monochromatic superradiant lasing, which is also in fact the same at opposite ends of the sample. Lasing would be monochromatic (accurate to the spectral line width) in the absence of the inversion grating (see the dashed line in Fig. 3a) since then the counterpropagating waves are amplified according to the local value of the stationary inversion profile (Fig. 3b) strictly within the framework of the unidirectional approximation. However, the inversion grating appearing in the central part of the sample (Fig. 3c) causes instability of monochromatic lasing due to a small redistribution of counterpropagating waves changing their amplification and providing the inversion increase in the sample center. This is accompanied by the quasiperiodic development of sporadic weak superradiant pulses alternately in one or another counterpropagating waves (solid curves in Fig. 3a), their concrete oscillograms being sensitive to quantum, thermal (and numerical) noises and, as a whole, greatly depending on the sample length $L$ and the pumping rate $\Gamma_1$.

It should be noted that the wave $a_+$ propagating to the right (Fig. 3d) has an almost constant amplitude in the left part of the sample, $|a_+(\zeta < 0)| \sim R|a_-(\zeta = -L/2)|$, and is amplified only in the right part of the sample, 'eliminating' there all the inversion produced by pumping and reducing it in fact to zero. The wave $a_-$ propagating to the left behaves symmetrically after the right $\rightleftarrows$ left change. The spectra of both waves are the same and contain, along with the quasimonochromatic component, a pedestal whose width is about some fraction of the cooperative frequency caused by the sporadic superradiant pulses mentioned above.

If the length of a sample containing active centers with a homogeneous spectral line is much greater than the cooperative length, $L \gg 1$, even a weak metastable inversion grating $n_z$ will not appear during superfluorescence or superradiant lasing because of the irregular reabsorption of superradiant pulses in regions with lengths on the order of the cooperative length. In this case, the output emission would be oscillating and weakly coherent (quasichaotic, taking into account real noises and stochastic initial conditions) with the spectral width $\sim \nu_c$ or even noticeably narrower due to the decrease in the field pulse steepness and its elongation in the sample caused by many reabsorptions. Because the effective rescattering of counterpopagating waves is absent, such dynamics can be adequately described in the unidirectional superradiance approximation [3, 12–14, 43, 46, 229].

For very short samples, $L \ll 1$, superradiant lasing is difficult to obtain, while superfluorescence is coherent and oscillatory (following, under certain conditions, the self-similar law [3, 230–232]). Its main part, in the form of an

elongated pulse with a duration of $\sim (v_c^2 T_E) \sim (v_c L)^{-1}$ is described well by the mean field model for the Bloch angle [4, 14, 46, 87, 110, 129, 233] (similar to a strongly decaying pendulum) giving a narrowed spectrum $\sim v_c L$ in width. The comparatively small amplitude of the field of counterpropagating waves, despite its quite regular character, excludes the formation of a noticeable inversion grating in the sample, and the unidirectional approximation can again be formally applied, although oscillograms of emission from opposite sample ends can significantly differ from each other, being nonsymmetrical. This is caused by differences in quantum and thermal fluctuations (initial and accompanying pumping) of the field and polarization at these ends and by the amplification of counterpropagating waves due to the common reservoir of inversion of active centers, resulting in their strong competition with each other.

### 3.5 Manifestations of the emission dynamics

The consideration of ohmic or diffraction (waveguide) losses in equations (19), which is important for $\Sigma_0 \gtrsim L^{-1}$, leads to an additional decrease in the emission intensity, elongation of pulses, and narrowing of the superradiance spectrum. Notice that, for $L \sim 1$, the dynamic inversion grating can play a prominent role only for $\Sigma_0 \lesssim 1$, while for $L \gg 1$ the formation of individual pulses inside a sample is greatly modified due to these losses only for $\Sigma_0 \gtrsim 1$, remaining in fact unidirectional and losing their oscillatory character at large losses $\Sigma_0 \gg 1$. The features of the influence of such distributed losses on the superradiance of waves with a continuous spectrum in the unidirectional approximation (in the absence of any reflections), including a passage from oscillatory superradiance to the single-pulse one, were considered in Refs [3, 87, 112, 233]. We will not discuss these losses further, assuming that $\Sigma_0 = 0$, because most of the interest is in emission itself through sample ends. This emission also plays the role of losses for the dissipative instability of polarization waves, and produces a strong inhomogeneity of the field and polarization in the sample under conditions of high amplification of waves in the active medium of oscillators during superradiance.[6]

As pointed out in many experiments and the superradiance theory, even weak reflections from sample ends, $R \ll 1$, which barely reduce the output radiation, can considerably affect the field, polarization, and inversion dynamics in the sample and, therefore, the properties of collective spontaneous emission pulses [3, 13, 36, 38, 40, 108, 115, 116, 127, 128, 194, 195, 224, 234–237]. Leaving aside until Section 5 the discussion of the influence of reflections on the field structure and the output pulse shape during superfluorescence and superradiant generation of discrete-spectrum modes, we note here only that, as in Refs [37, 197, 198, 238, 239], this influence will be levelled in fact by the unidirectional superradiance of continuous-spectrum waves in very long samples with

$$L \gg n_p^{-1/2} \ln |R|^{-1}, \text{ i.e. } v_c \sqrt{n_p} \gg T_E^{-1} > T_2^{-1}, \qquad (28)$$

$$L \gg \Delta_0 n_p^{-1} \ln |R|^{-1}, \text{ i.e. } \bar{\nu}_c n_p \gg T_E^{-1} > T_2^{-1}, \qquad (29)$$

[6] According to formulas (21) and (26), for a sample with homogeneous inversion and occupation factor of order $\bar{D} \sim 1$ and $\tilde{\Gamma} \sim 1$, respectively, the total gain of the monochromatic field varying as $\propto \exp(-i\tilde{\omega}t + ikz)$ with the complex wave number $k$ in the line center at $\tilde{\omega} = \bar{\omega}_{21}$ is large: $-B \operatorname{Im} k = (B/B_c)(\bar{D}/\tilde{\Gamma}) v_c/(T_2^{-1} + T_2^{*-1}) \gtrsim 1$ for both homogeneous ($T_2 \ll T_2^*$) and strongly inhomogeneous ($T_2 \gg T_2^*$) broadenings if $L \gtrsim 1$ and $L \gtrsim \Delta_0 \equiv (v_c T_2^*) \gg 1$, respectively.

in the case of homogeneous ($\Delta_0 < \Gamma_2$) and strongly inhomogeneous ($\Delta_0 \gg 1 \gtrsim \Gamma_2$) broadening, respectively. In this case, assuming for definiteness the use of strong continuous pumping, we can show that already near the first lasing threshold ($n_p \sim n_{p1}$) even for strong reflections ($\ln |R|^{-1} \sim 1$), local superradiant processes in separate regions of length $\delta L \sim 1$ and $\delta L \sim \Delta_0$, respectively, are typical (for inversion about unity). Pulses appearing in a variety of such regions will be weakly coherent between themselves and poorly separated, in particular, due to absorption in adjacent regions. As a result, the inversion supplied by pumping will be removed more or less uniformly over all the superradiant laser, producing noise-like low-coherent emission over all the spectral line, homogeneous ($2/T_2$) or inhomogeneous ($2/T_2^*$). In the latter case, even for samples with a smaller length for $L \gg \Delta_0^{-1}$, the superradiant lasing regime will simultaneously involve many modes, because the intermode interval $\pi c/(B\sqrt{\varepsilon_0}) \sim 1/T_E$ for such samples is small compared with the width $2/T_2^*$ of the inhomogeneous line broadening.[7] Then, at a considerable excess over the lasing threshold, lasing will be quasichaotic, not containing any noticeable separate superradiant mode pulses, while the difference in frequencies of active centers in the lasing band of each mode will facilitate the dephasing of their radiation and suppression of its collective character.

In such strongly nonstationary lasing regimes of a superradiant laser with a Fabry–Perot cavity, the emission spectrum has both a discrete component and a continuous component because of the nonlinear broadening and overlap of mode spectra and the overlap of spectral dips in the population inversion burnt by them (Fig. 4). To obtain separated collective spontaneous emission pulses in superradiant lasers with the inhomogeneous broadening of a spectral line, mode selection is required, i.e., an additional increase in the growth rate or gain in one or a few modes (see Section 5). It is important that for this purpose, as in the case of a homogeneously broadened spectral line, a low-$Q$ cavity is quite useful, which facilitates the realization of superradiance and provides its efficient outcoupling. However, the field in this cavity proves to be strongly inhomogeneous and, as a rule, multimode and, therefore, does not allow the correct description in the mean field model.

## 4. Observations of superfluorescence of dipole ensembles and the collective recombination of electrons and holes

### 4.1 Experiments are continued

The first experiments on superfluorescence were performed in the 1970s–1980s in the infrared and optical regions mainly with gases and activated crystals (see reviews [12, 14, 44, 45, 149, 210]). New recent experimental studies of the properties of the collective spontaneous emission of inverted active centers of various types, first of all, semiconductor structures, are presented in Refs [56–60, 62–68, 98–101, 103, 146, 193, 240–253]. These experiments are partially discussed in recent reviews [4, 5, 15, 47, 223]. We will present only several

[7] For very short samples with $B \sim T_2^* c/\sqrt{\varepsilon_0}$ and $\ln |R|^{-1} \gtrsim 1$, i.e. containing only one mode within the spectral line and being opened for superradiance outcoupling, the production of collective spontaneous emission requires too high a density of inverted active centers with $v_c \sim 1/T_2^*$, which is difficult to achieve in available active media.

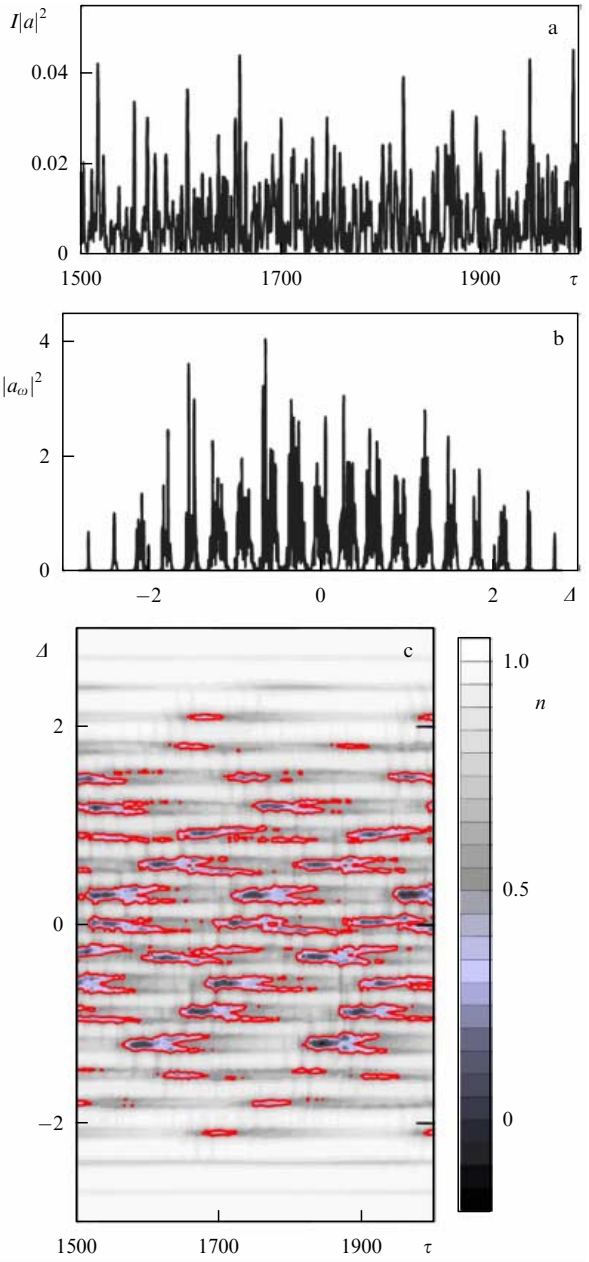


**Figure 4.** (Color online.) Quasichaotic dynamics of a multimode superradiant laser with a strongly inhomogeneously broadened spectral line and a low-$Q$ Fabry–Perot cavity: $R = 0.1$, $L = 10$, $\Delta_0 = 4$, $\Gamma_2 = 2\Gamma_1 = 0.02$, $n_p = 1$. (a) Oscillogram of the normalized output radiation intensity $I|a|^2$. (b) Spectral power $|a_\omega|^2$ of the radiation field. (c) Dynamic spectrum of the population inversion $n(\tau, \Delta)$ of active-center levels at the end $\zeta = L/2$.

examples from them, focusing our attention on the features of the superradiance phenomenon whose description is beyond the scope of the mean field model of a homogeneous ensemble of active centers and requires the consideration of its spectral–spatial inhomogeneity or the effects of propagation, distributed reflection, and interaction between counterpropagating, both electromagnetic and polarization waves.

Unfortunately, experimental data on the spatio-temporal dynamics of superradiance are scarce, and because of this we will illustrate our qualitative analysis by numerical simulations. Notice that the one-dimensional equations (19) that we use are practically universal and provide an adequate picture of superradiance phenomenon for most experiments, despite the variety of active centers studied. These include atoms and molecules in gases, molecular centers and activated dye centers in various matrices, molecular J and H aggregates and impurities in thin polymer films, quantum dots and nanocrystals, and electron–hole pairs and excitons in heterostructures and various traps. In some cases, it is necessary to discard the two-level approximation and take into account the coherent collective dynamics of transitions between many energy levels in active centers, as, for example, in the description of cascade superfluorescence of pulses at different frequencies upon laser pumping of the high-lying energy levels of Ca and Rb atoms in experiments considered below.

### 4.2 Example of the superfluorescence study in gas

Consider experiments [56] on superfluorescence at the 2-μm $3d4s\,^3D_J - 4s4p\,^3P_{J-1}$ transition in Ca vapors at temperatures of about 900 K and the Ca density $5 \times 10^{14}$ cm$^{-3}$. Excitation was performed by a 6-ns, 100-kW pulse from a 0.4-μm dye laser through higher-lying energy levels from which 'pulsed' pumping of this transition occurred for $\sim 100$ ns mainly due to spin-changing collisions with Ar atoms of a buffer gas with a partial pressure of 100–800 Torr. Inversion was produced by transverse laser excitation of the Ca and Ar gas mixture in a cylindrical volume with length $B \approx 50$ cm and cross section $S \approx (0.01 - 0.5)$ cm$^2$, so that the Fresnel number fell in the range $1 \lesssim F \lesssim 10$ and the length estimated by the authors exceeded by ten times or more the cooperative length: $B/B_c \gtrsim 10$.

As far as we know, this is the first detailed experiment [8] in which the influence of 'transverse' multimode properties of radiation and the 'longitudinal' reabsorption of superfluorescence was studied quantitatively in such long samples with the high density of active centers and their narrow spectral line, when the cooperative frequency $\nu_c$ reached $\sim 10^9$ s$^{-1}$ and could exceed the linewidth (mainly collisional) several-fold: $\nu_c \gtrsim 2/T_2 \gtrsim 3 \times 10^8$ s$^{-1} \sim 2/T_2^*$ (the inhomogeneous Doppler broadening was partially suppressed by collisions).[9] Parameters of the same order of magnitude were also achieved in experiments [222] on the superfluorescence of Ca atoms at the 5.5-μm $4s4p\,^1P_1 - 3d4s\,^1D_2$ transition observed as a precursor during the cascade relaxation of Ca excitations down to the $3d4s\,^3D_J$ level, which is the upper working level for forming collective spontaneous emission. The delay time of the latter was within 30–100 ns and was the sum of the 'cooperative' time $\sim 10\nu_c^{-1}$ required for the formation of the first pulse of this collective spontaneous emission in the end part of the sample with length $\sim 2B_c$ (i.e., about one or a few centimeters), the finite pumping pulse duration (a few dozen nanoseconds), and the subsequent time of inversion production at the working $3d4s\,^3D_J - 4s4p\,^3P_{J-1}$ transition after a series of cascade transitions between energy levels in Ca atoms caused by collisions with Ar atoms.

[8] The pioneering experiment on superfluorescence of Ca atoms was performed in Ref. [37] with $F \sim 1$ and $B \lesssim 3B_c$, where the dominating mechanism of polarization relaxation restricting collective spontaneous emission was Doppler broadening.

[9] These unique conditions $\nu_c > 2/T_2$, $\nu_c > 2/T_2^*$ for $B > B_c$ were also achieved in experiments [60, 123] with a dense rubidium gas nonresonantly pumped by 100-fs laser pulses. The single-oscillatory regime of cascade picosecond superfluorescence achieved in these experiments can be correctly described only beyond the framework of the unidirectional superradiance approximation.

The duration of the main (first) pulse was 5–50 ns, i.e., one–two orders of magnitude shorter than the radiative lifetime ($\approx 3$ ms) of the upper working $3d4s\,^3D_J$ level of an individual Ca atom. The total duration of collective spontaneous emission was on the order of the delay time and reached 100 ns, because fluorescence was maintained through all its way by additionally supplying Ca atoms inverted to the $3d4s\,^3D_J$ level mainly due to the collisions mentioned above. In this case, the oscillatory superradiance regime was usually reached, i.e., several coherent pulses were observed. They were either formed at different depths in layers with a thickness of about a few cooperative lengths $B_c$ in the sample and reached its ends after a number of reabsorptions or (for $F \gtrsim 3$) arrived at slightly different angles and were formed by weakly intersected beams producing thinner cylinders with the Fresnel number about unity in the inverted sample. As a Fresnel number $F$ of the whole sample was increased, the number of reoscillations observed was increased and their amplitude decreased, while for $F \sim 10$ superfluorescence oscillations completely disappeared after averaging over many laser shots. In this case, superfluorescence from opposite ends was in all cases approximately the same and corresponded to unidirectional superradiance, considered in Section 3.

### 4.3 Cooperative recombination of free electrons and holes

Let us consider now experiments [59, 146, 193, 248, 252] on the collective spontaneous recombination of free, unbound electrons and holes[10] initially produced by an incoherent 150-fs pumping pulse from a Ti:sapphire laser in barriers of a multilayer quantum-well heterostructure cooled to 4–150 K in a transverse quantizing magnetic field $B_0 = 4-17.5$ T. The heterostructure consisted of 15 layers of 8-nm $In_{0.2}Ga_{0.8}As$ quantum wells separated by 15-nm GaAs barriers. The laser beam spot on the sample was $\approx 0.5$ mm in diameter and the laser pulse energy density was about 10 mJ cm$^{-2}$. Taking into account the local neutrality, i.e., the equality between the electron and hole densities, equations for the difference between their populations at the corresponding Landau levels $N(K)$, polarization $P(K)$, and the superfluorescence field in the recombination frequency band for each Landau level $n_L = 0, 1, 2, \ldots$ are quite similar to equations (19) for the unidirectional superfluorescence of two-level active centers. It is important that the magnetic field weakens the polarization relaxation for electron–hole pairs, $T_2^{-1}$, and increases their dipole moment $d = d_{e,h}$, which is contained in the cooperative frequency (18) and is determined by the matrix element of the interband transition between the states of magnetized electrons and holes with energies (in the parabolic band approximation)

$$E_{e,h} = \pm\frac{E_g + (2n_L + 1)\hbar\omega_{B_{e,h}}}{2} \pm \frac{\hbar^2 K^2}{2m_{e,h}}, \qquad (30)$$

where $E_g$ is the bandgap energy, $\omega_{B_{e,h}} = eB_0/(cm_{e,h})$ are gyrofrequencies, $m_{e,h}$ are the electron and hole masses, respectively, and $K$ is their wave number in the Brillouin zone along the magnetic field $B_0$.

[10] The first proposals and theoretical grounds for these and other possible experiments on collective spontaneous emission upon the recombination of electrons and holes in semiconductors can be found in Refs [215, 254–256].

The spectral line shape $f_{n_L}(\Delta)$ as a function of the normalized detuning $\Delta = \hbar^2 K^2 (m_e^{-1} + m_h^{-1})/(2\nu_c)$ of the recombination frequency from the minimal value for the given Landau level $n_L$ is specified by the pumping and the relaxation of carriers. It seems unlikely that this shape is described by a Lorentzian 'bell'; rather, it should be similar to a blurred Fermi step and should depend on the density of electron–hole pairs and their departure from equilibrium state. The exact shape of this line is not of special interest, because, according to estimates, its width is smaller than the cooperative frequency for all recombination transitions between the corresponding Landau levels of electrons and holes $(0,0), (1,1), \ldots$ (up to $(9,9)$ depending on the pumping level, magnetic field, and temperature) demonstrating superfluorescence pulses.

Pulses were emitted in random directions, but always in the plane of quantum wells, because along them the gain is highest and additional waveguide properties exist which are caused by the presence of electron–hole plasma produced by pumping. The minimal pulse durations and the depletion time of an individual Landau level were $\sim 10$ ps, corresponding to the cooperative length $B_c$ on the order of the laser spot diameter and cooperative frequency $\nu_c \gtrsim 10^{11}$ s$^{-1}$ exceeding, according to estimates, the inverse relaxation time of dipole oscillations of a magnetized electron–hole pair ($T_2 \gtrsim 10$ ps). The pulse-emission delay time fluctuated within their duration from shot to shot, being $\sim 50$ ps for the highest Landau levels and reaching 300 ps for the lowest Landau levels. In this case, each lower $(n_L, n_L)$ transition emitted a pulse at once after the emission of a superfluorescence pulse from the preceding higher $(n_L + 1, n_L + 1)$ transition. This corresponds to a step decrease in the electron and hole Fermi quasilevels near which, as is known [257], the electron–hole recombination rate increases due to the Coulomb interaction of carriers.

In a weak magnetic field $B_0 < 0.4$ T or temperatures above 150 K, superfluorescence was not observed because Landau levels were not spectrally isolated and, for the density of electron–hole pairs $\sim 10^{12}$ cm$^{-2}$ providing the condition $\nu_c > T_2^{-1}$, the width of the inhomogeneously broadened spectral line exceeded the cooperative frequency, i.e., superradiance conditions (23) were not fulfilled. This experiment confirms the general conclusion [3, 198, 215, 258, 259] that in the absence of selection of electromagnetic modes, in particular, in the regime of unidirectional superradiance of continuous-spectrum waves considered here, the superfluorescence of a homogeneous ensemble of inverted active centers with the inhomogeneous broadening of the spectral line exceeding cooperative frequency (18) is impossible. To obtain collective spontaneous emission under these conditions, it is necessary to modify considerably the spectral line of dipole oscillators, for example, to detach a subensemble with the spectral linewidth smaller than the cooperative frequency calculated for the active centers of this subensemble. Another possibility not requiring the spectral line split-off consists in a considerable increase in the transition dipole moment and the spectral density of states in a narrow enough frequency band of inverted active centers, which is smaller than their cooperative frequency. In this case, their enhanced interaction via the self-consistent radiation field can overcome its decay caused by the dephasing of groups of spectrally adjacent active centers, inverted or noninverted.

This possibility was realized in experiments [65] on superfluorescence observed due to collective recombination

of free electrons and holes in a two-dimensional degenerate gas at a frequency determined by the difference between their Fermi quasilevels in 8-nm thick semiconductor quantum wells with the carrier density of $\sim 10^{12}$ cm$^{-2}$ mentioned above.[11] It is for electron–hole pairs formed by carriers with energies close to the corresponding jumps in the Fermi distribution that the Coulomb amplification of the radiative interaction takes place [257]. This provides the increase in the self-consistent field from the level of quantum or thermal noises and leads to the accelerated loss of field-producing electron–hole pairs due to their induced recombination. The Fermi quasilevels of electrons and holes approach each other during this process and the increase in the interaction due to Coulomb correlations is transferred to electron–hole pairs with lower recombination frequencies. For this reason, the total superfluorescence pulse emitted in random directions along quantum wells proves to be rather long (up to 200 ps), its dynamic spectrum shifts to the red (the difference between carrier frequencies at the pulse onset and its end amounts to 10%), and the superfluorescence lifetime at a fixed frequency is rather small (10–50 ps).

We will not further discuss the modification of the spectral line of active centers and only assume it to be smooth, single-scale, and without any specific features, i.e., being close to a Lorentzian or some other similar profile. Consider now the selection of electromagnetic waves involved in collective spontaneous emission, which is possible due to the inhomogeneous distribution of active centers in an extended sample, the matrix structure, or the presence of some boundaries or an electrodynamic system around the sample.

### 4.4 Problems of the physics of exciton superfluorescence

As a rather illustrative and pithy experiment, we consider recent observations in Refs [67, 68] of the signs of superfluorescence of nonequilibrium excitons (electron–hole pairs bound by Coulomb forces) located near 60 triplets of monolayer InAs quantum wells (separated by a pair of 10-nm thick GaAs barriers), which are assembled into a heterostructure with the repetition period $\lambda_0/2 \approx 120$ nm, approximately half the emission wavelength at the exciton recombination frequency ($\hbar\omega_{21\,\min} = 1.47$ eV) in GaAs with $\sqrt{\varepsilon_0} = 3.523$ (at a temperature of 5 K). Carriers in the heterostructure were produced at an initial density of $\sim 3 \times 10^{15}$ cm$^{-2}$ by a femtosecond laser pulse (with the surface energy density up to $w_\mathrm{p} \approx 1.5$ μJ cm$^{-2}$ and photon energy of about 1.54 eV) in a laser spot 150–200 μm in diameter and created excitons that were cooled during a time interval $\lesssim 400$ ps (depending on temperature in the interval of 5–100 K), in particular, due to stimulated scattering. Then, with the delay of $\lesssim 300$ ps (depending on the pumping level and temperature) and the same decay time, the accelerated recombination of electron–hole pairs was observed, which was most distinct for photon escape angles $\alpha = 30-70^\circ$ with respect to the normal to the heterostructure in the energy range $\hbar\tilde{\omega} = (1.475-1.495)$ eV. According to Snell's law, $\sin\alpha = \sqrt{\varepsilon_0}\sin\theta$, these angles correspond to the wave vectors in the structure forming angles $\theta \approx 8-15^\circ$ with the normal. As the angle $\theta$ was changed, the maximum of the emission spectrum approximately followed the Bragg resonance law

$$\hbar\tilde{\omega} \simeq \frac{2\pi\hbar c}{\lambda_0\sqrt{\varepsilon_0 - \sin^2\theta}}\,, \tag{31}$$

and the observed intensity increased superlinearly (approximately as $w_\mathrm{p}^{1.7}$) as pumping increased.

For small angles, $\theta \lesssim 5^\circ$, when $\alpha \lesssim 20^\circ$, superfluorescence was not observed probably because of the presence of a narrow background incoherent luminescence line of the main amount of cooled excitons in the energy range from 1.470 to 1.475 eV.[12] The spectral position of this line was almost independent of the pumping and observation angle, and its intensity linearly increased with increasing pumping and did not exceed the integrated intensity of the higher-energy emission only at the highest temperatures (50–100 K) and the maximum pumping $w_\mathrm{p} \sim 1.5$ μJ cm$^{-2}$. The higher-energy emission was difficult to observe at angles $\theta$ close to the total internal reflection angle $\theta \approx 15-16.5^\circ$, because the reflection coefficient from the heterostructure surface was close to unity, $1 - R \lesssim 0.1$ (for normal incidence, $R \approx 0.56$).

In the absence of information on radiation propagating along quantum wells and detailed data on the spatial and spectral distributions and dynamics of electrons, holes, and excitons, we can only make rather general assumptions about the fulfillment of conditions for the existence and realization of collective electron–hole recombination in experiments. The presence of the large inhomogeneous broadening $2/T_2^* \approx (0.01-0.02)\bar{\omega}_{21}$ (related, in particular, to the motion of particles and the inhomogeneity of the bandgap energy $E_\mathrm{g}$ near quantum wells due to the presence of In and electron–hole pairs at the high density), which is probably not smaller than the cooperative frequency of the exciton ensemble, which can be optimistically estimated as $\nu_\mathrm{c} \sim (10^{-3}-10^{-2})\bar{\omega}_{21}$, and the presence of a much smaller homogeneous broadening $2/T_2 \gtrsim 2/T_1 \sim 10^{-3}\bar{\omega}_{21}$ (mainly nonradiative and depending on the temperature and density of electron–hole pairs) means that superfluorescence should be dynamically determined by the effective cooperative frequency $\bar{\nu}_\mathrm{c} = \nu_\mathrm{c}^2 T_2^*$ and, according to formula (23), can exist in a homogeneous sample for $\bar{\nu}_\mathrm{c} > T_2^{-1}$. According to estimates [67, 68], superfluorescence can be described in the unidirectional approximation, because the Bragg rescattering of counterpropagating waves is almost absent due to a weak spatial modulation of the heterostructure permittivity (even probably taking into account the resonance contribution of the electron–hole plasma and excitons located near quantum wells).

The spectral selection of electromagnetic waves making a coherent contribution to emission at the given angle $\theta$, required for superfluorescence, can be provided [218, 260–

[11] We also mention paper [253] in which the IR emission band about 14 meV in width was observed in the energy interval from 100 to 200 meV at a temperature of $\sim 300$ K upon continuous thermal (current) pumping of $50 \times 50$-μm$^2$ plane samples with 18.5-nm- and 100-nm thick InGaAs quantum wells in AlInAs barrier plates with the carrier density of $1.5 \times 10^{13}$ cm$^{-2}$ and $8 \times 10^{13}$ cm$^{-2}$, respectively. The authors of Ref. [253] interpret this emission as a manifestation of collective spontaneous emission caused by electron–hole recombination with a characteristic time of no less than 100 fs (which was not measured in experiments). This interpretation based on the plasma emission mechanism is far from obvious in the case of an inhomogeneously broadened line observed in experiments (15–30 meV, depending on temperature) and should be verified, in particular, taking into account the features of superradiant lasing discussed in Section 5.

[12] The delay and decay times of this luminescence were 0.5–1 ns and 1–32 ns, respectively (depending on the pumping and temperature), i.e., were two–three times longer than these times for the higher-energy emission. As pointed out below, this luminescence observed across quantum wells can also contain part of the scattered superfluorescence developing along quantum wells.

265] by the periodic arrangement of layers of recombining electron–hole pairs, i.e., quantum wells in the direction across the heterostructure. The nondephasing coherent contribution to collective spontaneous emission in the vicinity of frequency (31) can be made only by electron–hole pairs with recombination frequencies in a narrow interval not exceeding, say, the carrier frequency divided by the quadruple number of the structure periods, $\Delta\omega \lesssim \bar{\omega}_{21}/240$. This frequency interval is only half the observed inhomogeneous broadening and, therefore, is greater than or on the order of the effective cooperative frequency: $\Delta\omega \gtrsim \bar{\nu}_c$. In the case of $\Delta\omega \gg \bar{\nu}_c$, the selection of waves for unidirectional superradiance becomes inefficient and superfluorescence would be suppressed, which allows us to estimate the cooperative frequency of all electron–hole pairs involved in cooperative recombination in the case of its occurrence: $\nu_c \sim (1-5) \times 10^{-3}\bar{\omega}_{21} \simeq (0.2-1) \times 10^{13}\ \mathrm{s}^{-1}$.

The corresponding effective cooperative frequency $\bar{\nu}_c \sim (1-50) \times 10^{-4}\bar{\omega}_{21}$ is higher than or around the experimental nonradiative exciton decay rate $T_1^{-1} \simeq 5 \times 10^{-4}\bar{\omega}_{21}$ and greatly exceeds the radiative decay lifetime $\sim 3 \times 10^{-5}\bar{\omega}_{21}$. Therefore, collective recombination could make the radiative lifetime of excitons subpicosecond (instead of 10–20 ps for an isolated exciton), shorter than or on the order of the nonradiative lifetime $T_1 \sim 1$ ps. However, this can be prevented in fact (within the uncertainty of parameters) by a small thickness of the layer with quantum dots ($B \approx 7.5$ μm) compared to the effective cooperative length $\bar{B}_c = c/(\sqrt{\bar{\varepsilon}_0}\,\bar{\nu}_c) \sim (400-7.5\ \mu)$m, i.e., a small value of the parameter $\bar{L} = B/\bar{B}_c \sim 0.02-1.00$, which elongates a superfluorescence pulse many times compared to the temporal scale $\bar{\nu}^{-1}$. As follows from numerical estimates, a superfluorescence pulse virtually disappears already for $\bar{L} \lesssim 0.3$ and its duration increases to a few picoseconds or more, i.e., up to a value considerably exceeding the maximum admissible duration $\sim T_1$. Therefore, the collective recombination considered is possible only for the maximum values of the indicated cooperative frequencies: $\nu_c \sim 2\bar{\nu}_c \sim 5 \times 10^{-3}\bar{\omega}_{21} \approx 10^{13}\ \mathrm{s}^{-1}$. The equipment available with a time resolution of about 20 ps could not ensure the observation of superfluorescence pulses.

The dynamic times $\gtrsim 100$ ps detected in experiments, which greatly exceed the oscillation relaxation time of an individual exciton, $T_2 \lesssim T_1 \sim 1$ ps, cannot be directly related to collective recombination and are determined first of all by the dynamics of formation, scattering, cooling, and nonradiative decay of excitons, as well as free electrons and holes. However, collective recombination in a certain part of the spectral line can repeat many times if cooled electron–hole pairs arrive rapidly enough, thereby accelerating the incoherent, as a whole, radiative decay of some excitons and the cooling of other excitons, producing a superlinear dependence of the recombination emission intensity on the pumping pulse energy.

The possibility of collective recombination of excitons can also occur due to the development of superfluorescence along quantum wells. Although the cooperative frequency for this process can be half the value of $\nu_c$ presented above, because of the differences in the occupation factors of superradiant modes and the different orientation of the exciton dipole moments in the plane of quantum wells, the decreased effective inhomogeneous broadening $2/T_2^* \lesssim 3 \times 10^{-3}\bar{\omega}_{21}$ and the increased spectral density of states and the dipole moment of the recombination transition in the main low-frequency part of the exciton spectral line and also a long path with electron–hole pairs excited by the pumping (150–200 μm, i.e., $L \sim 10$) can facilitate the proceeding of such a process, despite the presence of the inhomogeneous high-frequency wing of the exciton line and the absence of the superradiant Bragg selection for waveguide or 'diffraction' modes. The duration of a collective recombination event is again restricted by $\sim T_1$, i.e., by several picoseconds. However, due to the rapid arrival of new cooled excitons at the low-frequency part of the exciton line, for example, because of stimulated scattering from the nonequilibrium (heated) portion, the collective recombination events with emission of superfluorescence pulses along quantum wells (as in the event of emission across them considered above) can repeat many times, introducing a contribution, albeit small, to exciton losses with energies of 1.470–1.474 eV at long times ($\sim 1$ ns), as well, until the number of electron–hole pairs produced by pumping pulses capable of populating this low-frequency part of the exciton line is exhausted.

It should be noted that superfluorescence photons propagating along quantum wells can be reabsorbed and thus retained in the heterostructure, whereas photons in the same energy range resonantly scattered or spontaneously emitted during collective recombination in the transverse direction to the wells readily escape and can make a considerable contribution to the intensity of observable long-lived exciton luminescence line. The numerical simulation of this not one-dimensional but, in fact, three-dimensional problem, which also requires consideration of the spatio-temporal dependence of the shift of the bandgap energy $E_g$ proportional to the local carrier density, involves significant difficulties and has not been performed so far.

### 4.5 Superfluorescence simulation in a half-open Fabry–Perot cavity

We assume now that superfluorescence along quantum wells considered in Section 4.4 does not occur for some reason or is excluded by electrodynamic conditions, for example, by the formation of a two-dimensional Bragg grating creating a forbidden band for photons with energies of interest to us.[13] We will demonstrate the typical properties of superfluorescence in the direction across quantum wells using equations (19) at $n_p = 1$ for a one-dimensional layer of inverted dipole oscillators with thickness $B \gg \lambda_0$, having one negligibly weakly reflecting boundary, say, with $R_1 \approx 0.001$, and another boundary reflecting moderately with $R_2 \approx 0.1-0.9$.

For simplicity, we restrict ourselves to the case of a weak inhomogeneous broadening of the spectral line with the high cooperative frequency $\nu_c \gg 1/T_2^* \simeq 2T_2^{-1}$. Then, to obtain superfluorescence (unidirectional in fact, as in the experiment discussed in Section 4.4), no additional electrodynamic mode selection is required (for example, superradiant Bragg selection), whereas such dynamic selection was performed in this experiment. Taking into account this circumstance, we will assume that a layer of initially inverted two-level centers is spatially homogeneous with the occupation factor $\tilde{\Gamma} = 1$ and will use the following typical normalized parameters, which would be characteristic for this experiment in the case of a small inhomogeneous broadening of the exciton line:

[13] The quantum and classical features of collective spontaneous emission of a two-dimensional layer of inverted two-level active centers placed in a planar waveguide with a resonant two-dimensional Bragg structure admitting low-$Q$ (leaky) superradiant modes are considered in Refs [259] and [266], respectively.

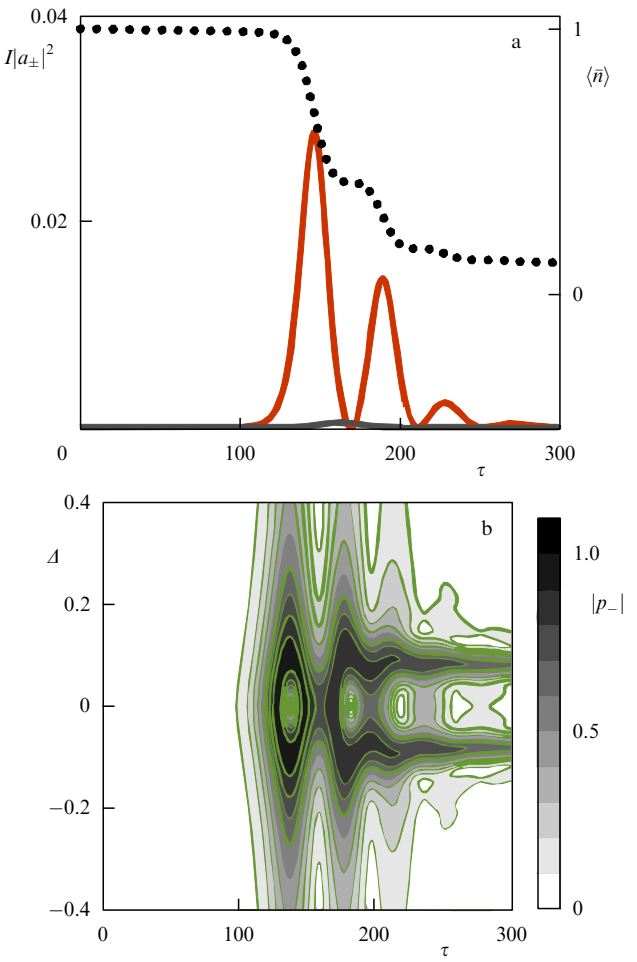


**Figure 5.** (Color online.) Oscillatory superfluorescence of a sample of length $L = 0.56$ in a Fabry–Perot cavity with negligibly weak reflections at one end ($R_1 = 10^{-3}$) and strong reflections at the other end ($R_2 = 0.3$) in the case of very small inhomogeneous spectral line broadening: $\Delta_0 = 0.046$, $\Gamma_2 = 2\Gamma_1 = 0.0026$. (a) Oscillograms of normalized output radiation intensities $I|a_\pm|^2$ (the upper and lower solid curves correspond to $a_-$ and $a_+$, respectively) and the inversion $\langle\bar{n}\rangle$ averaged over the sample (dotted curve). (b) Dynamic polarization spectrum $|p_-(\Delta,\tau)|$ at the facet with negligibly weak reflections.

$I = 10^{-4}$, $L = 0.56$, $R_2 = 0.3$, $\Delta_0 = 0.046$, $\Gamma_2 = 0.0026$, and $\Gamma_1 = 10^{-4}$.

According to calculations (Fig. 5), the wave field and polarization are amplified many times when passing both from the nonreflecting facet to the partially reflecting facet and during the passage back. After the delay time $\tau_d \simeq 150$, they begin to rapidly remove the inversion of active centers, first near the nonreflecting facet of the sample, where the field is maximal, and then also in its central part. Because reflection coefficients $R_1$ and $R_2$ are considerably different (in calculations, $R_2/R_1 = 300$), the intensity of emission escaping from the partially reflecting facet is a few dozen times lower than the emission intensity near the opposite facet, where superfluorescence reoscillations are stronger. In this case, the dynamic spectrum of the field is analogous to the dynamic spectrum of polarization and its width reaches a quarter of the cooperative frequency for the main output pulse with duration $\delta\tau \simeq 20$ (see Fig. 5). By the superfluorescence end time ($\tau \simeq 300$), the inversion averaged over the sample and spectral line remains positive ($\langle\bar{n}\rangle \sim 0.1$), but the mean inversion of the spectral line in the region adjacent to the nonreflecting facet is almost completely lost ($1 + \bar{n} \ll 1$). Therefore, the polarization of active centers in the main part of the inhomogeneously broadened line turns to be close to zero (as in the periods of the maxima of the main pulse and reoscillation pulses). In the half of the sample adjacent to the partially reflecting facet, the inversion expense is small ($\bar{n} \gtrsim 0.5$) and there in the regions of counterpropagating waves with comparable amplitudes ($|a_+| \sim |a_-|$) a noticeable inversion grating appears ($|n_z| \lesssim 0.3$). Nevertheless, it does not significantly change the gain of counterpropagating waves, leads only to weak reflections compared to the value of $R_2$, and does not considerably affect superfluorescence pulses.

The possible change in superfluorescence caused by the DFB of counterpropagating waves in a strongly nonsymmetrical cavity and repeated pulses of collective spontaneous emission upon prolonged pumping of a separated spectral line will be considered in Section 5.

To conclude this rather limited discussion of superfluorescence experiments, we point out the remarkable observation in paper [267] of the so-called superradiant decay of an ensemble of iron nuclei in an $^{57}FeBO_3$ crystal excited by a resonance 5-fs pulse 11-meV wide from a free-electron X-ray laser in the case of Bragg reflection from the $(1, 1, 1)$ plane at the 14,412-eV Mössbauer transition line. The coherent excitation of $N_{nuc} \approx 70$ nuclei with a lifetime of about 100 ns was achieved in experiments and all X-ray photons emitted by nuclei were detected with a time resolution of about 1 ns. In accordance with Dicke [1], the mean time of collective spontaneous emission of the first photon proved to be $N_{nuc}$ times smaller than the mean time of spontaneous emission for one isolated nucleus, and the common time profile of emission of all photons by $N_{nuc}$ nuclei coincides with the spontaneous decay curve for one nucleus.

The measured probabilities of these and other multiphoton observations, say, related to the probability distribution of the arrival time of the second or, for example, tenth photon were successfully reproduced analytically [267] based on simple statistics without the inclusion of the dynamics and propagation effects. The authors of Ref. [267] reasonably assumed that excited nuclei do not interact with each other and emit photons independently and spontaneously, but coherently, because their phase can be controlled by the coherent pumping pulse. In this connection, it is appropriate to repeat that, unlike the phenomenon observed in the given paper, in general the superradiance phenomenon is far from being exhausted by the coherence of emitters, but contains their coherent radiative interactions as the main component, which provides their spontaneous phasing under certain conditions via the self-consistent radiation field. We emphasized this effect in the description of experiments without cavities on unidirectional superfluorescence in this section, and we will discuss it in more detail in Section 5 for a number of problems on superradiance in low-$Q$ cavities using the language of waves and their instability and interactions.

## 5. Superfluorescence of modes upon pulsed pumping and superradiant lasing upon continuous pumping in a low-$Q$ cavity

### 5.1 Hot modes in the case of a homogeneously broadened spectral line

Most experiments on the collective spontaneous emission of ensembles of two-level active centers, as illustrated by

examples presented in Section 4, are related to continuous-spectrum waves and are rather adequately interpreted in the unidirectional approximation taking into account nonlinear effects of radiation propagation in the active medium. This interpretation is mainly based on semiclassical equations like (19) for weakly interacting counterpropagating waves supplied from the same energy reservoir — the inverse population of the energy levels in active centers. An example is the calculation of oscillatory superfluorescence [148] performed for parameters of experiments [189, 190] on the collective spontaneous emission of the gas of inverted $Te_2$ molecules.

However, it has been becoming clear recently that the use of low-$Q$ cavities, which do not really prevent the escape of radiation but often make important the interaction between counterpropagating waves, can considerably loosen requirements on the realization of superradiance and strongly enrich the spectral, temporal, and correlation features of these phenomena (see, for example, Refs [3, 12, 13, 38–40, 43, 48, 88, 108, 110, 114–116, 139, 194, 237]). As a result, the question arises as to the advantages and salient features of the realization of the instability and the superradiant dynamics of discrete hot modes of the field and polarization of the active medium filling a low-$Q$ cavity with a length smaller than or on the order of a few cooperative lengths $B_c$ or $\bar{B}_c$ [cf. formulas (28) and (29)] determined by the cooperative and effective cooperative frequencies (18) and (27) in the cases of homogeneous and inhomogeneous broadening of spectral lines, respectively. These modes in the simplest one-dimensional geometry include inhomogeneous self-consistent counterpropagating waves, which are nonlinearly self-modulated due to the coherent dynamics of two inversion components: smoothly inhomogeneous $n(\zeta, \tau, \Delta)$ and small-scale $n_z(\zeta, \tau, \Delta)$.

At the linear stage of superfluorescence and the initiated superradiance processes, the mode amplitudes increase exponentially in time, $\sim \exp(\omega_m'' t)$, with their growth rates $\omega_m''$ which under certain conditions can be close to the maximum values equal to cooperative frequencies $v_c$ and $\bar{v}_c$ (depending on the type of spectral line broadening). Therefore, discrete modes having the largest growth rates can dominate over continuous-spectrum waves[14] and will be the first to reach the nonlinear stage, ensuring the removal of population inversion in the active medium. Such a process in the case of the homogeneously broadened line was described for an active single-mode waveguide with a small feedback coefficient closed in a circle [3], and was also analyzed in a Fabry–Perot cavity in Refs [43, 195, 236, 237, 268]. It was found that even weak reflections $|R| \gtrsim R_c$, where $R_c$ is determined by the relation

$$\ln R_c^{-1} \sim \frac{\ln (N_0 S B)^{1/4}}{1 + \sqrt{1 + (1/4) \ln (N_0 S B)^{1/4}}}, \qquad (32)$$

at the ends of a cylindrical sample with the Fresnel number $F = S/(\lambda_0 B) \sim 1$ corresponding to the model of a one-dimensional Fabry–Perot cavity, lead to the synchronous emission of counterpropagating superfluorescent waves in the form of discrete modes whose field considerably exceeds the field of continuous-spectrum waves (in most real experiments, $R_c \lesssim 0.1$).

Recall that, according to Eqns (1)–(3), the polariton spectrum of homogeneous plane waves, $\sim \exp(-i\omega t + ikz)$, $\operatorname{Im} k = 0$, in a homogeneous two-level medium with the homogeneously broadened spectral line and homogeneous inversion $n$ contains two waves: an electromagnetic wave and a polarization wave with complex frequencies

$$\omega_{e,p} = \omega_{21} - \frac{i}{T_2} + \frac{1}{2}\left[c_0 k - \omega_{21} + i(T_2^{-1} - 2\pi\tilde{\sigma}_0)\right] \times \left\{1 \pm \left[1 - \frac{4 n v_c^2}{\left[c_0 k - \omega_{21} + i(T_2^{-1} - 2\pi\tilde{\sigma}_0)\right]^2}\right]^{1/2}\right\}. \qquad (33)$$

Standard concepts in laser physics about the induced instability of an electromagnetic wave, $\operatorname{Im}\omega_e > 0$, and the incoherent superluminescence process described by balance equations are related to the case of strong polarization relaxation. In this case, $T_2^{-1} > v_c\sqrt{n} > 2\pi\tilde{\sigma}_0$ (see definitions (4) and (5) and system of equations (19) while ignoring the derivative $\partial p_\pm/\partial\tau$). In the case of weak polarization relaxation of interest to us,[15] when $T_2^{-1} < 2\pi\tilde{\sigma}_0$, the instability takes place (for $2\pi\tilde{\sigma}_0 < n v_c^2 T_2$) only for the polarization wave, $\operatorname{Im}\omega_p > 0$, which has a negative energy and leads to the process of coherent superfluorescence or initiated superradiance. Here, as explained in Refs [3, 125], collective spontaneous emission is the induced emission of the internal energy of active centers under the action of the self-consistent field of the polarization wave.

The above is also valid for polariton modes in a low-$Q$ cavity. In this case, it is necessary, in accordance with the boundary conditions, to take into account the consistence of counterpropagating waves by choosing certain discrete wave numbers and the presence of radiative losses by making the substitution $\tilde{\sigma}_0 \to \tilde{\sigma} = \tilde{\sigma}_0 + \tilde{\sigma}_{rad}$ in formula (33) and in the inequalities presented below [197, 198] (as was indicated in Section 2 in the discussion of the mean field model). For a Fabry–Perot cavity with the reflection coefficients $R_{1,2}$ of the end mirrors, we have $\tilde{\sigma}_{rad} = (c_0/4\pi B)\ln|R_1 R_2|^{-1}$ and frequencies (33) correspond to hot modes, each of them being produced by two inhomogeneous counterpropagating waves. The amplitudes of these waves depend on the coordinate $z$ and exponentially increase $1/\sqrt{|R_1 R_2|}$ times after passage through the sample, while the real parts of wave numbers are described as $k = l\pi/B$, $l = 1, 2, \ldots$. The most unstable mode having the maximum growth rate $\operatorname{Im}\omega_{p l_0} \equiv \omega_{p l_0}''$ is the one with the number $l_0$ giving the value $c_0 k = l_0 \pi c_0/B$ closest to the resonance frequency $(\omega_{21}^2 + T_2^{-2})^{1/2}$ of active centers. For a short inverted sample with $\lambda_0 \ll B \ll B_c$ and $R_c \lesssim |R_{1,2}| \lesssim 1/2$ for $\sqrt{n} v_c \gg T_2^{-1}$ and $2\pi\tilde{\sigma}_0 \ll 2\pi\tilde{\sigma}_{rad} \simeq T_E^{-1} \ll n v_c^2 T_2$, the radiative (dissipative) instability is developed in fact only for this single polariton mode having the growth rate

$$\omega_{p l_0}'' \approx \frac{n v_c^2}{2\pi\tilde{\sigma}_{rad}} - \frac{1}{T_2} \approx n v_c^2 T_E - \frac{1}{T_2}. \qquad (34)$$

[14] The coherent increase in these waves in the inverted medium is restricted from above by the self-similar law $\sim \exp(\sqrt{\omega_c^2 z t/c})$ [230–232] in the case of the homogeneously broadened line and is completely impossible in the case of large inhomogeneous broadening.

[15] Expression (33) and everything said based on it about the instability of a polarization wave and a polariton mode, including expression (34), are also correct for the case of the Lorentzian inhomogeneous line for $1/T_2 \lesssim 1/T_2^* < \sqrt{n} v_c$, if the substitution $T_2^{-1} \to 1/T_2 + 1/T_2^*$ is made everywhere. We will use this below, beginning with expression (46). For $1/T_2^* > \sqrt{n} v_c$, only electromagnetic waves and modes prove to be unstable, and without their special selection superfluorescence and superradiant lasing become problematic.

This directly follows from the characteristic and dispersion equations (24) and (25) and remains qualitatively valid for a combined Fabry–Perot cavity with a small integrated Bragg reflection coefficient $\beta L \equiv \bar{\beta} B \omega_0 / c_0 \lesssim 1$. In particular, the growth rate for this resonance polariton mode is still determined by expression (34) if $\ln |R|^{-1}$ in the expression for the radiative lifetime $T_E$ of a photon (see footnote 5) is replaced by the approximate expression $\ln |R - i\beta L / \ln |R|^{-2}|^{-1}$, where we assume for simplicity that $R_1 = R_2 = R$ (for $|R| \ll \beta L/2$, the replacement $\ln |R|^{-1} \to \ln |\beta L/2|^{-1}$ should be made).

### 5.2 Analytic inversion 'unloading' theory in a Fabry–Perot cavity

The nonlinear stage in the crude adiabatic mean field approximation (with the replacement of the inhomogeneous inversion $n(z, t)$ by the instantaneous value $\langle n(t) \rangle$ averaged over a sample) is described by the solution of equations (19). By disregarding relaxation processes in the medium (for $\Delta_0, \Gamma_1 \lesssim \Gamma_2 \ll 1$) and the inversion grating ($n_z = 0$), this solution represents single-pulse superradiance with the field amplitude $|\mathcal{E}| \propto 1/\cosh [\omega''_{p l_0} (t - t_d)]$, where the growth rate contains the initial inversion $n(t = 0)$. The ratio of the delay time $t_d$ to the pulse duration $\tau \simeq 1/\omega''_{p l_0}$ is a multiple of the logarithm of the ratio between the maximum and initial emission intensities: $t_d \simeq \tau \ln |\mathcal{E}_{max}/\mathcal{E}(t = 0)|$.

In paper [237], a more accurate and general equation was obtained for mode superfluorescence in a Fabry–Perot cavity also by ignoring the spectral line broadening, but taking into account the development of the 'unloading wave' of the inversion of active centers, having a strongly inhomogeneous profile. Approximate analytic solutions show that this 'unloading' begins from the ends of the sample and moves inside it with the velocity determined by the group velocity of inhomogeneous polarization waves. This equation and its solutions are written out in Ref. [237] for a symmetric Fabry–Perot cavity uniformly filled with an active medium ($\tilde{\Gamma} = 1$, $\varepsilon_0 = \text{const}$) and featuring real reflection coefficients ($R_1 = R_2 = R$) for the so-called amplitude $\Theta(t)$ of the Bloch angle $\phi$ represented approximately in the factorized form

$$\phi(t, z) \simeq \Theta(t) \sqrt{\sin^2 \frac{\omega_{21}(z + B/2)}{c_0} + \sinh^2 \frac{(\ln R^{-1}) z}{B}} \qquad (35)$$

for an active sample with a length falling within the limits

$$\frac{\pi c_0}{\omega_{21} R} (1 + \ln R^{-1}) \ll B \lesssim B_c (1 + \ln R^{-1}) , \qquad (36)$$

i.e., many times exceeding the wavelength but smaller than or around the cooperative length. Spatial structure of angle (35) corresponds to the profile of the most unstable polariton mode only at the linear stage of superfluorescence for small $\Theta$.

At the nonlinear stage, the Bloch angle (35) completely describes the inversion structure, $D = \cos \phi$, and determines to a great extent the wavy form of the polarization $\mathcal{P}$ and field $\mathcal{E}$, which no longer correspond to any mode. We will not present here cumbersome expressions for them and only note that, according to the law of conservation of the Bloch vector length and the law of Rabi oscillations, the amplitudes of inhomogeneous polarization and field waves are specified by the quantities $dN_0 \sin \phi$ and $(\hbar/d)\, d\Theta/dt$, respectively. For simplicity, we will present the equation for the evolution of the Bloch angle amplitude 'starting' from a small value $\Theta(0) \ll \sqrt{R}$ (virtually the completely inverted medium) only in the case of predominantly single-pulse superfluorescence:[16]

$$\frac{d\Theta}{d(t v_c)} \simeq - \frac{4}{B_c (R^{-1} - R)} \int_{-B/2}^{B/2} \frac{\partial \cos \phi(t, z)}{\partial \Theta} \, dz . \qquad (37)$$

According to formula (35), the right-hand part of equation (37) considerably depends on the reflection coefficient $R$ and for no value of $R$ is reduced to the function $\sin \Theta$ declared in the mean field model [10, 11, 13, 43, 51, 225, 226, 268]. However, for $R \gtrsim 1/2$, it proves to be close to the Bessel function $J_1(\Theta)$ similar to $\sin \Theta$ and leading to the implicit solution in the form

$$t(\Theta) = \frac{\pi c_0 \ln R^{-1}}{4 v_c^2 B} \int_{\Theta(0)}^{\Theta} \frac{d\Theta'}{J_1(\Theta')} . \qquad (38)$$

The assumption about single-pulse superfluorescence, as in equation (37), means that, according to the right inequality in expression (36), the factor $(\ln R^{-1}) c_0 / B = T_E^{-1}$, equal to the inverse photon lifetime in a cold cavity (see footnote 5), exceeds the cooperative frequency $v_c$, so that the pulse duration is determined by the growth rate of the polariton mode and is described by the expression $\delta t \sim (v_c^2 T_E)^{-1}$. In such a low-$Q$ cavity, even for $R > \exp(-2)$ at which the right-hand side of equation (37) as a function of $\Theta$ still has noticeable oscillations, collective spontaneous emission weakly oscillates and reaches a maximum in the first, main pulse at the Bloch angle amplitude $\Theta = \Theta_d \simeq \pi/2$ corresponding to the delay time $t_d \sim \delta t \ln (N_0 B^2 \lambda_0 R)$.

In the limit of a very low-$Q$ cavity for $R \lesssim \exp(-2)$, the right-hand side of equation (37) is approximately described by the monotonic MacDonald function $K_0(\Theta)$, so that the superfluorescence pulse duration and its delay time $t_d$ increase logarithmically as $\delta \tilde{t} \propto \ln R^{-1}$. The pulse reaches its maximum for lower $\Theta = \tilde{\Theta}_d \simeq \pi R^{1/2}$ and corresponds to the maximum density of the electromagnetic energy flux (from one end) logarithmically dependent on the reflection coefficient:

$$F(t_d) \sim \frac{c_0}{\varepsilon_0} \left( \frac{dN_0 B \omega_{21}}{c_0 \ln R^{-1}} \right)^2 . \qquad (39)$$

Under these conditions, the temporal shape of the field pulse $|\mathcal{E}(t)| \propto d\Theta/dt$, which exponentially increases at the linear stage of superfluorescence for $\Theta(0) \leqslant \Theta \lesssim R^{1/2}\pi/2$, changes to hyperbolically decreasing function $\propto (t - t_i)^{-\alpha_i}$, first with the index $\alpha_1 \lesssim 3/2$ for $\pi R^{1/2} \lesssim \Theta \lesssim 1$ and then with the index $\alpha_2 = 1$. As the reflection coefficient increases for $R_{cr} \lesssim R \lesssim \exp(-2)$, the superfluorescence pulse shape greatly sharpens, and for $R \gtrsim 1/2$, it is almost independent of the reflection coefficient, although, as $R$ approaches unity, the pulse duration continues to decrease, while the superluminesence field continues to increase until the corresponding quantities reach their minimum, $\min(\delta t) \simeq 2/v_c$, and maximum, $\max [F(t_d)/(1 - R_{opt})] \approx \hbar \omega_{21} N_0 c_0 / 3$, values for the *optimal reflection coefficient*, determined by the boundary between the single-pulse and oscillatory regimes, i.e., by the condition $T_E \sim \sqrt{2}/v_c$:

$$\ln R_{opt}^{-1} \sim \frac{B v_c}{\sqrt{2} c_0} \equiv \frac{B}{\sqrt{2} B_c} . \qquad (40)$$

[16] Excluding high-$Q$ cavities in which oscillatory superradiance is possible [114, 126, 194, 225, 226, 237].

If, along with the single-pulse superfluorescence regime, the oscillatory regime is taken into account, the universal estimate of the maximum density of the electromagnetic energy flux in the first, main pulse takes the form [17] [237]

$$F(t_{\rm d}) \sim \frac{c_0(1-R)}{\varepsilon_0} \frac{(dD_0N_0B\omega_{21}/c_0)^2}{(\ln R^{-1})^2 + \left[B/(2B_{\rm c})\right]^2}\,, \qquad (41)$$

where the possibility of incomplete initial inversion of active centers, $D_0 \lesssim 1$, is also taken into account. It follows from the above consideration that the use of weakly reflecting mirrors with reflection coefficients $R_{\rm cr} \lesssim R \lesssim R_{\rm opt}$ for short samples of length $B \lesssim B_{\rm c}$ considerably increases the superfluorescence intensity and reduces its duration compared to its intensity and duration in the unidirectional regime in the absence of mirrors. The produced multimode superfluorescence cannot be described by the mean field model and is single-pulse, unlike unidirectional superfluorescence of the oscillatory self-similar type. For very short samples with $B \ll B_{\rm c}$, i.e., for $L \ll 1$, the employment of mirrors with the optimal reflection coefficient $R \sim R_{\rm opt} \simeq \exp(-L/\sqrt{2}) \simeq 1 - L/\sqrt{2}$ transforms unidirectional superfluorescence into almost single-mode, as predicted by the mean field model, and gives the limiting pulse intensity and duration, which can be achieved in the unidirectional regime (without mirrors) only in long samples with $B \sim 2B_{\rm c}$ (for the same parameters of the active medium).

Even for a sample with the *optimal length* (at $n \sim 1$) $B \sim 2B_{\rm c}$, i.e., $L \sim 2$, the use of an open Fabry–Perot cavity with the mirror reflection coefficients $R \sim R_{\rm opt} \simeq 0.3$ can weaken oscillations and make the superfluorescence pulse more compressed and more powerful. This is demonstrated in Fig. 6 for the case of $L = 2$, $R = 0.37$, in which the Rabi frequency of the pulse field in the pulse maximum region is on the order of the cooperative frequency, $\sqrt{I}|a_\pm| \sim 1$, the pulse spectrum width is close to the double cooperative frequency, $\delta\tilde{\omega} \sim 2\nu_{\rm c}$, and its duration is about three inverse cooperative frequencies, $\delta t \approx 2\pi/\delta\tilde{\omega} \sim 3\nu_{\rm c}^{-1}$. Numerical calculations confirm that on such short time scales neither the appearance of a self-consistent inversion grating nor the presence of pumping with $\Gamma_1 \lesssim 0.01$ at $n_{\rm p} = 1$ affect the shape of the superfluorescence pulse or the inversion evolution in the sample (lasing in this case is demonstrated in Fig. 13 in Section 5.6).

Notice that, to completely realize the advantages of mode superradiance, the reflection coefficients of the sample ends need not necessarily be the same, but both should have values close to optimal. If the reflection coefficient of one of the ends is too small, as in the numerical example in Fig. 5, where $R_1 = 0.001 < R_{\rm cr}$ and $R_2 = 0.3 \approx R_{\rm opt}/2$, superfluorescence will not differ much from unidirectional, and the pulse duration will exceed by many times the cooperative frequency, even in the case of $L \sim 2$, and even more so for $L \ll 1$.

### 5.3 Low-$Q$ cavity with distributed feedback of waves

The presence of a low-$Q$ cavity required for improving the mode superfluorescence can be provided by the resonance DFB of counterpropagating electromagnetic waves (for simplicity, we assume here that the parameter $\beta$ is real). In the simplest case of weak integral Bragg reflection with the coefficient $\tanh\beta L < 1/2$, the DFB can replace the local coupling of wave amplitudes due to reflections from the sample ends, which will lead to the same photon lifetime $T_{\rm E} \approx B/\{c_0 \ln[1 + \pi/(\beta L)]\}$ as in a Fabry–Perot cavity, $T_{\rm E} \approx B/(c_0 \ln|R_1R_2|^{-1/2})$, if the Bragg wave coupling coefficient, i.e., the DFB coefficient, satisfies the condition $\beta \simeq \pi\sqrt{|R_1R_2|}/L \lesssim 1/L$. As a result, general qualitative conclusions about mode superfluorescence made in Sections 5.1 and 5.2 for an open Fabry–Perot cavity can also be applied to a great extent to an open purely Bragg cavity, despite the absence of the corresponding detailed analytic nonlinear theory of inversion 'unloading' in the active medium of the cavity.

However, it is important that for short samples with $L \ll 1$, the creation of a Bragg cavity providing the maximum superfluorescence pulse intensity and the minimal pulse

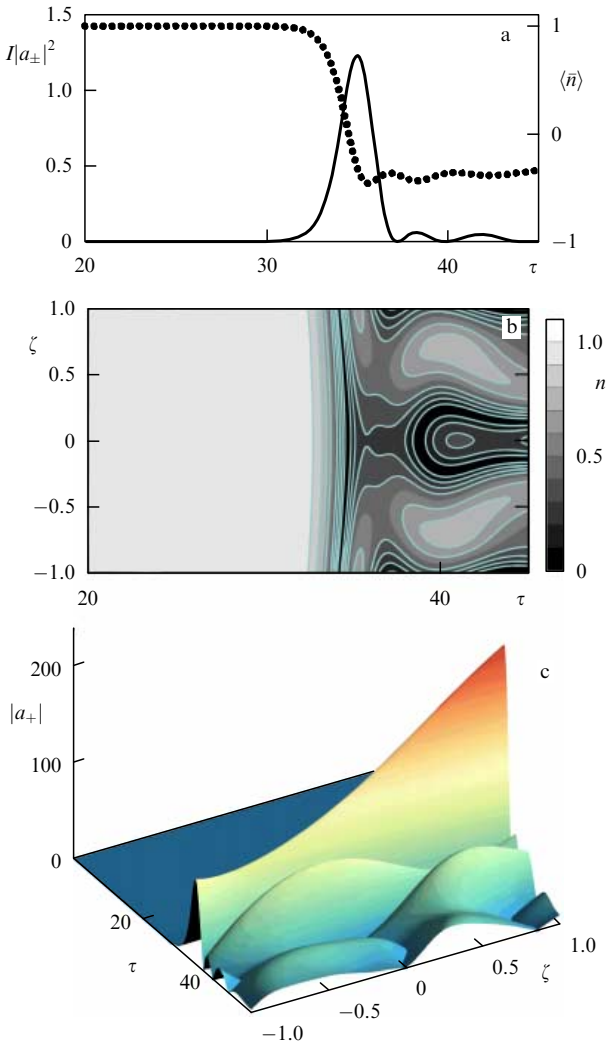


**Figure 6.** (Color online.) Superfluorescence of a sample of length $L = 2$ in a Fabry–Perot cavity with moderate reflection at laser ends ($R = 0.37$) in the case of slow continuous pumping ($n_{\rm p} = 1$) and a homogeneously broadened spectral line: $\Gamma_2 = 2\Gamma_1 = 0.02 \gg \Delta_0 = 0.002$. (a) Oscillograms of the normalized output radiation intensity $I|a_\pm|^2$ and the inversion $\langle\bar{n}\rangle$ averaged over the sample (dotted curve). (b) Spatio-temporal evolution of the inversion $n(\zeta,\tau)$ over the sample. (c) Spatio-temporal evolution of the amplitude $|a_+(\zeta,\tau)|$ of the wave running to the right.

[17] The inversion grating $n_z$ produced by the first pulse plays a secondary role for the pulse itself, but can considerably affect the next pulses generated by the active medium in a low-$Q$ cavity (Fabry–Perot, Bragg, or combined). We will consider this question in Sections 5.6 and 5.7 in the case of continuous pumping, i.e., for superradiant lasers, where it is of special interest.

duration ($\gtrsim v_c^{-1}$), similarly to condition (40), where $R_{opt} \sim \exp(-L/\sqrt{2})$ is close to unity, requires that the integrated reflection coefficient $\tanh \beta L$ be close to unity (and, therefore, the parameter $\beta L \gg 1$) and the photonic bandgap be large. The latter has a width of $2\beta v_c \gg v_c/L = c_0/B \gg T_2^{-1}$, and collective spontaneous emission in it is impossible. Therefore, based on the mean field model (see Section 2), the effective mode superfluorescence can naturally be related to cold modes at the edge of this forbidden band, for which the normalized complex frequency detuning $\Omega_E = (\tilde{\omega} - \omega_0)/v_c$ satisfies the equation [199]

$$\Omega_E^2 = \kappa^2 + \beta^2, \qquad \kappa \equiv \frac{(k-k_0)c_0}{v_c} \simeq \frac{\pi m}{L}\left(1 - \frac{i}{\beta L}\right), \qquad m = \pm 1, \pm 2, \ldots, \pm \bar{M} \lesssim \frac{\beta L}{\pi}, \tag{42}$$

and photon lifetimes are described by the expression

$$T_{Em} \simeq \left(\frac{\beta L}{\pi m}\right)^2 \frac{B}{c_0} \gtrsim \frac{B}{c_0}, \quad \beta L \gg 1. \tag{43}$$

Under these conditions, low-$Q$ modes with $T_{Em}^{-1} \gtrsim v_c$ required for single-pulse superfluorescence have numbers $|m| \gtrsim \beta L\sqrt{L}/\pi$ and, in particular, the first mode is a low-$Q$ one for $\beta L \lesssim \pi/\sqrt{L}$. By tuning the spectral line, for example, to this first mode, setting $|\Phi| \simeq B[1 + (\pi/\beta L)^2/2]$, and choosing the optimal Bragg coupling $\beta_{opt}$ for counterpropagating waves, from condition $T_{E1} \sim \sqrt{2}/v_c$ (40), i.e.,

$$\beta_{opt} \sim \frac{\pi}{L}\sqrt{\frac{\sqrt{2}}{L}}, \tag{44}$$

then, due to the spontaneous growth of the most unstable hot polariton mode, we can again obtain, in fact, single-pulse superfluorescence with the ultimate pulse intensity and minimum pulse duration ($\sim v_c^{-1}$) without considerable oscillations, because the adjacent electromagnetic mode of the cold cavity is detuned under condition (44) by a frequency exceeding the cooperative frequency: $|\Omega_{E2} - \Omega_{E1}| \simeq 3\pi^2/(2\beta L^2) \sim \pi/\sqrt{L} > 1$.

Everywhere below, except in one example of 'exotic' multimode superradiant lasing presented in Section 5.8 in Fig. 20, we will consider only weak Bragg reflections with $\beta L \lesssim \pi$ leveling the inhomogeneity of counterpropagating waves along the active sample but not especially preventing the appearance of collective spontaneous emission. In particular, for an active sample, with the optimal length $L \sim 2$, the value of $\beta \sim 1$ corresponds to the best DFB level providing the most rapid and powerful single-pulse superfluorescence. In this case, when the Bragg resonance is tuned to the spectral line center ($\Phi = 0$), the photonic bandgap is not formed yet, as for $\beta L \gg 1$, and Bragg rescattering does not prevent but, on the contrary, facilitates the formation of a high-power superfluorescence pulse. The corresponding example at $\beta L = 2$ is presented in Fig. 7, where all the time and spectral scales of the inversion dynamics of active centers and the evolution of the emitted field differ by no more than two–three times[18] from those for superfluorescence in an open Fabry–Perot cavity ($R = 0.37$) with the same active sample and the same photon lifetime $T_E = 2/v_c$, equal for

[18] Frequency detunings $\Omega'_{1,2}$ and growth rates $\Omega''_{1,2}$ differ two–three times for two unstable polariton modes responsible for superfluorescence in two compared cases.

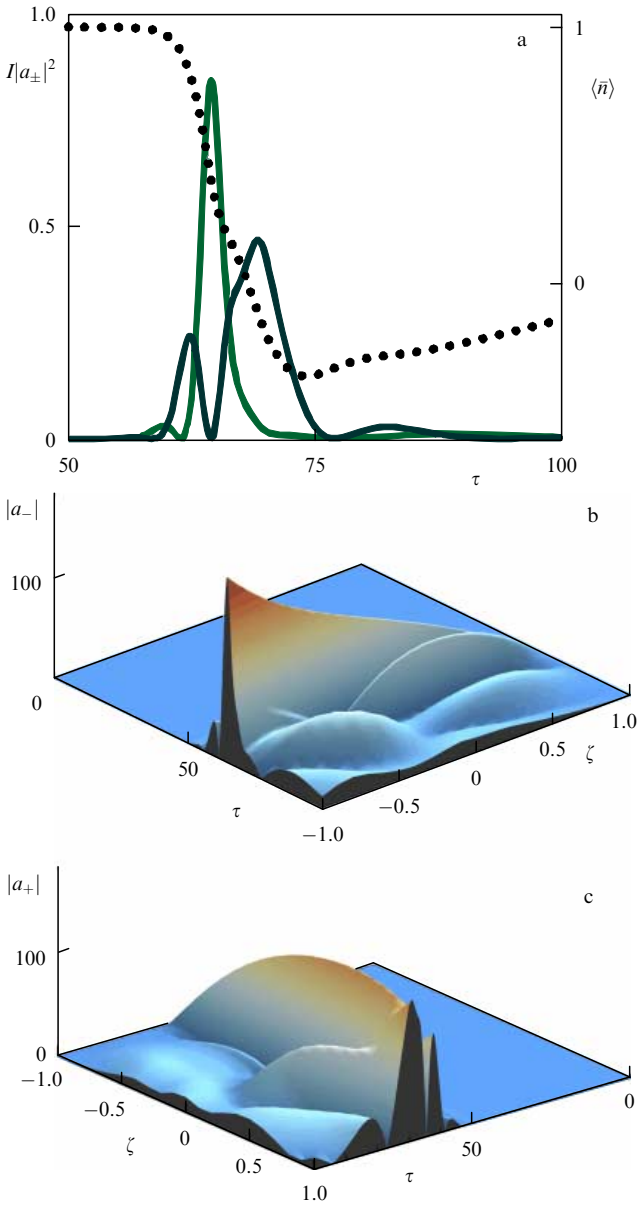


**Figure 7.** (Color online.) Superfluorescence of a sample of length $L = 2$ in a Bragg cavity with the DFB coefficient $\beta = 1$ in the case of weak continuous pumping ($n_p = 1$) and a homogeneously broadened spectral line: $\Gamma_2 = 2\Gamma_1 = 0.02 \gg \Delta_0 = 0.002$, $\Phi = 0$. (a) Oscillograms of the normalized output radiation intensity $I|a_\pm|^2$ (the upper and lower solid curves correspond to $a_-$ and $a_+$, respectively) and the inversion $\langle\bar{n}\rangle$ averaged over the sample (dotted curve). (b, c) Spatio-temporal evolution of the amplitudes $|a_-(\zeta,\tau)|$ and $|a_+(\zeta,\tau)|$ of a wave running to the left and right, respectively.

chosen Fabry–Perot and Bragg cavities (see Fig. 6). Two of a few qualitative differences caused by the DFB are the larger homogeneity of each of the counterpropagating waves of the field during main superfluorescence emission and the more noticeable difference between pulses escaping from opposite ends of the sample, which experience a different action of the self-consistent inversion grating.

The introduction of a moderate DFB leveling the inhomogeneous profile of partial waves forming an unstable mode responsible for superfluorescence improves, as a rule, the characteristics of the pulse that would be emitted without application of the wave feedback by increasing its energy and power, decreasing the pulse duration and delay time and

suppressing reoscillations after the main pulse. Thus, if we apply a rather weak resonance DFB[19] with $\beta = 0.9$ at $\Phi = 0$ in the example of unidirectional superfluorescence of an active sample of length $L = 0.56$ in a strongly asymmetric Fabry–Perot cavity with $R_1 = 0.001$ and $R_2 = 0.3 \sim R_{\rm opt}$, where $T_{\rm E} = 0.135/v_{\rm c}$ (see Fig. 5 in Section 4.5), the mode superfluorescence pulse power (Fig. 8a) will increase 2.5 times and its duration $\delta\tau$ decrease from $\approx 20$ to $\approx 10$ (i.e., will become only three times longer than the minimal pulse duration in a symmetric Fabry–Perot cavity with $R_1 = R_2 = R_{\rm opt}$). In this case, the intensities of output pulses from the opposite ends of the sample differ only two times (rather than a few dozen times, as in Fig. 5a), because the field and polarization in the sample become more homogeneous and inversion, as a whole, is removed more completely. As is seen from the dynamic spectrum of one of the polarization components $p_-(\tau, \Delta)$ taken at the virtually nonreflecting end of the sample (Fig. 8b), active centers in the main part of the inhomogeneously broadened line $|\Delta| \lesssim \Delta_0$ completely give to the superfluorescence pulse all their energy stored on the upper energy level, and therefore their dipole oscillations are absent (cf. Fig. 5b in which the spectral band with polarization close to zero, $p(\tau, \Delta \simeq 0)$, is narrower and dipole oscillations in this band appear again after the reabsorption of repeated pulses). Outside this spectral band, the number of active centers is small, but they give information on the spectrum of the emitted rapid superfluorescence pulse covering a broader frequency region in Fig. 8b than that in Fig. 5b and leaving the memory about itself in free dipole oscillations with long lifetimes $\sim T_2 = 500/v_{\rm c}$.

### 5.4 Superfluorescence in a combined cavity in the case of a moderately inhomogeneously broadened spectral line

Consider now the problem of exploiting low-$Q$ cavities to *overcome inhomogeneous spectral line broadening*, which is one of the main obstacles in the way of obtaining intense collective spontaneous emission.[20] As noted, an increase in the density of active centers, which is natural for heightening the cooperative frequency [see formulas (4) and (18)] and emission power and, therefore, for shortening the superfluorescence pulse duration, usually enhances some incoherent interactions of dipole oscillators and leads to dispersion in their partial oscillation frequencies preventing superradiance. Thus, if we raise the inhomogeneous broadening several-fold in the example considered at the end of Section 5.3 (see Fig. 8), taking, for example, $\Delta_0 = 0.25$, superfluorescence in the unidirectional regime without the DFB will be virtually impossible in a short sample with length $L = 0.56$ and $T_{\rm E} = 0.135/v_{\rm c}$.

However, one can see from Fig. 9 that the presence of a moderate DFB with $\beta L = 0.5$ increasing the photon lifetime by 2.5 times in a low-$Q$ cavity ($T_{\rm E} = 0.32/v_{\rm c}$) preserves superfluorescence, although an order of magnitude weaker. The DFB also ensures the existence of an unstable hot polariton mode for any position of the spectral line in the region of a weakly manifested photonic bandgap $\sim 2\beta = 1.8$

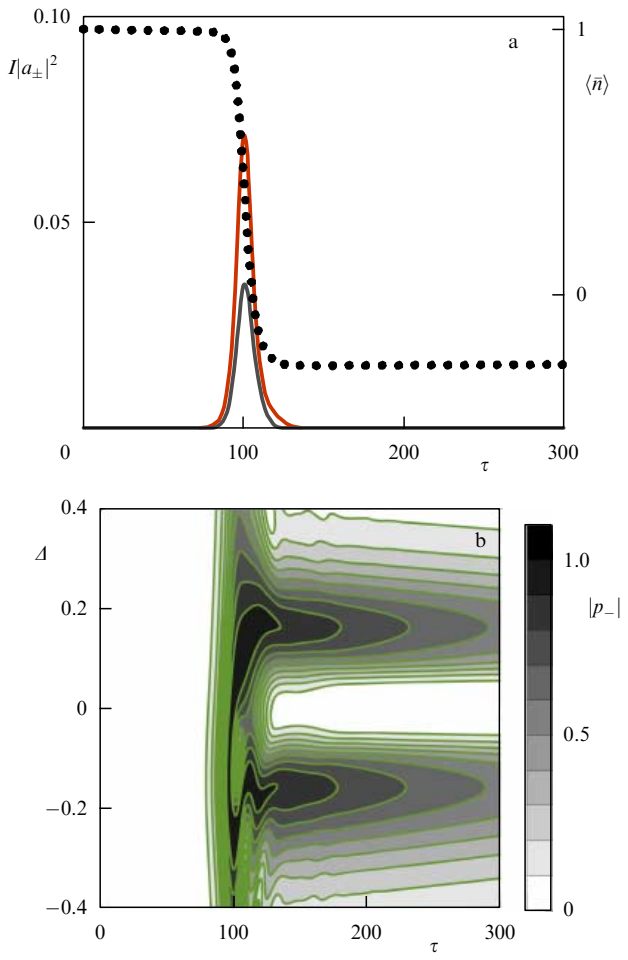


**Figure 8.** (Color online.) Superfluorescence of a sample of length $L = 0.56$ in a combined Fabry–Perot cavity with negligibly weak reflections at one end ($R_1 = 10^{-3}$) and strong reflections at the other end ($R_2 = 0.3$) with the DFB coefficient $\beta = 0.9$ in the case of very small inhomogeneous spectral line broadening: $\Delta_0 = 0.046$, $\Gamma_2 = 0.0026$, $\Gamma_1 = 0.001$, $\Phi = 0$. (a) Oscillograms of normalized output radiation intensities $I|a_\pm|^2$ (the upper and lower solid curves correspond to $a_-$ and $a_+$, respectively) and the inversion $\langle\bar{n}\rangle$ averaged over the sample (dotted curve). (b) Dynamic polarization spectrum $|p_-(\Delta, \tau)|$ at the end with negligibly weak reflections.

in width. For the parameters chosen, the growth rate of this mode $\omega''/v_{\rm c} \sim 0.1-0.2$ (depending on the value of $|\Phi| \lesssim \beta$) exceeds the homogeneous spectral line width $2\Gamma_2$ by several dozen times, providing distinct superfluorescence, but at the same time this growth rate is several times smaller than the cooperative frequency and the inhomogeneous linewidth $2\Delta_0$, which leads to the long pulse duration ($\delta\tau \approx 20$ in Fig. 9a). As a result, only a small fraction of active centers in the central part of the line ($|\Delta| \lesssim 0.1$, Fig. 9b) are involved in superfluorescence, whereas others do not emit the stored energy, which makes the level of the residual mean inversion high in the sample ($\langle\bar{n}\rangle \simeq 0.8$) and the delay time long[21] ($\tau_{\rm d} \simeq 180$).

The general analysis of mode instability for not too large Lorentzian inhomogeneous spectral line broadening, when $1/T_2 \ll 1/T_2^* \lesssim v_{\rm c}$, i.e., $\Gamma_2 \ll \Delta_0 \lesssim 1$, is identical to that

[19] An order of magnitude smaller than the optimal DFB (44) for $\Phi \approx 10$, but nonetheless providing the integrated reflection coefficient $\beta L = 0.5 \approx R_{\rm opt} = \exp(-L/\sqrt{2})$, and the 2.5 times longer photon lifetime $T_{\rm E} = 0.32/v_{\rm c}$.

[20] Theoretical and experimental studies of superfluorescence of spin ensembles with the large inhomogeneous broadening of spectral lines, in particular, in the presence of a cavity, are considered in Refs [269–271].

[21] However, due to general distributed reflection of counterpropagating waves ($|a_+| \sim |a_-|$), a pulse escaping through the partially reflecting facet of the sample becomes quite comparable to a similar pulse in the unidirectional superfluorescence regime without the DFB for a very small inhomogeneous broadening $\Delta_0 = 0.046$ (Fig. 5a).

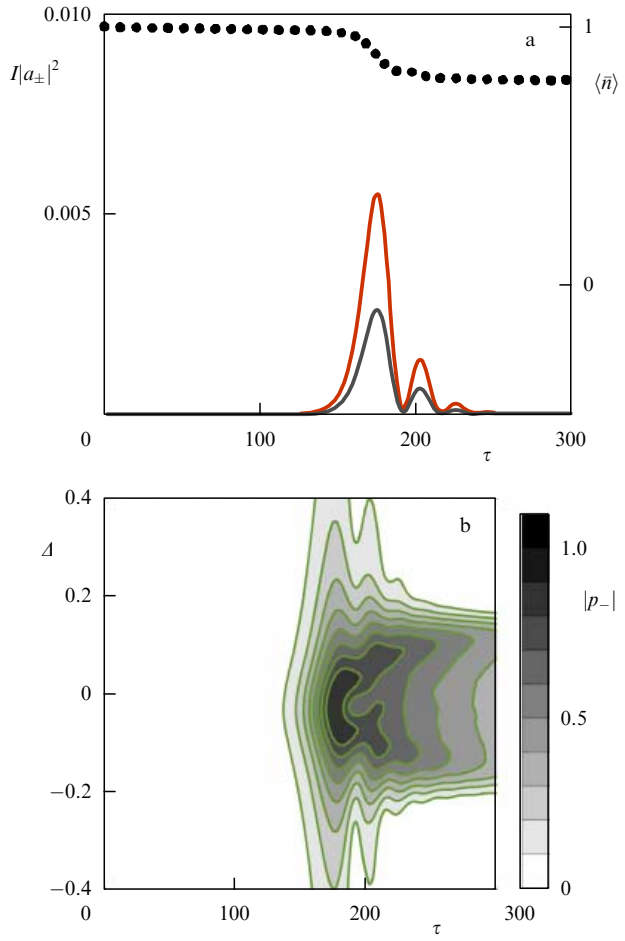


**Figure 9.** (Color online.) Restricted superfluorescence of a sample of length $L = 0.56$ in a combined Fabry–Perot cavity with negligibly weak reflections at one end ($R_1 = 10^{-3}$) and strong reflections at the other end ($R_2 = 0.3$) for the DFB coefficient $\beta = 0.9$ in the case of inhomogeneous spectral line broadening: $\Delta_0 = 0.25 \gg \Gamma_2 = 0.0026$, $\Gamma_1 = 0.001$, $\Phi = 1$. (a) Oscillograms of normalized output radiation intensities $I|a_\pm|^2$ (the upper and lower solid curves correspond to $a_-$ and $a_+$, respectively) and the inversion $\langle\bar{n}\rangle$ averaged over the spectral line and the sample (dotted curve). (b) Dynamic polarization spectrum $|p_-(\Delta,\tau)|$ at the end with negligibly weak reflections.

presented after expression (33) in the case of homogeneous broadening with the substitution $1/T_2 \to 1/T_2 + 1/T_2^* \simeq 1/T_2^*$ in expressions indicated there (see Refs [197, 198]). By excluding samples that are too long (28) and of no interest for mode superfluorescence, we will consider only comparatively short open active samples in a symmetric low-$Q$ combined cavity with $R_1 = R_2 = R$ and $\beta L \sim 1$ and with the comparatively short photon lifetime

$$T_E \simeq \frac{B/c_0}{\ln\left|R - i\beta L/\ln|R|^{-2}\right|^{-1}} \lesssim \frac{1}{\sqrt{n}v_c}\,. \qquad (45)$$

Then, the existence of mode superfluorescence is provided by the presence of an unstable resonant polariton mode with the growth rate exceeding the relaxation rate of individual dipole oscillations of active centers:

$$\omega''_{pl_0} \simeq nv_c^2 T_E - \frac{1}{T_2^*} > \frac{1}{T_2}\,. \qquad (46)$$

This requirement represented in the form $nv_c^2 T_E \gtrsim 1/T_2 + 1/T_2^*$ coincides, in fact, with the earlier-used condition (22) of emerging mode superradiance. Under these conditions, which can be reduced as a whole to the form

$$\Gamma_2 + \Delta_0 < \frac{n}{\Gamma_E} \simeq \frac{nL}{\ln\left|R - i\beta L/\ln|R|^{-2}\right|^{-1}} \lesssim \sqrt{n}\,, \qquad (47)$$

mode superfluorescence has the single-pulse character (with the pulse duration $\sim 1/\omega''_{pl_0}$) and is developed only when the inhomogeneous line broadening $\Delta_0 = (v_c T_2^*)^{-1}$ does not exceed the value on the order of the normalized length $L = Bv_c/c_0$ of the sample. In this case, most of the active centers will be involved in collective spontaneous emission only if the growth rate exceeds not only homogeneous but also inhomogeneous broadening, i.e., when inequality (46) is enhanced to $\omega''_{pl_0} > 1/T_2^*$ and, consequently, in fact the left-hand side of inequality (47) is doubled:

$$2\Delta_0 < nv_c T_E \simeq \frac{nL}{\ln\left|R - i\beta L/\ln|R|^{-2}\right|^{-1}} \lesssim \sqrt{n}\,. \qquad (48)$$

Otherwise, mode superfluorescence cannot be strong and will lead in the best case to the formation of a narrow dip of width $\sim \omega''_{pl_0} < 1/T_2^*$ in the inversion spectrum $n(\Delta)$, as shown in the example in Fig. 9.

For an active sample with the optimal length $L \sim 2$ (for $n \sim 1$), the efficient superfluorescence related to the radiative instability of polariton modes is possible even for inhomogeneous broadening on the order of the cooperative frequency, when $\Gamma_2 \ll \Delta_0 \sim 1$. Figure 10 shows the example for a purely Bragg cavity with $\Phi = 0$ and the photon lifetime $T_E = 2/v_c$ for the two highest-$Q$ cold modes, which is the same as in Figs 6 and 7 where the inhomogeneous broadening is negligibly small ($\Delta_0 = 0.002$). Compared to single-pulse superfluorescence in Fig. 7, the superfluorescence demonstrated in Fig. 10 is an order of magnitude weaker in intensity, slightly delayed in development, much longer, and more oscillatory. At first glance, it represents the spatially inhomogeneous (Fig. 10b) and symmetric (with respect to the cavity center) (Fig. 10b) beats of two initial unstable polariton modes with large growth rates[22] ($\sim v_c/3$) and symmetric frequency detunings from the Bragg resonance ($\sim \pm v_c/3$) and two nonadiabatically excited by them electromagnetic modes with the same wave numbers but with larger frequency detunings from the Bragg resonance ($\sim \pm v_c$) (see also the discussion of Fig. 19 in Section 5.7). In this case, the emission of active centers in the central part of the spectral line was very weak, as in the central part of the sample, where the field of collective spontaneous emission is considerably weaker (Figs 10b, c). As a whole, superfluorescence carried away only 1/5 of the energy stored in the sample, rather than 2/3, as in the case of the homogeneous broadening shown in Fig. 7. The spontaneous symmetry breaking caused by the difference between counterpropagating waves became less manifested, in particular, due to the more symmetric and uniform action

[22] In the case of the homogeneous spectral line broadening shown in Fig. 7, the growth rates of two such polariton modes responsible for superfluorescence were approximately three times smaller. However, due to the higher power and, hence, the higher Rabi frequency of the collective spontaneous emission field, its resulting spectrum had the width on the order of the cooperative frequency and overlapped all the photonic bandgap of the Bragg resonance of width $\sim \beta = 1$.

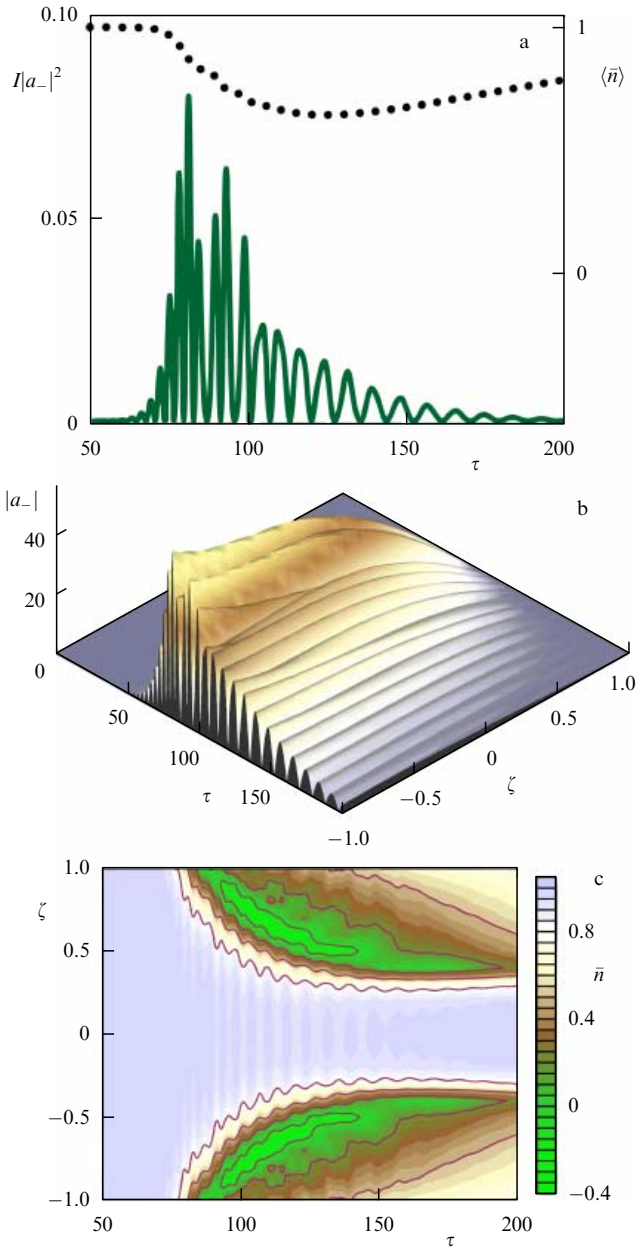


**Figure 10.** (Color online.) Oscillatory superfluorescence of a sample of length $L = 2$ in a Bragg cavity with the DFB coefficient $\beta = 1$ in the case of weak continuous pumping ($n_p = 1$) and inhomogeneous spectral line broadening: $\Delta_0 = 1 \gg \Gamma_2 = 2\Gamma_1 = 0.02$. (a) Oscillograms of the normalized output radiation intensity $I|a_-|^2$ (solid curve) and the inversion $\langle\bar{n}\rangle$ averaged over the spectral line and sample (dotted curve). (b) Spatio-temporal evolution of the amplitude $|a_-(\zeta,\tau)|$ of the wave running to the left. (c) Spatio-temporal evolution of the inversion $\bar{n}(\zeta,\tau)$ averaged over the spectral line.

of a self-consistent inversion grating appearing at the initial, nonlinear superfluorescence stage and leveling the amplification asymmetry of counterpropagating waves due to its spectral alternation and efficient averaging over the spectrum during the formation of output emission pulses.

### 5.5 Superfluorescence in the case of a strongly inhomogeneously broadened spectral line

In the case of the large inhomogeneous broadening of a spectral line $\Delta_0 \gtrsim 1 \gg \Gamma_2$, the most important property of a low-$Q$ Bragg cavity with $\beta L \sim 1$ or a related combined cavity (in the case of finite reflections $R$ from the ends of a sample) for obtaining superfluorescence is a possibility of creation and control of the considerable difference between the growth rates of the most unstable modes via line tuning to the Bragg resonance, when $|\Phi| \lesssim \Delta_0$. The point is that for $\Delta_0 \gtrsim 1$, as mentioned above, superfluorescence is impossible in the unidirectional regime, and for obtaining it a mode selection is required, which suppresses the interaction of electromagnetic waves with some of the active centers in certain intervals of their partial frequencies and enhances this interaction in other spectral parts of the inhomogeneously broadened line.

By excluding cavities that are too long and of no interest for mode superradiance and satisfy condition (29), we consider only low-$Q$ cavities with rather short photon lifetimes restricted by the same inequality (45), but making the substitution $v_c \to \bar{v}_c\sqrt{n}$:

$$T_E \lesssim \frac{1}{n\bar{v}_c} < T_2\,. \tag{49}$$

Then, the mode selection preventing the dephasing of dipole oscillations of active centers during collective spontaneous emission is optimal if, for spectral regions with enhanced interaction with the electromagnetic field, the formally calculated cooperative frequency (see formula (4) or (18)) of active centers from a separated spectral region singled out by a particular cold mode will be about the relaxation rate $T_E^{-1}$ of this mode and will considerably exceed the relaxation rate $T_2^{-1}$ of their individual dipole oscillations. In other words, the growth rate of the corresponding resonance hot electromagnetic mode, which has the form (33)

$$\omega''_{el_0} = nv_c^2 T_2^* - 2\pi\tilde{\sigma} \equiv n\bar{v}_c - T_E^{-1}\,, \tag{50}$$

should be on the order of the relaxation rate $T_E^{-1}$ of the initial cold mode, which, taking into account the inequality $T_E < T_2$, gives

$$2\Delta_0 \sim nv_c T_E \simeq \frac{nL}{\ln\left|R - i\beta L/\ln|R|^{-2}\right|^{-1}} \tag{51}$$

(cf. formula (48)), and then mode superfluorescence will be maximally fast and powerful.

However, for extended samples with the *optimal length on the order of the effective cooperative length* $B \sim 2\bar{B}_c = 2c_0/\bar{v}_c$ (i.e., $L \sim 2\Delta_0$ for $n \sim 1$), required in the latter case, a great number of modes $\sim \Delta_0^2$ will be excited in a Fabry–Perot cavity without the frequency dispersion. Therefore, without taking special precautions, a superfluorescence pulse will be a superposition of the same number of incoherent random emission pulses of separate modes, i.e., it will be referred to the quasichaotic type with a broad spectrum.

Figure 11 demonstrates the spectrum of such low-coherence superfluorescence pulse with duration $\delta\tau \sim 50$ and delay time $\tau_d \sim 100$ for a sample with length $L = 2.5\Delta_0 = 10$ placed into an open Fabry–Perot cavity with $R = 0.15$ and the photon lifetime $T_E \simeq 5.5/v_c$. We see that the superfluorescence of inhomogeneously broadened line is caused by approximately ten equidistant electromagnetic modes with comparable amplitudes and growth rates $\omega''_e \leqslant 0.06v_c \simeq \bar{v}_c/4$. By the way, returning to Fig. 4, we see that, in the presence of continuous pumping due to the nonlinear interaction of modes in a similar sample with even two thirds of the reflection coefficients of the ends, a greater

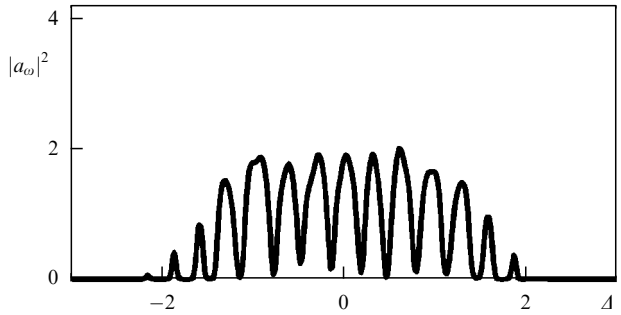


**Figure 11.** Low-coherence superfluorescence spectrum of a sample of length $L = 10$ in a Fabry–Perot cavity with weak reflections at the ends, $R = 0.15$, in the case of large inhomogeneous spectral line broadening: $\Delta_0 = 4 \gg \Gamma_2 = 10\Gamma_1 = 0.02$.

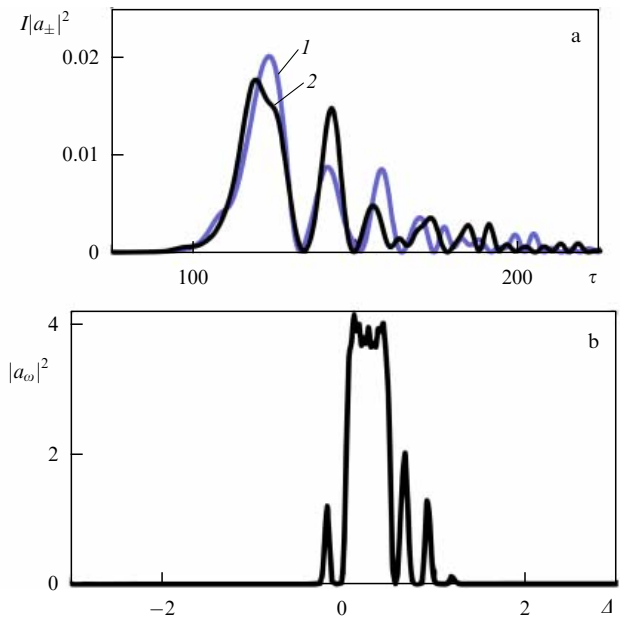


**Figure 12.** Oscillatory superfluorescence of a sample with length $L = 10$ in a combined Fabry–Perot cavity with small reflection coefficients $R = 0.1$ at the ends and the DFB coefficient $\beta = 0.06$ in the case of large inhomogeneous spectral line broadening: $\Delta_0 = 4 \gg \Gamma_2 = 10\Gamma_1 = 0.02$, $\Phi = 0$. (a) Oscillograms of normalized output radiation intensities $I|a_\pm|^2$ (curves *1* and *2* correspond to $a_+$ and $a_-$, respectively). (b) Spectral power $|a_\omega|^2$ of the radiation field at the end $\zeta = L/2$.

number of modes are involved in the steady superradiant lasing.

The application of the DFB into an active sample even with a small integrated reflection coefficient $\beta L \sim 1$ considerably changes the growth rates of modes at frequencies in the photonic bandgap, even weakly manifested. Depending on the reflection coefficients at the sample ends, this change can be nonsymmetric, differently increasing or decreasing mode growth rates on different sides of this band. Such a selection makes is possible to obtain highly coherent single-mode superfluorescence in a rather broad range of parameters by using the highest-$Q$ modes with the maximum growth rate and suppressing the emission of other modes.

A corresponding example is presented in Fig. 12 for the same active sample as in Fig. 11 with the additional DFB coefficient $\beta = 0.06$, i.e., with the parameter $\beta L = 0.6$. In addition, the reflection coefficient of the ends in the Fabry–Perot cavity is decreased by two third to $R = 0.1$ (as in Fig. 4) to retain the photon lifetime in the highest-$Q$ modes at the previous level: $T_E = (6-5)/v_c$. Superfluorescence in this combined cavity is caused by only one mode with the growth rate increased to $\omega_e'' \sim 0.08v_c \sim \bar{\nu}_c/3$, whereas all the adjacent modes with reduced growth rates at the level of $0.05v_c$ proved to be noncompeting. In this case, only about 10% of active centers are involved in collective spontaneous emission. This emission acquired a highly coherent and distinct oscillatory character, retaining the same total duration $\delta\tau \sim 50$ and delay time $\tau_d \sim 100$, but the maximum main pulse intensity decreased by approximately an order of magnitude (Figure 12 shows the Rabi frequency squared at the end normalized to the cooperative frequency).

### 5.6 Superradiance upon continuous pumping and laser dynamics

Selective properties of low-$Q$ Bragg cavities and combined Fabry–Perot cavities with the DFB are especially important for superradiant lasers using collective spontaneous emission upon continuous (CW) pumping of active media with inhomogeneous spectral lines. Lasers of this type have the richest dynamics. Prior to their discussion, we will briefly recall the classification of lasers in the two-level model of the active medium and demonstrate the simplest operating regimes of superradiant lasers with these cavities in the limit of the homogeneously broadened spectral line of active centers (see details in Refs [197, 198]).[23] We will consider mainly the dynamic aspect of the problem concerning the dissipative instability of waves and the coherent type of interaction of active centers with the self-consistent field inherent in collective spontaneous emission, and first of all the pulsed dynamics of the Dicke superradiance as a whole. Therefore, we will still use semiclassical equations (19) as the initial model of a two-level laser, by assuming for simplicity that $\Sigma_0 = 0$, $\Gamma_{1z} = \Gamma_1$, and $\beta = \mathrm{Re}\,\beta$, $\Phi = 0$, $R_1 = R_2 = R$, and $R = \mathrm{Re}\,R$ (if not specially specified).

The various quantum-mechanical models of lasers are presented in Refs [95, 102, 278–284] mainly devoted to quasistationary single-mode lasing, in particular, to the influence of collective spontaneous emission of active centers on the laser line width, which can be much narrower than the spectral width of a laser mode in a low-$Q$ cavity. It is known that in conventional lasers this is the main factor limiting the narrowing of a single-mode laser line. Hopes for obtaining quasistationary single-mode superradiant lasing in low-$Q$ cavities with a homogeneous spectral line are based on the promising results of experiments with rare-earth and alkali metal atoms in cooled gases [285–288] and with dipolar excitons in cooled semiconductor heterostructures with open traps [242, 244, 246, 289].

Depending on the relation between the inversion, polarization, and field relaxation parameters, four dynamic classes of lasers are considered [198, 215, 290, 291] (see Table 1). In most lasers, except class A ones, the relaxation rate $T_1^{-1}$ of the population inversion of levels in the active medium is the lowest. The polarization relaxation rate $(T_2^{-1})$ for active centers is most often highest, including most semiconductor lasers, and such lasers belong to class B lasers. To obtain lasing in them, high-$Q$ cavities are required, in which the field

[23] Because of the limited scope of this review, we omit other possible schemes of superradiant lasers, for example, based on the nonlinear, say, Raman (Mandelstam–Brillouin) scattering of pumping and generated waves [272, 273] or on wave feedback due to scattering by random inhomogeneities of the active medium or its matrix [274–277].

**Table 1.** Dynamic classes of lasers.

| Class | Relations between relaxation rates | Adiabatically excluded variables |
|---|---|---|
| A | $T_E^{-1} \ll T_1^{-1}, T_2^{-1}$ | Polarization, inversion |
| B | $T_1^{-1} \ll T_E^{-1} \ll T_2^{-1}$ | Polarization |
| C | $T_1^{-1} \ll T_E^{-1} \sim T_2^{-1}$ | |
| D | $T_1^{-1}, T_2^{-1} \ll T_E^{-1}$ | Electromagnetic field if $\omega_R < T_E^{-1}$ |

relaxation rate $T_E^{-1}$ is low, and therefore the field (along with the active-medium inversion) determines the dynamics adiabatically traced by polarization, i.e., by the density of high-frequency dipole moments of active centers.

The intrinsic polarization dynamics begin to develop already in the intermediate case of $T_E^{-1} \sim T_2^{-1}$, i.e., for class C lasers (see Refs [199, 290]). However, this dynamics play an important role only for $T_E^{-1} > T_2^{-1}$, i.e., in *class* D *lasers*, where, however, the dynamic role of the electromagnetic field is not passive either. This role is not reduced to the adiabatic tracing of polarization because, due to superradiance for long time intervals, the field amplitude $\mathcal{E}$ is so large that the field relaxation rate $T_E^{-1}$ in the cavity proves to be lower than the Rabi frequency $\omega_R = d|\mathcal{E}|/\hbar$ and, therefore, than the rate of induced transitions between the energy levels of active centers [290]. Then, adiabatic field exclusion is impossible, as a rule, the coherent interaction of modes occurs, the fields in them rapidly change, and nonstationary lasing is typical. In this case, a major part of the field appearing in a class D laser has time to escape from the cavity (because of the low $Q$-factor) for a transit time $B/c_0$ in the cavity.

In a class C laser, where by definition the times $T_E$ and $T_2$ do not greatly differ, the coherent dynamics of modes are also possible; however, they are of self-modulation type with period $\sim T_E \sim T_2$, do not change the inversion sign in the medium, and are not accompanied by distinct emission pulses similar to collective spontaneous emission pulses. These lasers were studied experimentally and numerically for the case of small inhomogeneous broadening, $1/T_2^* \lesssim 1/T_2$ (see, for example, Refs [292–296]).

The emission dynamics in class D lasers are even more diverse and the dynamic mode spectrum is very sensitive to changes in the cavity and/or pumping parameters, which provides the possibility of efficiently controling spectral, temporal, and correlation characteristics of the emission obtained. This circumstance gives hope that class D lasers, which have not been created yet, will be essential for solving problems of data processing and in the spectroscopy and diagnostics of various media and processes proceeding in them. Class D lasers can probably be created by modifying semiconductor lasers based on heterostructures containing many layers of closely packed quantum dots with the lateral modulation of facing waveguide layers providing the DFB for waves [297–299]. By varying the values of parameters of a class D laser, one can efficiently control the number of longitudinal lasing modes, their spectral width and mutual phase difference, the pulse and pulse train duration and amplitude, and the coherence degree of laser pulses (and modes).

It is known that lasing appears with increasing pumping level or changing the active-medium and cavity parameters when one of the hot modes acquires a growth rate under conditions of decay of other modes. Above this threshold, which is called the first lasing threshold, lasing, as a rule, is stationary and single-mode. However, as pumping is further increased or laser parameters are changed, lasing can become nonstationary (in particular, two- or three-mode), which is called the excess over the second lasing threshold. In class D lasers with a short photon lifetime $T_E \lesssim (v_c\sqrt{n_p})^{-1}$ or $T_E \lesssim (\bar{v}_c n_p)^{-1}$ (see formula (45) or (49), respectively),[24] there is also another one the *superradiance* threshold, above which collective spontaneous emission pulses with a small duration $\delta t \lesssim T_2$ appear. As a rule, this threshold can be related to the fulfillment of the superradiance condition $\omega''_{p|_0} > T_2^{-1}$ for the most unstable hot mode.

This condition for not too large inhomogeneous broadening $1/T_2 < 1/T_2^* < v_c\sqrt{n_p}$ formally coincides with the superfluorescence condition (46), (47) discussed above if the inversion level specified by pumping is chosen. In this case, as in the case of the homogeneous broadening of a spectral line, pulsed lasing is due to the development of the radiative instability of polariton modes rather than electromagnetic modes. Polariton modes have negative energy and, according to characteristic and dispersion equations (24) and (25), for the specified inversion $n = n_p$ lie in the spectral interval of the width which does not exceed the value

$$\delta\omega_p \simeq 2n_p v_c^2 T_E \tag{52}$$

and can exceed the spectral line width $\delta\omega_L = 2/T_2^* + 2/T_2$ only by the number of times equal to the ratio between $\delta\omega_p/\delta\omega_L$ and its value ($\sim 1$) at the first lasing threshold. This conclusion and expression (52) are also qualitatively correct for a set of quasistationary lasing modes (in the absence of superradiant pulses) if the inversion $n_p$ specified by pumping is replaced by the average inversion $\langle\bar{n}\rangle$ of the active medium in the laser.[25]

The strong nonlinearity of the laser is manifested, of course, already in the quasistationary lasing regime, and the self-consistent spatial structure of the field, polarization, and inversion can considerably differ from the structure of hot modes and/or their superposition in a homogeneous active sample. In particular, the steady lasing can correspond to the strongly nonsymmetric structure of the field, polarization, and inversion in a laser with identically reflecting ends ($R_1 = R_2$) and a homogeneous or, as a whole, symmetric (with respect to the center $\zeta = 0$) active medium and pumping. An example of *such a spontaneous symmetry breaking* in the steady regime is presented in Fig. 13, where the fields of counterpropagating waves significantly differ and are not mirror-symmetric with respect to each other, in accordance with the nonsymmetric profiles of the smoothly inhomogeneous inversion component $\bar{n}$ and inversion grating $n_z$ pressed to one of the ends of the sample (to which one

[24] These inequalities exclude too long active samples, in which chaotic superradiance is inevitable, as, for example, in cases (28) and (29) for a Fabry–Perot cavity.

[25] Strictly speaking, the interpretation of nonstationary laser dynamics based on the concept of hot modes is restricted and requires at least the consideration of the dependences of their frequencies, growth rates, structure, and nonadiabatic and/or nonlinear interaction on the spatial and spectral inhomogeneity of the inversion and its possible rapid variations in time. The nonstationary and possibly superradiant lasing dynamics can be more efficiently analyzed with the help of so-called spatio-temporal empirical modes. These modes are determined by the eigenvectors of the time-averaged covariance matrix of the complex amplitudes of the fields on a large enough set of points inside the sample with a rather small time step [300]. Nevertheless, the conditions for the development of various lasing regimes and their qualitative features can be determined by analyzing hot polariton and/or electromagnetic modes.

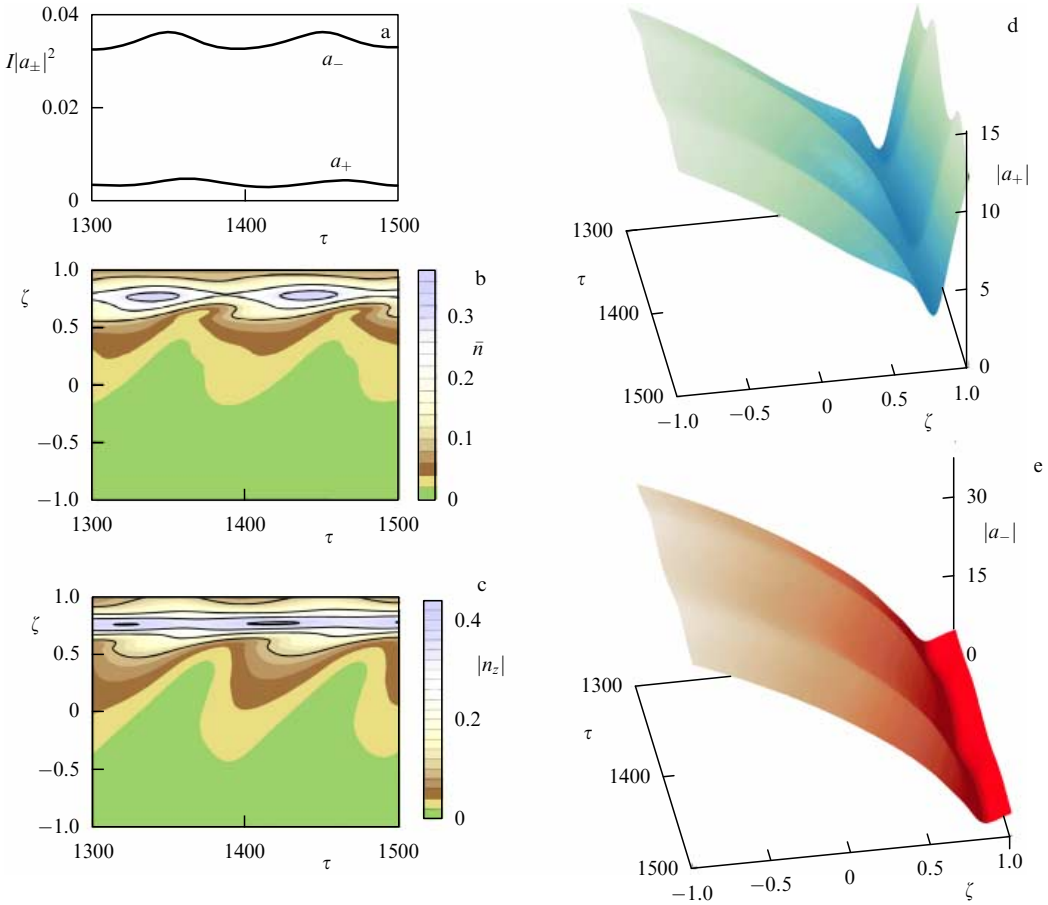


**Figure 13.** (Color online.) Weakly modulated superradiant lasing of a sample of length $L = 2$ in a Fabry–Perot cavity with moderately reflecting ends ($R = 0.37$) in the case of weak continuous pumping ($n_p = 1$) and an almost homogeneously broadened spectral line: $\Gamma_2 = 2\Gamma_1 = 0.02 \gg \Delta_0 = 0.002$. (a) Oscillograms of normalized output radiation intensities $I|a_\pm|^2$. (b, c) Spatio-temporal evolution of the inversion $\bar{n}(\zeta, \tau)$ and the inversion grating amplitude $|n_z(\zeta, \tau, \Delta = 0)|$. (d, e) Spatio-temporal evolution of the amplitudes of the waves running to the right, $|a_+(\zeta, \tau)|$, and left, $|a_-(\zeta, \tau)|$.

depends on the initial conditions) and experiencing a slow self-modulation with the period specified by the pumping rate: $\tau_M \simeq \Gamma_1^{-1} = 100$.

It should be noted that, according to Fig. 6, the mutual mirror symmetry of the amplitude profiles of counterpropagating waves $|a_+(\zeta)|$ and $|a_-(\zeta)|$ and the symmetry of the spatial inversion distribution in this laser with the total initial inversion of the active medium are well preserved during the main part of the superfluorescence process. The symmetry breaking occurs during the long stage of moving to steady lasing.

In general, in any, even strongly, nonstationary superradiance regime, a dynamic spontaneous symmetry breaking takes place (at $R_1 = R_2$) for the profiles of mode fields and the consistent inversion profile averaged over a long enough time interval $\delta T \gg T_1$ containing several characteristic sets of pulses of all lasing modes. The appearing asymmetry can be metastable and the regions of the maximum inversion of the medium and the minimum intensity of the mode field can displace alternately to one side or another from the cavity center. Such spontaneous switchings of metastable laser states can cause temporal changes in the average (over $\delta T$) emission intensity and in the correlation properties of pulses, these averages being considerably different for opposite ends of the laser.

Above the superradiance threshold, which can slightly differ from or even coincide with the second laser threshold, the repeating sporadic or quasiperiodic generation of short (with duration $< T_2$) pulses of collective spontaneous emission occurs in one or several modes, and the spectral width of the emitted field can exceed (and greatly exceed in the developed superradiant regime) the homogeneous line width $2/T_2$. In the case of small inhomogeneous line broadening, $2/T_2 < 2/T_2^* < v_c$, i.e., $\Gamma_2 < \Delta_0 < 1/2$, the width of the lasing spectrum can exceed $2/T_2^*$. In this case, the lasing dynamics not too far away from the superradiance threshold are still mainly determined by one, two, or several hot modes which are coupled with the highest-$Q$ cold modes of a low-$Q$ cavity, but are modified and nonstationary due to the presence of the time-dependent inhomogeneous inversion profile and self-consistent inversion grating. However, continuous-spectrum waves also can be essential, because the cavity is open, and lasing in class D lasers is nonstationary and nonlinear, unlike usual class B and A lasers in which high-$Q$ cavities are used.

### 5.7 Pulsed lasing in superradiant lasers

Besides the mechanisms[26] of quasistationary lasing instability inherent in class A, B, and C lasers, class D lasers have

[26] For example, intermode scattering by a self-consistent inversion grating, the parametric decay of a lasing mode to adjacent modes due to its Rabi splitting, or the so-called Risken–Nummedal–Graham–Haken mechanism [290, 291].

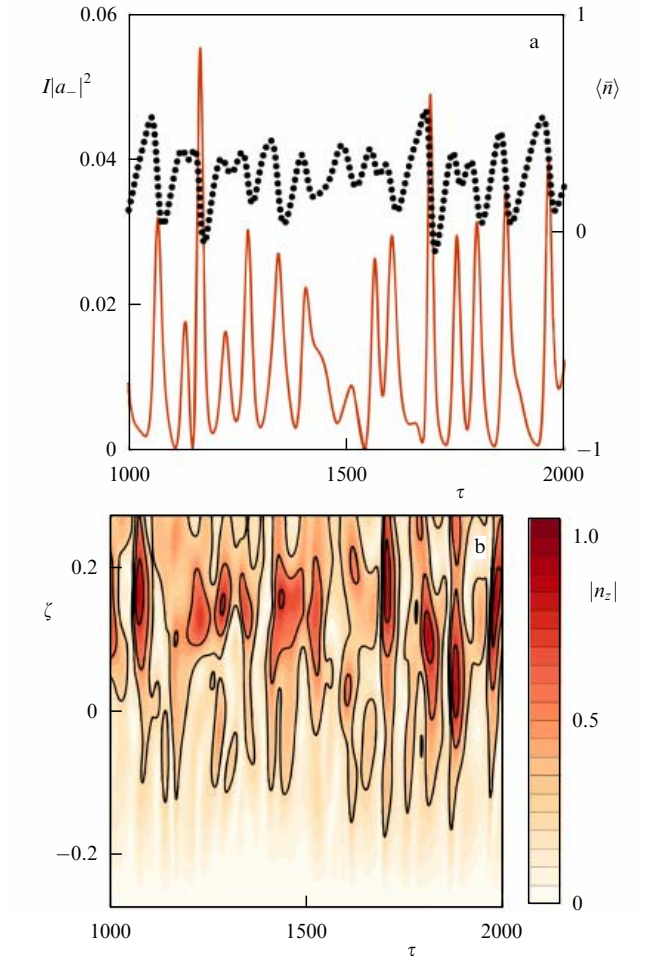


**Figure 14.** (Color online.) Nonstationary superradiant lasing of a sample of length $L = 0.56$ in a combined Fabry–Perot cavity with negligibly small reflections at one end ($R_1 = 10^{-3}$) and moderate reflections at the other ($R_2 = 0.3$) and the DFB coefficient $\beta = 0.9$ in the case of strong pumping ($n_p = 1$) and small inhomogeneous spectral line broadening: $\Delta_0 = 0.046 > \Gamma_2 \sim \Gamma_1 = 0.02$, $\Phi = 0$. (a) Oscillograms of the normalized output radiation intensity $I|a|^2$ from the nonreflecting end (solid curve) and inversion $\langle\bar{n}\rangle$ averaged over the spectral line and sample (dotted curve). (b) Spatio-temporal evolution of the inversion grating amplitude $|n_z(\zeta, \tau)|$ over the sample.

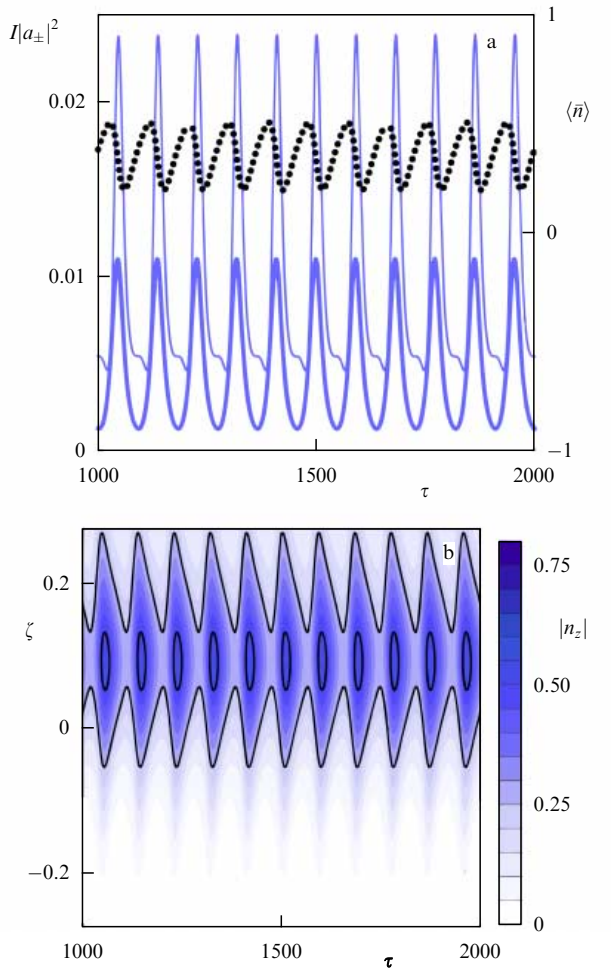


**Figure 15.** (Color online.) Periodic superradiant lasing of a sample of length $L = 0.56$ in a combined Fabry–Perot cavity with negligibly small reflections at one end ($R_1 = 10^{-3}$) and moderate reflections at the other ($R_2 = 0.3$) and the DFB coefficient $\beta = 0.9$ in the case of strong pumping ($n_p = 1$) and the same homogeneous and inhomogeneous spectral line broadenings: $\Delta_0 = \Gamma_2 = 0.046$, $\Gamma_1 = 0.02$, $\Phi = 0$. (a) Oscillograms of normalized output radiation intensities $I|a_\pm|^2$ from nonreflecting and reflecting ends (thin ($a_+$) and thick ($a_-$) solid curves) and inversion $\langle\bar{n}\rangle$ averaged over the spectral line and sample (dotted curve). (b) Spatio-temporal evolution of the inversion grating amplitude $|n_z(\zeta, \tau)|$.

another unique mechanism of mode generation instability caused by the initiated collective spontaneous emission from the central region of the laser sample. In this mechanism, due to the low $Q$-factor of the cavity, the noticeable (possibly manifold) inversion excess is produced over the average level corresponding to steady lasing. This makes it possible to 'take off' very rapidly the energy of active centers, i.e., to decrease the population inversion of their energy levels to negative values, which is followed by the temporary loss of amplifying properties in a greater part of the active medium of the laser. This leads to nonstationary pulsed lasing upon stationary pumping: the field rapidly decreases due to its escape from the open cavity and begins to increase only after the pumping restores a high enough inversion level for a time of about $T_1$.

An example of such dynamics is presented in Fig. 14 showing the mean inversion and laser radiation intensity for a combined cavity encompassed by a DFB loop with the integrated reflection coefficient $\beta L = 0.5$ and highly nonsymmetric mirrors ($R_2 = 300R_1 = 0.3$). As it should be for typical superradiant lasers, the laser pulses have considerably different amplitudes, durations ($\delta\tau \sim 20$ on average), and delay times ($\tau_d \sim 50-100$). This is explained by the fact that the superradiant instability initiating them greatly depends on the inversion distribution, and each time 'starts' with new configurations of the self-consistent inversion grating and weak fields and polarization remained in the cavity after the previous pulse. Notice that the large width of the quasi-continuous lasing spectrum, about $\nu_c/4$, is caused first of all by the polarization dynamics, because the field dynamics are damped by its large relaxation rate $\Gamma_E \simeq 3$ (this is also valid for unidirectional (see Fig. 5) and mode (see Fig. 8) superfluorescences of this laser system in the absence of pumping).

This circumstance and the laser dynamics complexity are confirmed by the fact that, as the homogeneous broadening is increased to the inhomogeneous broadening level, $\Gamma_2 = \Delta_0 = 0.046$ (other parameters being invariable (Fig. 15)), quasichaotic lasing gives way to strictly periodic lasing corresponding to the self-modulation of one effective polar-

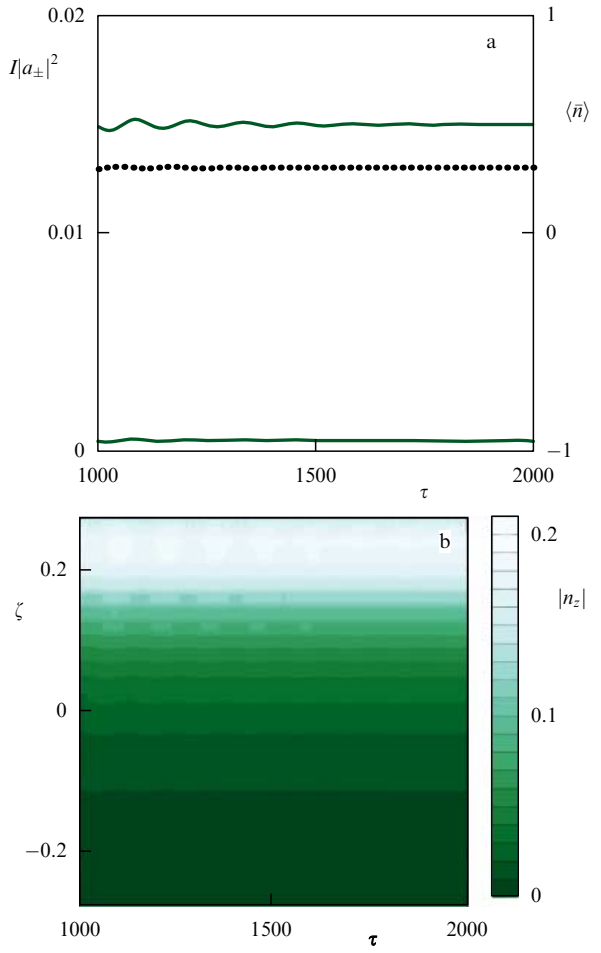


**Figure 16.** (Color online.) Going to stationary superradiant lasing of a sample of length $L = 0.56$ in a combined Fabry–Perot cavity with negligibly small reflections at one end ($R_1 = 10^{-3}$) and moderate reflections at the other ($R_2 = 0.3$) and the small DFB coefficient $\beta = 0.18$ in the case of strong pumping ($n_p = 1$) and the same homogeneous and inhomogeneous spectral line broadenings: $\Delta_0 = \Gamma_2 = 0.046$, $\Gamma_1 = 0.02$, $\Phi = 0$. (a) Oscillograms of normalized output radiation intensities $I|a_\pm|^2$ from nonreflecting and reflecting ends (upper ($a_+$) and lower ($a_-$) solid curves) and inversion $\langle\bar{n}\rangle$ averaged over the spectral line and sample (dotted curve). (b) Spatio-temporal evolution of the inversion grating amplitude $|n_z(\zeta, \tau)|$.

iton mode and the inversion grating consistent with it.[27] Generated regular laser pulses have a superradiant nature, their intensity varies within an order of magnitude, and the repetition period exceeds their duration $\delta\tau \simeq 23$ by approximately four times. Due to the DFB, the intensities of laser pulses escaping from the opposite ends with quite different reflection coefficients differ only twice, as similar superfluorescence pulses in Fig. 8. If the DFB coefficient is decreased to one fifth or less for the parameters indicated (as in Fig. 16), by taking $\beta \lesssim 0.2$ (i.e., $\beta L \lesssim 0.1$) and, therefore, making the sample in fact open ($\Gamma_E \sim 5$), although with a highly nonsymmetric output of counterpropagating waves, the self-consistent inversion grating will weaken ($|n_z| \lesssim 0.1$) and lasing will be monochromatic and stationary, with radiation intensities from the opposite ends differing by several dozen times, and almost independent of the DFB.

[27] By ignoring the inversion grating, i.e., at $n_z \equiv 0$, equations (19) lead in the case considered to purely monochromatic (single-mode) lasing.

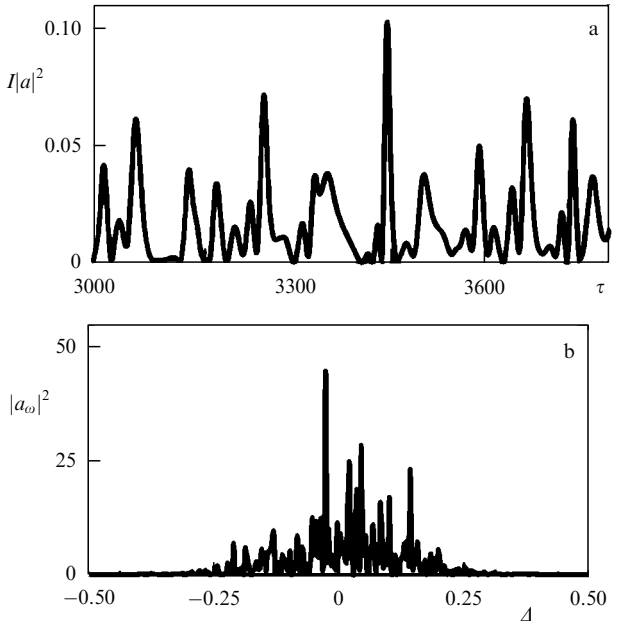


**Figure 17.** Broadband superradiant lasing of a distributed sample of length $L = 2$ in a Bragg cavity with the DFB coefficient $\beta = 1$ in the case of strong pumping ($n_p = 1$) and homogeneous spectral line broadening: $\Gamma_2 = 2\Gamma_1 = 0.02 \gg \Delta_0 = 0.002$, $\Phi = 0$. (a) Oscillogram of the normalized output radiation intensity $I|a|^2$. (b) Spectral power $|a_\omega|^2$ of the radiation field at the end of a sample.

Another example of broadband superradiant lasing is presented in Fig. 17 for a Bragg cavity with the DFB parameter $\beta L = 2$ in the absence of reflections from the sample ends, when $T_E \simeq 2 \ll T_2 = 50$. We see that, compared to the superfluorescence pulse from the same sample in Fig. 7, superradiant laser pulses are several times longer and their intensity is an order of magnitude smaller. Their inverse normalized Rabi frequencies $(\sqrt{I}|a|)^{-1} \sim 3-10$, as they should be, are several times smaller than the duration $\delta\tau \sim 10-30$ and the width of the total lasing spectrum reaches half the cooperative frequency and covers all the central part of the photonic bandgap. When the pumping level $n_p$ was decreased from 1 to 0.25 and the homogeneously broadened line shifted to the edge of the photonic bandgap, $\Phi = 1$, the quasichaotic pulsed superradiant lasing gave way to the single-mode self-modulation regime with a period $\tau_M \simeq 80 \sim \Gamma_1^{-1}$ (Fig. 18). The efficient control of the lasing regime in a class D laser illustrated by the last example can also be performed by changing the parameters of the cavity and active medium in it, including the sample length.

However, upon passing from homogeneous to inhomogeneous line broadening, especially in the case of the large linewidth exceeding the cooperative frequency, $\Delta_0 > 1$, superradiant lasing in such Bragg and related combined cavities with $\beta L \lesssim \pi$, as a rule, proves to be nonstationary and, for the required long sample lengths $L \gtrsim 1$, also multimode. As is clear from the discussion of an analogous superfluorescence problem in Sections 5.3 and 5.4, the appearance of superradiance upon continuous pumping and its realization in a quite regular 'few-mode' regime with distinct collective spontaneous emission pulses are determined to a great extent by the selection of unstable hot electromagnetic modes due to DFB dispersion properties, which are absent in a Fabry–Perot cavity.

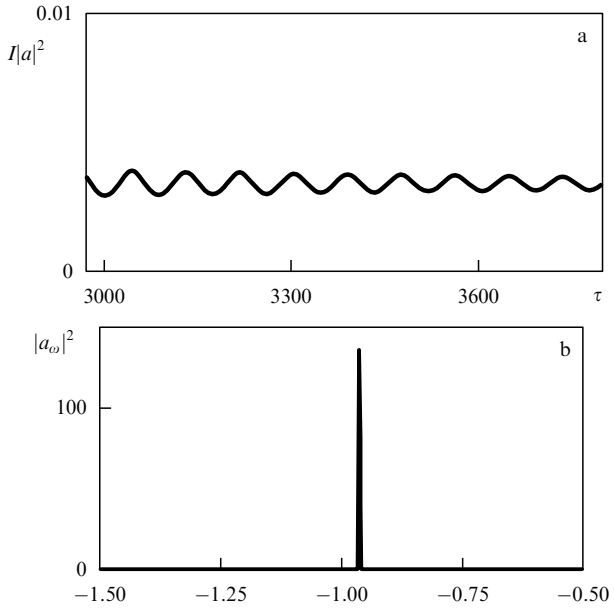


**Figure 18.** Superradiant lasing in the single-mode self-modulation regime of a sample of length $L = 2$ in a Bragg cavity with the DFB coefficient $\beta = 1$ in the case of weak pumping ($n_p = 0.25$) and homogeneous spectral line broadening: $\Gamma_2 = 2\Gamma_1 = 0.02 \gg \Delta_0 = 0.002$, $\Phi = 1$. (a) Oscillogram of the normalized output radiation intensity $I|a|^2$. (b) Spectral power $|a_\omega|^2$ of the radiation field at the end of a sample.

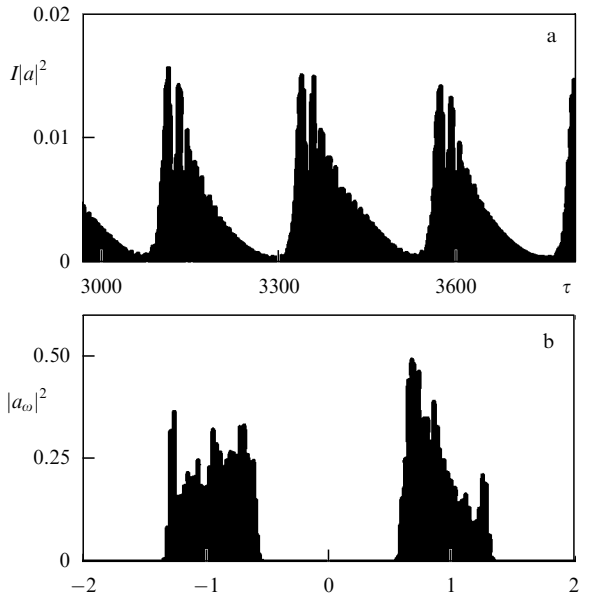


**Figure 19.** Two-band superradiant lasing of a sample of length $L = 2$ in a Bragg cavity with the DFB coefficient $\beta L = 2$ in the case of strong pumping ($n_p = 1$) and inhomogeneous spectral line broadening: $\Delta_0 = 1 \gg \Gamma_2 = 2\Gamma_1 = 0.02$, $\Phi = 0$. (a) Oscillograms of the normalized output radiation intensity $I|a|^2$ at the end. (b) Spectral power $|a_\omega|^2$ of the radiation field at the end of a sample.

However, as a consequence of deep spectral dips produced in the population inversion of energy levels of active centers and its drastic spatio-temporal evolution caused by the whole prehistory of moving to steady lasing it often turns out that the concept of electromagnetic and polariton modes with a fixed spatial structure becomes invalid in principle and inefficient for the quantitative description of the nonlinear dynamics of superradiant lasing. Therefore, although we use below the mode language, in particular, in the discussion of Figs 19–24, we do it only to explain qualitatively the phenomenon, to invoke some analogies, or for the identification of isolated components of the lasing spectrum. Such a nonstrict mode language was also used above in a number of cases.

We will illustrate the complexity of the mode description of the superradiant laser dynamics by considering the intermediate case of $\Delta_0 = 1$ presented in Fig. 19 for a typical Bragg cavity with the DFB parameter $\beta L = 2$ and $T_E \simeq 2 \ll T_2 = 50$. Superfluorescence, as an initial stage of lasing in this case, was considered above in the discussion concerning Fig. 10. Its spectrum consisted of two symmetric bands, each of which could be interpreted as the result of the nonadiabatic evolution and nonlinear interaction of two modes: a polariton mode with frequency near the inner edge of bands ($\Delta \simeq \pm 0.3$), and an electromagnetic mode with frequency near the external edge ($\Delta \simeq \pm 1$), if such hot modes are to be calculated for a homogeneous completely inverted sample. Oscillatory superradiance pulses obtained in the course of steady lasing (Fig. 19a) are quite similar to oscillatory superfluorescence pulses (Fig. 10a) and could also be qualitatively interpreted as a result of the interaction and beats of a few excited and slowly decaying modes, for example, two modes resembling polariton modes and two modes resembling electromagnetic modes. Their amplitudes should be half as large, and frequencies one and a half times higher than for the corresponding modes forming a superfluorescence pulse, because the intensity of the two-band spectrum decreased and its width increased namely in this way upon moving from superfluorescence process to lasing.

However, such an interpretation of the shape and spectrum of both superfluorescence and especially superradiant laser pulses appears very naïve due to the complexity of the spatio-temporal and spectral structures of the field, polarization, and inversion (including the inversion grating) in the sample, which follow from the numerical solution of equations (19). A description of such structures with the aid of four or some other small number of modes determined by irregular instantaneous inversion profiles would require more time-consuming calculations without any guarantee that disregarding other modes or continuous-spectrum waves is justified. It seems that in this case the method of empirical modes with the unfixed spatio-temporal structure, developed in Ref. [300], is more convenient, but its description is beyond the scope of this review.

### 5.8 Superradiant lasers with a strongly inhomogeneously broadened spectral line

In the case of very strong inhomogeneous spectral line broadening, $\Delta_0 \gg 1$, the concept of hot electromagnetic modes and their selection during lasing is partially more justified, at least for the low-$Q$ cavities of interest to us with the optimal photon lifetime and length (51) indicated in Section 5.5 in the discussion of the corresponding superfluorescence problem. In this case, electromagnetic modes are well separated in frequencies and do not experience any strong nonlinear interaction with each other or rapid nonadiabatic evolution, although they do not give the general solution to the 'unloading' problem for the pulsed collective spontaneous emission process in an extended sample without involving continuous-spectrum waves (cf.

analytic theory (35)–(41) for a similar inversion 'unloading' problem for superfluorescence in the active medium with a homogeneous spectral line broadening in a Fabry–Perot cavity).

Superradiant lasing regimes in a Bragg cavity with the DFB parameter $\beta L \lesssim \pi$ upon continuous pumping were recently analyzed in Ref. [199] and we will not repeat it here. We present only one representative example of multimode lasing in which three types of mode dynamics coexist: superradiant, self-modulation, and quasistationary, and then move at once to a general qualitative description of the features and possible operating regimes of superradiant lasers with open combined cavities, including, in particular, a Bragg cavity.

Figure 20a plots the steady lasing spectrum of a very long laser ($L = 20$, $I = 0.25 \times 10^{-4}$) containing an active medium with the strong inhomogeneous broadening ($\Delta_0 = 4 \gg \Gamma_2 = 0.03$) placed into a comparatively high-$Q$ Bragg cavity with the DFB parameter $\beta L = 6$. Such a cavity has two cold high-$Q$ modes at the edges of the photonic bandgap for $\Delta \simeq \pm\beta = \pm 0.3$ with frequency detunings $\Omega_{\mathrm{E}m} \approx 1/3$, $m = \pm 1$ and the photon lifetime $T_{\mathrm{E}} \simeq 90/v_{\mathrm{c}} > T_2 = 33/v_{\mathrm{c}}$ (Fig. 20c) [see formulas (42) and (43)]. The two corresponding hot electromagnetic modes at the complete inversion $n = 1$ have the maximum growth rates $\Omega''_{\mathrm{e},\pm 1} \equiv \omega''_{\mathrm{e},\pm 1}/v_{\mathrm{c}} \simeq 0.25$ and almost unshifted frequency detunings $\Omega'_{\mathrm{e},\pm 1} \simeq \pm 0.3$. Upon continuous pumping, they provide the generation of two quasimonochromatic fields with the highest spectral amplitudes $|a_{\omega,\pm 1}| \sim 20$ (Fig. 20a), forming two broad spectral dips in the inversion spectrum, as usual during quasistationary generation of modes in a class B laser. The next cold modes $\Omega_{\mathrm{E}m}$, $m = \pm 2, \pm 3, \ldots$ with frequencies lying on the slopes of the spectral line of the Bragg cavity adjacent to the photonic bandgap have the photon lifetime $T_{\mathrm{E}} < T_2$ (Fig. 20c), so that the generation of the corresponding hot modes, due to a large enough growth rate $\Omega''_{em} \gtrsim \Gamma_2$ [for the complete inversion $n = 1$ (Fig. 20b)], corresponds to class C lasers (for close values of $T_{\mathrm{E}}$ and $T_2$, as with $m = \pm 2$) or class D lasers (when $T_2$ considerably exceeds $T_{\mathrm{E}}$, as with $m = \pm 3, \pm 4, \ldots$). Therefore, as is clear from the right inset to Fig. 20a, $m = \pm 2$ modes emit in the self-modulation regime, not producing isolated pulses, while $m = \pm 3, \pm 4, \ldots$ modes emit in the superradiant regime with quite distinct collective spontaneous emission pulses, thereby having considerably larger spectral broadening. Finally, cold modes with $T_{\mathrm{E}} \sim \Delta_0/v_{\mathrm{c}} = 1/\bar{\nu}_{\mathrm{c}}$ at the line wings $|\Delta| > \Delta_0/2 = 2$ correspond to hot modes with small growth rates $\Omega''_{em} \lesssim \Gamma_2$ (Fig. 20b) and, for the low pumping rate $\Gamma_1 = 0.01$, lie below the superradiant threshold, i.e., they are generated in the quasistationary regime with low intensity (see the left inset to Fig. 20a). Of course, in the presence of several dozen laser modes, whose total number is estimated as $M \lesssim \beta L/[\pi \exp(-nL/\Delta_0)]$, according to formulas (33), (49) for $R \ll \beta L$, the lasing regime for an individual mode can be determined only using spectral filters, because the oscillogram of the total emission field is quasichaotic.

Consider now some general properties of class D lasers with low-$Q$ combined cavities in which the photon lifetime (see formula (45)) is shorter than the relaxation time of individual dipole oscillations of active centers: $T_{\mathrm{E}} < T_2$. For definiteness, we will rely on lasers with the optimal length $L \sim 2\Delta_0$ (see formula (51)) in which collective spontaneous emission effects are manifested most distinctly. We can distinguish [197, 198] at least *five qualitatively different operation regimes* of such lasers: quasistationary, self-modulation, regular pulsed, irregular pulsed with quasiperiodic pulse trains, and quasistochastic. Under typical conditions, the field of each superradiant mode $a(\tau)$ generated by the laser is coherent and the spectral width of the mode is determined by the corresponding Rabi frequency $\omega_{\mathrm{R}} = v_{\mathrm{c}}\sqrt{I}\,|a|$, which at strong enough pumping can reach the effective cooperative frequency $\bar{\nu}_{\mathrm{c}} = v_{\mathrm{c}}^2 T_2^*$, resulting in the overlapping of spectra of adjacent modes. Therefore, the emission spectrum of a class D laser can be both quasidiscrete and quasicontinuous (see, for example, Figs 4, 20–24). Notice that many special

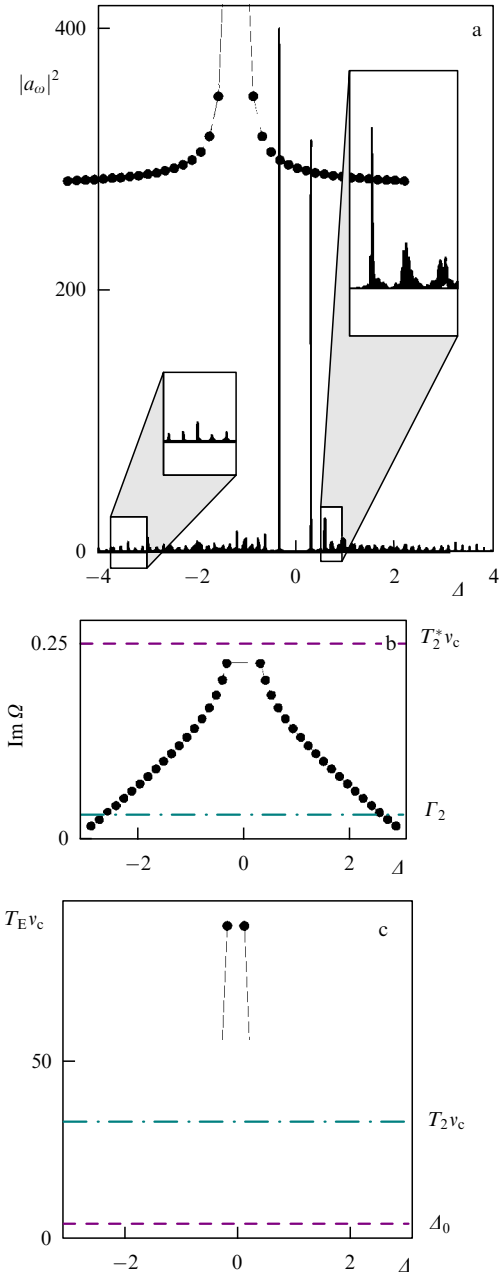


**Figure 20.** Mixed generation of superradiant and quasistationary modes of a sample of length $L = 20$ in a high-$Q$ Bragg cavity with the DFB coefficient $\beta = 0.3$ in the case of strong pumping ($n_{\mathrm{p}} = 1$) and large homogeneous spectral line broadening: $\Delta_0 = 4 \gg \Gamma_2 = 3\Gamma_1 = 0.03$, $\Phi = 0$. (a) Spectral power $|a_\omega|^2$ of the radiation field at the end; the left inset shows quasimonochromatic modes at the lasing band edge; the right inset illustrates superradiant modes near the photonic bandgap. (b) Calculated spectrum of growth rates of hot modes. (c) Calculated spectrum of photon lifetimes $T_{\mathrm{E}}$ of cold electromagnetic modes.

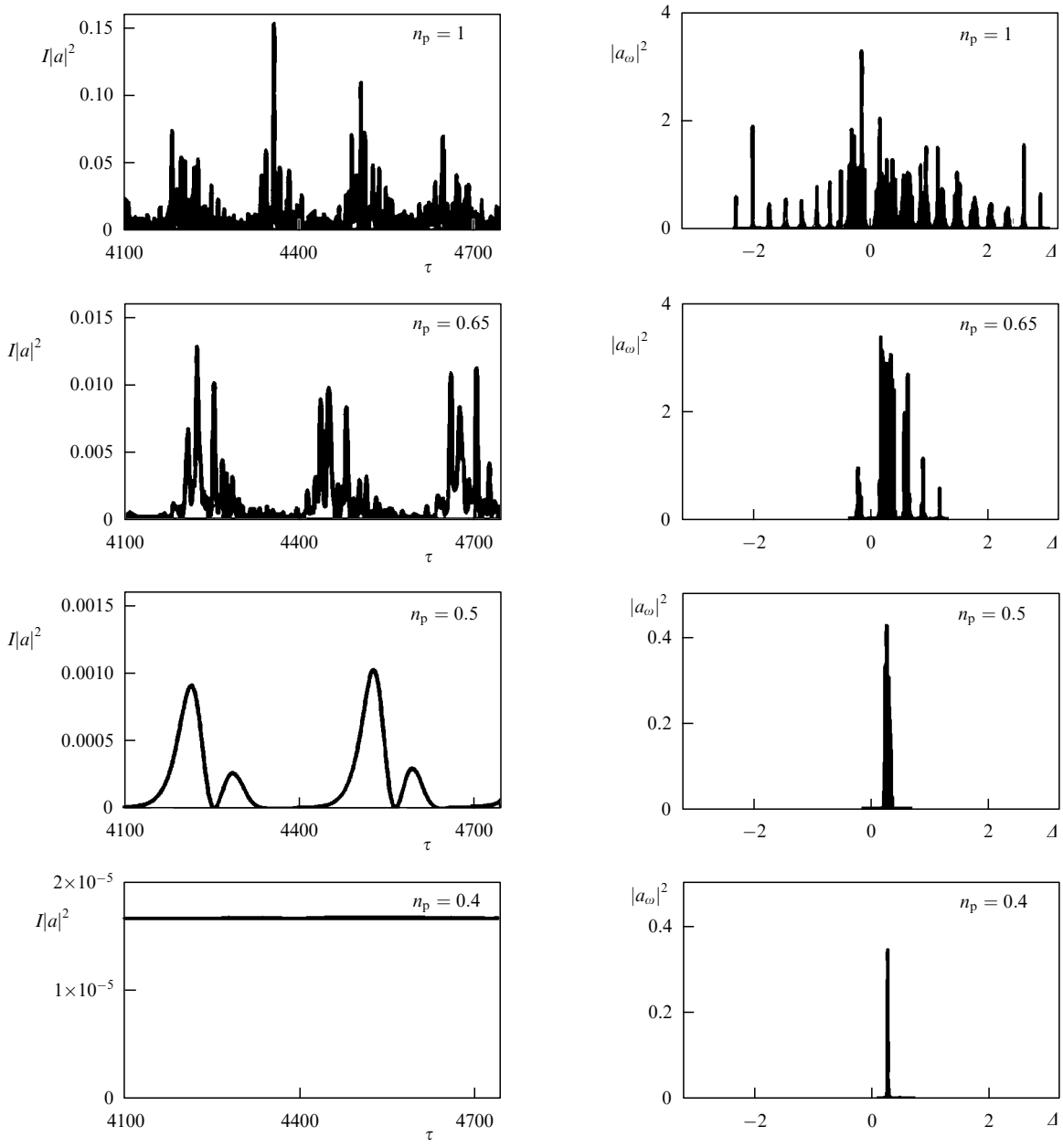


**Figure 21.** Influence of the pumping level on the lasing regime of a sample of length $L = 10$ in a combined Fabry–Perot cavity ($R = 0.1$) with the DFB coefficient $\beta = 0.1$ in the case of strong inhomogeneous spectral line broadening: $\Delta_0 = 4 \gg \Gamma_2 = 3\Gamma_1 = 0.03$, $\Phi = 0$. At the left of the figure are presented oscillograms of the normalized output radiation intensity $I|a|^2$ for different pumping levels $n_p$. At the right of the figure are presented spectral powers $|a_\omega|^2$ of the radiation field at the end of a cavity for the corresponding pumping level $n_p$.

superradiant lasing regimes have not in fact been studied so far.

Unlike a class B laser, a class D laser does not actually allow the stationary mode generation, i.e., the second laser threshold is very close to the first threshold having a pumping level of approximately $n_p^{th} \simeq 2\Delta_0/L$. Because lasing conditions depend in one way or another on many laser parameters, by varying any of them it is possible to pass through the first, second, and superradiant thresholds and to control the lasing regime as a whole or its individual modes, thereby changing the spectral and correlation properties of emission. Examples of the influence of the pumping level $n_p$, the active sample length $L$, and the homogeneous broadening $\Gamma_2$ on the laser operation (the osilllogram and its emission spectrum) for other parameters fixed are presented in Figs 21–23.

We see that all five lasing regimes are realized, and the superradiance of some modes often coexists with the self-modulation or quasistationary generation of other modes if the spectral inhomogeneous bands of active centers responsible for maintaining the field of corresponding modes do not overlap. In this case, the spectral bands of superradiant modes are especially broad due to the broad spectrum of the field of their collective spontaneous emission pulses. This pulsed emission in an individual spectral band is mainly proceeds similar to that for the superfluorescence of a sample with a homogeneously or slightly inhomogeneously broadened spectral line and sometimes causes drastic decreases in the inversion level to negative values (cf. Figs 2, 4, 6, and 10). Spectral inversion dips produced in this case are compensated for by the pumping for the time $\sim T_1$, which ensures the

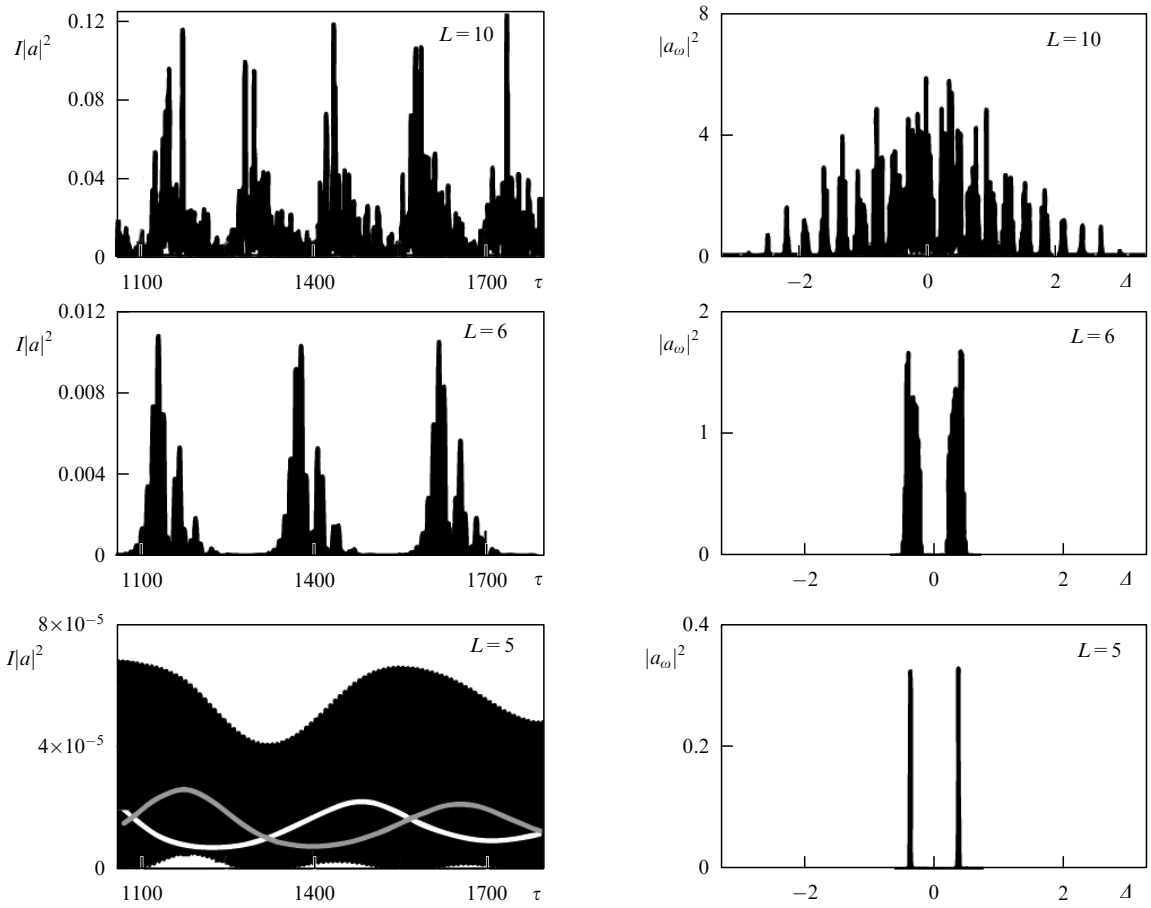


**Figure 22.** Influence of the sample length on lasing regimes in a combined Fabry–Perot cavity ($R = 0.1\exp(i\pi/2)$) with the DFB coefficient $\beta = 0.1$ in the case of strong pumping ($n_p = 1$) and large inhomogeneous spectral line broadening: $\Delta_0 = 4 \gg \Gamma_2 = 2\Gamma_1 = 0.02$, $\Phi = 0$. At the left of the figure are presented oscillograms of the normalized output radiation intensity $I|a|^2$ for different active sample lengths $L$. For the case of $L = 5$, oscillograms of the fields of each of the two coherent modes are shown by light curves. (The dark background is caused by frequent intensity oscillations with a frequency on the order of the cooperative frequency.) At the right of the figure are presented spectral powers $|a_\omega|^2$ of the radiation field at the end of a cavity for the corresponding sample lengths $L$.

repeated emission of the superradiant mode pulse. Depending on the number of superradiant modes, the generated train of superradiant pulses can be quasiperiodic, regular nonperiodic, or completely irregular.

The origin of superradiant pulses can be analyzed with the help of dynamic inversion spectra at the working transition, which are completely consistent with the temporal dynamics of the field spectrum [197, 198, 301]. A comparison of dynamic inversion spectra and field intensity at the laser end in a broad range of parameters shows that these pulses are generated and emitted independently, each in its spectral interval, forming trains containing, generally speaking, several pulses in the frequency band of each superradiant mode. Due to the broad spectrum, superradiant pulses from different spectral channels related to adjacent hot modes or even separated by the photonic bandgap can be emitted synchronously during a number of pulse trains. Several simultaneously emitted coherent pulses from different spectral regions at the sample edge interfere and can produce higher-power and short-emission pulses.

The presence of a fairly weak modulation of the inversion grating $n_z(\tau, \zeta, \Delta)$ in class D lasers leads to the loss of strict periodicity of superradiant pulse trains. The appearing local amplification, absorption, or distributed reflection, which are different for counterpropagating waves, are nonstationary and affect the phase properties of emission, decreasing its coherence, by introducing the randomness to the formation and emission of each individual pulse and the train as a whole. It can also be shown that, when the superradiant threshold is greatly exceeded, independent collective spontaneous emission pulses have time to form in relatively short parts of the sample. These pulses propagating in the sample are many times reabsorbed by active centers and nonlinearly interact with each other, producing weakly modulated and low-coherent emission of continuous-spectrum waves, which is typical for unidirectional superradiance in long samples (see formulas (28), (29)) and suppresses mode superradiance. According to formula (51), this bounds from above the optimal length of a superradiant laser.

### 5.9 Mode interaction effects in multimode superradiant lasers

Even in the case of a weak, seemingly insignificant overlapping of the spectra of adjacent modes, including superradiant modes, in a class D laser, as in a conventional multimode class B laser, an intermode interaction can exist, which is maintained by continuous pumping and is especially efficient in the case of the quasiequidistant mode spectrum. The two effects of this interaction are illustrated in Fig. 24 for a class D laser with a long combined cavity possessing the quasiequidistant spectrum of cold electromagnetic modes and the active medium with a strong inhomogeneous line broad-

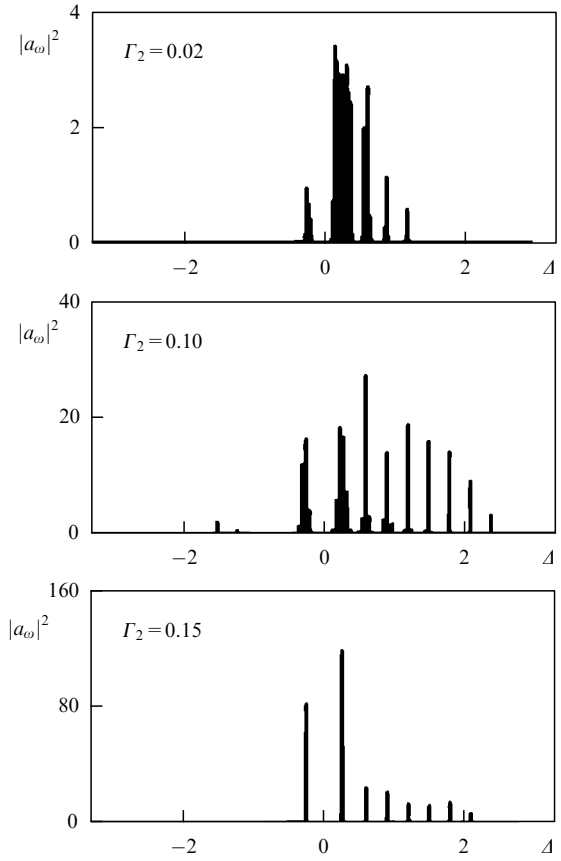


**Figure 23.** Influence of the homogeneous spectral line broadening on the lasing spectrum of a sample of length $L = 10$ in a combined Fabry–Perot cavity ($R = 0.1$) with the DFB coefficient $\beta = 0.1$ in the case of moderate pumping ($n_p = 0.65$) and large inhomogeneous spectral line broadening: $\Delta_0 = 4 \gg \Gamma_2 = 2\Gamma_1 = 0.02$, $\Phi = 0$. The spectral power $|a_\omega|^2$ of the radiation field at the end of a cavity is demonstrated for different relaxation rates $\Gamma_2$ of dipole oscillations of the active centers shown in the figure.

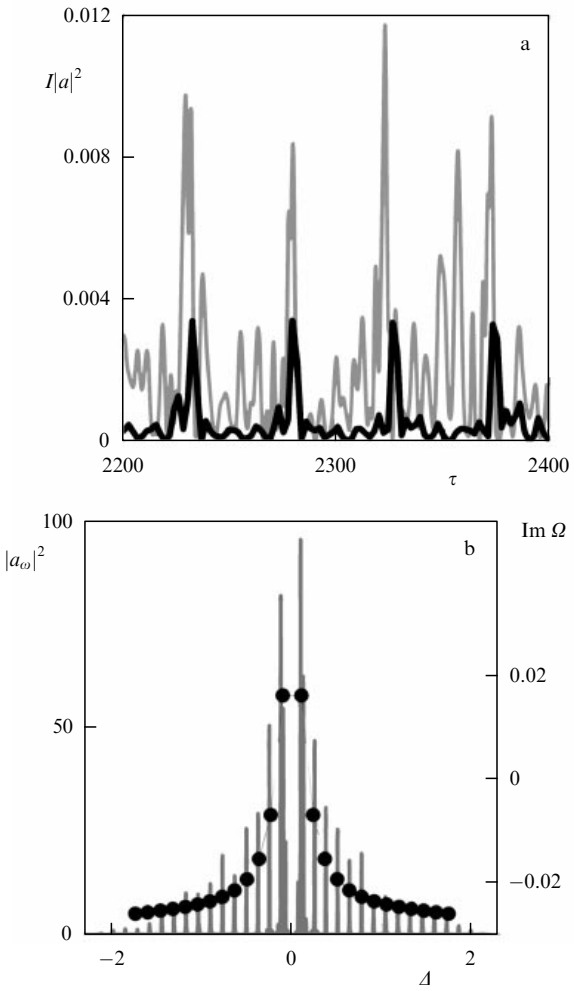


**Figure 24.** Generation of two superradiant modes of a sample of length $L = 22.5$ in a combined Fabry–Perot cavity ($R = 0.1 \exp(i\pi/2)$) with the DFB coefficient $\beta = 0.04$ in the case of strong pumping ($n_p = 1$) and very large inhomogeneous spectral line broadening: $\Delta_0 = 13$, $\Gamma_2 = 3\Gamma_1 = 0.03$, $\Phi = 0$. (a) Oscillograms of the normalized output radiation intensity $I|a|^2$: quasichaotic total radiation (grey curve) and quasiperiodic radiation produced by the ten extreme modes of the right wing of the lasing spectrum (black curve). (b) Spectral power $|a_\omega|^2$ of the radiation field at the end of a cavity. Dots mark growth rates of the corresponding hot modes.

ening providing the growth rates only for two of the highest-$Q$ modes.

First, albeit for the maximum pumping $n_p = 1$, other separate modes decay in the absence of lasing (Fig. 24b), many of them are involved in quasistationary lasing and have large amplitudes due to the repeated formation of short superradiant pulses by the two highest-$Q$ modes. The dynamic spectrum of these pulses covers adjacent modes. Such parametric action produces multimode lasing covering about 30 quasistationary narrowband modes and two nonstationary broadband modes. Collective spontaneous emission in these two modes imparts the element of randomness to the total emission field (Fig. 24a), representing a partially coherent superposition of the fields of all generated modes.

Second, a spectacular intermode interaction effect in a class D laser with a combined cavity is the *partial self-locking* of quasistationary modes in the presence of one or more superradiant modes. The numerical solution of equations (19) shows [197, 198, 300] that it is possible in a broad range of laser parameters in the absence of both the external modulation of its properties and any absorbers to generate in the laser a quasiregular train of radiation pulses with durations shorter than the relaxation times of the population of energy levels and polarization of the active medium; the superradiant pulses of modes with the highest growth rates, following quasiperiodically with the period close to the pumping time $T_1$, burn out deep dips in the population of the active medium, up to removing the population inversion in it, in certain spectral intervals and in certain time intervals. As a result, modes with smaller growth rates and frequencies lying farther from the photonic bandgap are capable of partial locking maintained by coherent interaction with superradiant modes. In this case, if the reflection coefficients $R$ from the ends are not too small compared to $\beta L$, then, due to mode-locking of some modes, another pulsed quasiperiodic component appears in emission with the period approximately equal to the travel time of light in the cavity (see the oscillogram of the field of ten modes in Fig. 24). Superradiant modes can also make contributions to a mode-locked pulse circulating in the cavity.

It should be noted that the dynamic spontaneous symmetry breaking in the inversion distribution and mode profiles in a laser with a symmetric combined Fabry–Perot cavity and large inhomogeneous broadening of the spectral

line is, as a rule, manifested much weaker (and occurs only during short time intervals) than this effect in the case of a homogeneously broadened line. One of the manifestations of such a symmetry breaking is the appearance of a pulse circulating in the cavity and formed by partially mode-locked modes.

It is interesting that the mutual coherence of superradiant pulse trains can be lower than the mutual coherence of individual mode-locked emission pulses even in widely separated trains, which is natural for multimode lasing with partial mode-locking. Moreover, it seems unlikely that many nonsuperradiant quasistationary modes would appear in steady lasing in the absence of superradiant modes, because, according to the linear theory, they would not have the growth rate, as discussed above in presenting Fig. 24. This operation regime is promising for generating a quasiregular train of high-power ultrashort coherent emission pulses upon continuous pumping in the absence of additional elements or devices providing mode-locking. Such a laser can be realized, for example, exploiting a heterostructure with submonolayer InAs/GaAs quantum dot layers and a lateral Bragg structure providing the proper selection of longitudinal laser modes [197, 302].

## 6. Conclusions

The aim of the present review was to discuss recent experiments and theoretical advances concerning the collective spontaneous emission of an ensemble of dipole oscillators and to attract attention to some physically interesting problems in the field of studies of coherent radiative interaction in many-particle systems.

We considered the following issues, which are relevant for both experimental and theoretical investigations:

- the unified interpretation of various aspects of this phenomenon, which is classically macroscopic in its manifestation and quantum-mechanical by nature, in ensembles of active centers of various types;
- the role of propagation effects and nonlinear spatio-temporal correlation effects in the dynamics of collective spontaneous emission;
- the influence of low-$Q$ cavities on the realization and development of superfluorescence and initiated superradiance.

In the last case, we are dealing in fact with an important experimental and theoretical problem in this field of physics: the development and adequate description of superradiant lasers in which the collective spontaneous emission of continuously pumped active centers leads to the generation of coherent emission with a variety of spectral correlation properties. The study of these properties is necessary for the numerous applications, from information optics and dynamic spectroscopy to diagnostics of the states of many-particle systems and the development of the concepts of quantum-dynamical and nonequilibrium phase transitions.

Despite more than a half-century history of studying this scope of problems associated with Dicke superradiance, the issues mentioned above and many other ones remain far from exhausted. Moreover, recently the superradiance phenomenon has been extensively studied. We can expect in the near future the experimental demonstration of various schemes and practical applications of superradiant semiconductor lasers based on special multilayer heterostructures with quantum dots or excitons as active centers. The investigation of these and other ensembles of active centers with dominating radiative interaction is promising, and it will undoubtedly lead to the formulation of profound new questions and the discovery of unexpected physical effects.

In this review, we have shown by numerous examples that, when superradiance plays a dominant role in the pulsed dynamics of an initially inverted sample and in the laser dynamics upon continuous pumping, unique possibilities appear for controling qualitative and quantitative lasing characteristics, such as the spectral width, duration, and coherence degree of various pulsed components of output radiation. In other words, by controling the parameters of the ensemble of particles and the set of hot modes determined by the cavity and pumping, we can control the output radiation. On the other hand, by studying changes in spectral correlation properties of the output radiation, we can judge the reconstruction of collective states of a many-particle system, in particular, detect phase transitions in it.

No less exciting are recently initiated extensive studies of collective states in many-particle systems experiencing, along with the radiative interaction, other interactions of comparable strength, for example, the Coulomb, magnetic dipole (spin), phonon interactions, or interactions related to some other scattering of particles or their quantum statistics.

Various analogies or relations with the superradiance phenomenon are highly sought after, beginning with the similarity of model Hamiltonians to the Dicke Hamiltonian and ending with the similarity of spatio-temporal, spectral, and correlation characteristics of the collective behavior of particles or simply the statement of their phased contribution to some self-consistent field determining the properties of the states in a many-particle system. Although problems of this type have not been discussed in the review, we mention briefly some recent work in this area, especially devoted to quite open many-particle systems in which the excessive, sometimes undesirable, accumulation of the field in the cavity inherent in conventional lasers is absent, and the 'exotic' states of active centers can be formed due to their collective interaction with the self-consistent field. Notice that different manifestations of collective spontaneous emission, first of all nonstationary, can be characterized, on the one hand, by quite unusual physical properties and, on the other hand, can be used for studying other, nonradiative interactions and related 'exotic' states of active centers.

Examples of various corresponding experimental results include:

(1) The discovery of spontaneous symmetry breaking in the Dicke quantum phase transition in a Bose–Einstein condensate of rubidium atoms placed into the central region of a high-$Q$ Fabry–Perot cavity pumped by a continuous-wave laser [71].

(2) The demonstration of a so-called paired superradiance upon coherent two-photon emission from the first vibrational level of molecular hydrogen in the radiation field of two lasers [303].

(3) The use of superfluorescence of cesium atoms distributed along a quasi-one-dimensional photonic-crystal waveguide for studying the features of the radiative interaction between atoms [304].

(4) The observation of a so-called single-photon superfluorescence from a quantum dot, opening the possibility of studying quantum effects of the Coulomb interaction between electrons and holes in low-dimensional semiconductor structures [305].

(5) The creation and study of a subemitting coherent state in a large cloud of cold rubidium atoms ($\sim 10^9$ atoms in a 3 $mm^3$ volume) with a radiative decay time two orders of magnitude longer than the spontaneous emission lifetime of an atom [306].

Among theoretical results, we only mention a few recent studies generalizing the Dicke phase transition model for boson and fermion many-particle systems subjected to some external actions [98, 307–314].

The study of various types of such many-particle states, transitions between them, and their spatio-temporal dynamics was initiated only recently and is undoubtedly promising from both the fundamental and applied points of view.

**Acknowledgments**

This study was supported by the state program of the IAP RAS for scientific studies by projects Nos 0035-2014-0029 and 0035-2014-0005 (Sections 1 and 2), the program of fundamental studies of the DPS RAS IV.2.6, Fundamental Basis and Experimental Realization of Promising Semiconductor Lasers for Industry and Technologies' (Section 3), the Program of Fundamental Studies of the RAS Presidium P-1, Nanostructures: Physics, Chemistry, Biology, Basic of Technology (Section 4), and the Russian Foundation for Basic Research (grant No. 16-02-00714) (Section 5).

## References

1. Dicke R H *Phys. Rev.* **93** 99 (1954)
2. Siegman A E *Lasers* (Mill Valley, Calif.: Univ. Science Books, 1986)
3. Zheleznyakov V V, Kocharovskii V V, Kocharovskii Vl V *Sov. Phys. Usp.* **32** 835 (1989); *Usp. Fiz. Nauk* **159** 193 (1989)
4. Lugiato L, Prati F, Brambilla M *Nonlinear Optical Systems* (Cambridge: Cambridge Univ. Press, 2015)
5. Cong K et al. *J. Opt. Soc. Am. B* **33** C80 (2016)
6. Fain V M *Kvantovaya Radiofizika* (Quantum Radiophysics) Vol. 1 (Moscow: Sov. Radio, 1972)
7. Fain B *Nuovo Cimento B* **68** 73 (1982)
8. Ginzburg V L *Sov. Phys. Usp.* **26** 713 (1983); *Usp. Fiz. Nauk* **140** 687 (1983)
9. Ginzburg V L *Applications of Electrodynamics in Theoretical Physics and Astrophysics* 2nd ed. (New York: Gordon and Breach Sci. Publ., 1989); Translated from Russian: *Teoreticheskaya Fizika i Astrofizika*: *Dopolnitel'nye Glavy* 3rd ed. (Moscow: Nauka, 1987)
10. Bonifacio R, Schwendimann P, Haake F *Phys. Rev. A* **4** 302 (1971)
11. Bonifacio R, Schwendimann P, Haake F *Phys. Rev. A* **4** 854 (1971)
12. Gross M, Haroche S *Phys. Rep.* **93** 301 (1982)
13. Andreev A V *Sov. Phys. Usp.* **33** 997 (1990); *Usp. Fiz. Nauk* **160** (12) 1 (1990)
14. Benedict M G et al. *Super-radiance*: *Multiatomic Coherent Emission* (Bristol: Institute of Physics Publ., 1996)
15. Brandes T *Phys. Rep.* **408** 315 (2005)
16. Zheleznyakov V V, Kocharovskii V V, Kocharovskii Vl V *Sov. Phys. Usp.* **29** 1059 (1986); *Usp. Fiz. Nauk* **150** 455 (1986)
17. Kocharovsky V V, Kocharovsky Vl V, Belyanin A A *Phys. Rev. Lett.* **76** 3285 (1996)
18. Gaponov A V, Petelin M I, Yulpatov V K *Radiophys. Quantum Electron.* **10** 794 (1967); *Izv. Vyssh. Uchebn. Zaved. Radiofiz.* **10** 1414 (1967)
19. Bonifacio R et al. *Phys. Rev. Lett.* **73** 70 (1994)
20. Men'shikov L I *Phys. Usp.* **42** 107 (1999); *Usp. Fiz. Nauk* **169** 113 (1999)
21. Agarwal G S, in *Quantum Optics* (Springer Tracts in Modern Physics, Vol. 70) (Berlin: Springer-Verlag, 1974) p. 1
22. Suryan G *Current Sci.* **18** 203 (1949)
23. Bloembergen N, Pound R V *Phys. Rev.* **95** 8 (1954)
24. Bloom S *J. Appl. Phys.* **28** 800 (1957)
25. Eberly J H *Am. J. Phys.* **40** 1374 (1972)
26. Krishnan V, Murali N *Prog. Nucl. Magn. Reson. Spectrosc.* **68** 41 (2013)
27. Kiselev Yu F et al. *Sov. Phys. JETP* **67** 413 (1988); *Zh. Eksp. Teor. Fiz.* **94** 344 (1988)
28. Warren W S, Hammes S L, Bates J L *J. Chem. Phys.* **91** 5895 (1989)
29. Kiselev Yu F, Aliskenderov E I *JETP Lett.* **51** 15 (1990); *Pis'ma Zh. Eksp. Teor. Fiz.* **51** 14 (1990)
30. Bazhanov N A et al. *Sov. Phys. Solid State* **31** 291 (1989); *Fiz. Tverd. Tela* **31** 206 (1989)
31. Boscaino R, Gelardi F M, Korb J P *Phys. Rev. B* **48** 7077 (1993)
32. Barjat H et al. *J. Magn. Reson. A* **117** 109 (1995)
33. Agnello S et al. *Phys. Rev. A* **59** 4087 (1999)
34. Shishmarev D, Otting G *J. Magn. Reson.* **213** 76 (2011)
35. Skribanowitz N et al. *Phys. Rev. Lett.* **30** 309 (1973)
36. MacGillivray J C, Feld M S *Phys. Rev. A* **14** 1169 (1976)
37. Gibbs H M, Vrehen Q H F, Hikspoors H M J *Phys. Rev. Lett.* **39** 547 (1977)
38. Moi L et al. *Phys. Rev. A* **27** 2043 (1983)
39. Goy P et al. *Phys. Rev. A* **27** 2065 (1983)
40. Florian R, Schwan L O, Schmid D *Phys. Rev. A* **29** 2709 (1984)
41. Varnavskii O P et al. *Sov. Phys. JETP* **59** 716 (1984); *Zh. Eksp. Teor. Fiz.* **86** 1227 (1984)
42. Varnavskii O P et al. *Sov. Phys. JETP* **63** 937 (1986); *Zh. Eksp. Teor. Fiz.* **90** 1596 (1986)
43. MacGillivray J C, Feld M S *Contemp. Phys.* **22** 299 (1981)
44. Vrehen Q H F, Gibbs H M, in *Dissipative Systems in Quantum Optics*: *Resonance Fluorescence, Optical Bistability, Superfluorescence* (Topics in Current Physics, Vol. 27, Ed. R Bonifacio) (Berlin: Springer, 1982) p. 111
45. Schuurmans M F H et al. *Adv. At. Mol. Phys.* **17** 167 (1982)
46. Andreev A V, Emelyanov V I, Ilinskii Yu A *Cooperative Effects in Optics*: *Superradiance and Phase Transitions* (Bristol: Institute of Physics Publ., 1993); Translated from Russian: *Kooperativnye Yavleniya v Optike*: *Sverkhizluchenie, Bistabil'nost', Fazovye Perekhody* (Moscow: Nauka, 1988)
47. Kalachev A A, Samartsev V V *Laser Phys.* **12** 1114 (2002)
48. Zheleznyakov V V, Kocharovskii V V, Kocharovskii Vl V *Sov. Phys. JETP* **60** 897 (1984); *Zh. Eksp. Teor. Fiz.* **87** 1565 (1984)
49. Bonifacio R, Lugiato L *Phys. Rev. A* **11** 1507 (1975)
50. Bonifacio R, Lugiato L *Phys. Rev. A* **12** 587 (1975)
51. Haake F et al. *Phys. Rev. A* **20** 2047 (1979)
52. Haake F et al. *Phys. Rev. Lett.* **42** 1740 (1979)
53. Polder D, Schuurmans M F H, Vrehen Q H F *Phys. Rev. A* **19** 1192 (1979)
54. Emel'yanov V I, Seminogov V N *Sov. Phys. JETP* **49** 17 (1979); *Zh. Eksp. Teor. Fiz.* **76** 34 (1979)
55. Leonardi C, Vaglica A *Nuovo Cimento* **67** 233 (1982)
56. Kumarakrishnan A, Chudasama S, Han X *J. Opt. Soc. Am. B* **22** 1538 (2005)
57. Scheibner M et al. *Nature Phys.* **3** 106 (2007)
58. Paradis E et al. *Phys. Rev. A* **77** 043419 (2008)
59. Jho Y D et al. *Phys. Rev. B* **81** 155314 (2010)
60. Ariunbold G O et al. *Phys. Rev. A* **82** 043421 (2010)
61. Basharov A M, Znamenskii N V, Shashkov A Yu *Bull. Russ. Acad. Sci. Phys.* **74** 943 (2010); *Izv. Ross. Akad. Nauk Ser. Fiz.* **74** 984 (2010)
62. Dai D, Monkman A P *Phys. Rev. B* **84** 115206 (2011)
63. Ariunbold G O, Sautenkov V A, Scully M O *Phys. Lett. A* **376** 335 (2012)
64. Suh J Y et al. *Nano Lett.* **12** 5769 (2012)
65. Kim J-H et al. *Sci. Rep.* **3** 3283 (2013)
66. Akselrod G et al. *Phys. Rev. B* **90** 035209 (2014)
67. Pozina G et al. *Sci. Rep.* **5** 14911 (2015)
68. Pozina G et al. *Phys. Status Solidi B* **254** 1600402 (2016)
69. Black A T, Chan H W, Vuletić V *Phys. Rev. Lett.* **91** 203001 (2003)
70. Baumann K et al. *Nature* **464** 1301 (2010)
71. Baumann K et al. *Phys. Rev. Lett.* **107** 140402 (2011)
72. Keßler H et al. *Phys. Rev. Lett.* **113** 070404 (2014)
73. Klinder J et al. *Proc. Natl. Acad. Sci. USA* **112** 3290 (2015)
74. Dimer F et al. *Phys. Rev. A* **75** 013804 (2007)
75. Hepp K, Lieb E H *Ann. Physics* **76** 360 (1973)
76. Hepp K, Lieb E H *Phys. Rev. A* **8** 2517 (1973)
77. Wang Y K, Hioe F T *Phys. Rev. A* **7** 831 (1973)

78. Rzażewski K, Wódkiewicz K, Żakowicz W *Phys. Rev. Lett.* **35** 432 (1975)
79. Bialynicki-Birula I, Rzażewski K *Phys. Rev. A* **19** 301 (1979)
80. Gawedzki K, Rzaźewski K *Phys. Rev. A* **23** 2134 (1981)
81. Rzaewski K, Wódkiewicz K *Phys. Rev. A* **43** 593 (1991)
82. Rzażewski K, Wódkiewicz K *Phys. Rev. Lett.* **96** 089301 (2006)
83. Lambert N, Emary C, Brandes T *Phys. Rev. Lett.* **92** 073602 (2004)
84. Bužek V, Orszag M, Roško M *Phys. Rev. Lett.* **94** 163601 (2005)
85. Nataf P, Ciuti C *Nature Commun.* **1** 72 (2010)
86. Ritsch H et al. *Rev. Mod. Phys.* **85** 553 (2013)
87. Saunders R, Bullough R, in *Cooperative Effects in Matter and Radiation* (Eds C M Bowden, D W Howgate, H R Robl) (New York: Plenum Press, 1977) p. 209
88. Zheleznyakov V V, Kocharovsky V V, Kocharovsky Vl V, in *Nonlinear Waves 2. Dynamics and Evolution* (Research Reports in Physic, Eds A V Gaponov-Grekhov, M I Rabinovich, J Engelbrecht) (Berlin: Springer 1989) p. 136; Translated from Russian: in *Nelineinye Volny. Dinamika i Evolyutsiya* (Eds A V Gaponov-Grekhov, M I Rabinovich) (Moscow: Nauka, 1989) p. 358
89. Andreev A V, Emel'yanov V I, Il'inskii Yu A *Sov. Phys. Usp.* **23** 493 (1980); *Usp. Fiz. Nauk* **131** 653 (1980)
90. Bienaime T et al. *Fortschr. Phys.* **61** 377 (2013)
91. Temnov V V,Woggon U *Opt. Express* **17** 5774 (2009)
92. Su Y et al. *Phys. Rev. Lett.* **110** 113604 (2013)
93. Mlynek J A et al. *Nature Commun.* **5** 5186 (2014)
94. Bhatti D, von Zanthier J, Agarwal G S *Sci. Rep.* **5** 17335 (2015)
95. Leymann H A M et al. *Phys. Rev. Appl.* **4** 044018 (2015)
96. Jahnke F et al. *Nature Commun.* **7** 11540 (2016)
97. Klimontovich Yu L *Kinetic Theory of Electromagnetic Processes* (Berlin: Springer-Verlag, 1983); Translated from Russian: *Kineticheskaya Teoriya Elektromagnitnykh Protsessov* (Moscow: Nauka, 1980)
98. Kozub M, Pawicki L, Machnikowski P *Phys. Rev. B* **86** 121305(R) (2012)
99. Okuyama R, Eto M *J. Phys. Conf. Ser.* **400** 042049 (2012)
100. Ichimiya M et al. *J. Non-Cryst. Solids* **358** 2357 (2012)
101. Phuong L et al. *J. Lumin.* **133** 77 (2013)
102. Jen H H *Phys. Rev. A* **94** 053813 (2016)
103. Bradac C et al., arXiv:1608.03119
104. Tighineanu P et al. *Phys. Rev. Lett.* **116** 163604 (2016)
105. Kocharovsky V V, Kocharovsky Vl V, Kukushkin V A *Radiophys. Quantum Electron.* **44** 161 (2001); *Izv. Vyssh. Uchebn. Zaved. Radiofiz.* **44** 174 (2001)
106. Belenov E M, Oraevskii A N, Shcheglov V A *Sov. Phys. JETP* **29** 1153 (1969); *Zh. Eksp. Teor. Fiz.* **56** 2143 (1969)
107. Bonifacio R, Lugiato L A *Phys. Rev. A* **18** 1129 (1978)
108. Bonifacio R, Lugiato L *Opt. Commun.* **47** 79 (1983)
109. Gronchi M et al. *Phys. Rev. A* **24** 1419 (1981)
110. Basharov A M et al. *JETP* **102** 206 (2006); *Zh. Eksp. Teor. Fiz.* **129** 239 (2006)
111. Mattar F P et al. *Phys. Rev. Lett.* **46** 1123 (1981)
112. Watson E A et al. *Phys. Rev. A* **27** 1427 (1983)
113. You L, Cooper J, Trippenbach M *J. Opt. Soc. Am. B* **8** 1139 (1991)
114. Basharov A M et al. *Quantum Electron.* **39** 251 (2009); *Kvantovaya Elektron.* **39** 251 (2009)
115. Schiller A, Schwan L O, Schmid H D *J. Lumin.* **38** 243 (1987)
116. Schiller A, Schwan L O, Schmid H D *J. Lumin.* **40** 541 (1988)
117. Bonifacio R, Maroli C, Piovella N *Opt. Commun.* **68** 369 (1988)
118. Vainshtein L A, Kleev A I *Sov. Phys. Dokl.* **35** 359 (1990); *Dokl. Akad. Nauk SSSR* **311** 862 (1990)
119. Scherrer D et al. *Appl. Phys. B* **53** 250 (1991)
120. Bonifacio R, Piovella N, McNeil B W J *Phys. Rev. A* **44** R3441 (1991)
121. Brownell J H, Lu X, Hartmann S R *Phys. Rev. Lett.* **75** 3265 (1995)
122. Kocharovsky V V, Kocharovsky Vl V *Infrared Phys. Technol.* **36** 1003 (1995)
123. Lvovsky A I, Hartmann S R, Moshary F *Phys. Rev. Lett.* **82** 4420 (1999)
124. Zuikov V et al. *Laser Phys.* **10** 364 (2000)
125. Berezovsky V et al. *J. Opt. Soc. Am. B* **25** 458 (2008)
126. Kocharovskii V V, Kocharovskii Vl V *Radiophys. Quantum Electron.* **28** 756 (1985); *Izv. Vyssh. Uchebn. Zaved. Radiofiz.* **28** 1009 (1985)
127. Kaluzny Y et al. *Phys. Rev. Lett.* **51** 1175 (1983)
128. Brecha R et al. *J. Opt. Soc. Am. B* **12** 2329 (1995)
129. Maimistov A I, Basharov A M *Nonlinear Optical Waves* (Dordrecht: Kluwer Acad., 1999)
130. Zheleznyakov V V, Kocharovsky V V, Kocharovsky Vl V *Izv. Akad. Nauk SSSR Ser. Fiz.* **56** 1321 (1992)
131. Kocharovsky V V, Kocharovsky Vl V *Pure Appl. Opt. J. Eur. Opt. Soc. A* **3** 29 (1994)
132. Pustovit V N, Shahbazyan T V *Phys. Rev. B* **82** 075429 (2010)
133. Pustovit V N et al. *Phys. Rev. B* **93** 165432 (2016)
134. Pustovit V N, Shahbazyan T V *Phys. Rev. Lett.* **102** 077401 (2009)
135. Dorofeenko A V et al. *Opt. Express* **21** 14539 (2013)
136. Meng X et al. *Sci. Rep.* **3** 01241 (2013)
137. Martín-Cano D et al. *Nano Lett.* **10** 3129 (2010)
138. Kocharovsky V V, Kocharovsky Vl V *Opt. Commun.* **53** 345 (1985)
139. Kocharovsky V V, Kocharovsky Vl V, in *Nonlinear Waves 3. Physics and Astrophysics. Proc. of the Gorky School 1989* (Eds A V Gaponov-Grekhov, M I Rabinovich, J Engelbrecht) (Berlin: Springer-Verlag, 1990) p. 146; Translated from Russian: in *Nelineinye Volny. Fizika i Astrofizika* (Exec. Eds A V Gaponov-Grekhov, M I Rabinovich) (Moscow: Nauka, 1993) p. 176
140. Rupasov V I, Yudson V I *Sov. Phys. JETP* **60** 927 (1984); *Zh. Eksp. Teor. Fiz.* **87** 1617 (1984)
141. Dekker H *Phys. Rep.* **80** 1 (1981)
142. Dekker H *Physica A* **144** 445 (1987)
143. Dekker H *Physica A* **144** 453 (1987)
144. Glauber R, Man'ko V I *Sov. Phys. JETP* **60** 450 (1984); *Zh. Eksp. Teor. Fiz.* **87** 790 (1984)
145. Vrehen Q, Schuurmans M, Polder D *Nature* **285** 5760 (1980)
146. Jho Y D et al. *Phys. Rev. Lett.* **96** 237401 (2006)
147. Reibold R *Phys. Lett. A* **115** 325 (1986)
148. Meziane J et al. *Chem. Phys. Lett.* **363** 573 (2002)
149. Haake F et al. *Phys. Rev. A* **23** 1322 (1981)
150. Mostowski J, Sobolewska B *Phys. Rev. A* **28** 2573(R) (1983)
151. Mostowski J, Sobolewska B *Phys. Rev. A* **30** 610 (1984)
152. Mostowski J, Sobolewska B *Phys. Rev. A* **30** 1392 (1984)
153. Wenzel R G, Telle J M, Carlsten J L *J. Opt. Soc. Am. A* **3** 838 (1986)
154. Leung P T, Liu S Y, Young K *Phys. Rev. A* **49** 3057 (1994)
155. Leung P T et al. *Phys. Rev. A* **49** 3068 (1994)
156. Leung P T, Liu S Y, Young K *Phys. Rev. A* **49** 3982 (1994)
157. Vrehen Q H F, der Weduwe J J *Phys. Rev. A* **24** 2857(R) (1981)
158. Nattermann K, Fabricius N, von der Linde D *Opt. Commun.* **57** 212 (1986)
159. Lim S-H et al. *Phys. Rev. Lett.* **92** 107402 (2004)
160. Arikawa T et al. *Phys. Rev. B* **84** 241307(R) (2011)
161. Zhang Q et al. *Phys. Rev. Lett.* **113** 047601 (2014)
162. Il'inskii Yu A, Maslova N S *Sov. Phys. JETP* **67** 96 (1988); *Zh. Eksp. Teor. Fiz.* **94** 171 (1988)
163. Becker T, Rinkleff R-H *Phys. Rev. A* **44** 1806 (1991)
164. Bartholdtsen D, Becker T, Rinkleff R-H *Phys. Rev. A* **46** 5801 (1992)
165. Kumarakrishnan A, Han X *Opt. Commun.* **109** 348 (1994)
166. Prozument K et al. *Phys. Rev. Lett.* **107** 143001 (2011)
167. Zhou Y et al. *Chem. Phys. Lett.* **640** 124 (2015)
168. Will S A et al. *Phys. Rev. Lett.* **116** 225306 (2016)
169. Jaroszynski D A et al. *Phys. Rev. Lett.* **78** 1699 (1997)
170. Ginzburg N S et al. *Phys. Rev. Lett.* **78** 2365 (1997)
171. Ginzburg N S et al. *Opt. Commun.* **175** 139 (2000)
172. Ginzburg N S et al. *Phys. Plasmas* **10** 4494 (2003)
173. Korovin S D et al. *Phys. Rev. E* **74** 016501 (2006)
174. Ginzburg N S et al. *Radiophys. Quantum Electron.* **50** 762 (2007); *Izv. Vyssh. Uchebn. Zaved. Radiofiz.* **50** 839 (2007)
175. Ginzburg N S et al. *IEEE Trans. Plasma Sci.* **41** 646 (2013)
176. Bonifacio R, Pellegrini C, Narducci L *Opt. Commun.* **50** 373 (1984)
177. Bonifacio R, McNeil B W J, Pierini P *Phys. Rev. A* **40** 4467 (1989)
178. Bonifacio R et al. *Phys. Rev. A* **50** 1716 (1994)
179. Kim K-J *Phys. Rev. Lett.* **57** 1871 (1986)
180. Vinokurov N et al. *Nucl. Instrum. Meth. Phys. Res. A* **475** 74 (2001)
181. Shevchenko O A, Vinokurov N A *Radiophys. Quantum Electron.* **60** (1) (2017); *Izv. Vyssh. Uchebn. Zaved. Radiofiz.* **60** 41 (2017)
182. Zheleznyakov V V, Kocharovsky V V, Kocharovsky Vl V *Radiophys. Quantum Electron.* **29** 830 (1986); *Izv. Vyssh. Uchebn. Zaved. Radiofiz.* **29** 1095 (1986)

183. Zheleznyakov V V, Kocharovskii V V, Kocharovskii Vl V *Sov. Phys. Usp.* **30** 1009 (1987); *Usp. Fiz. Nauk* **153** 525 (1987)
184. Kuzelev M V, Rukhadze A A *Elektrodinamika Plotnykh Elektronnykh Puchkov v Plazme* (Electrodynamics of Dense Electron Beams in Plasma) (Moscow: Nauka, 1990)
185. Drummond P D, Eberly J H *Phys. Rev. A* **25** 3446(R) (1982)
186. Heinzen D J, Thomas J E, Feld M S *Phys. Rev. Lett.* **54** 677 (1985)
187. Prasad S, Glauber R J *Phys. Rev. A* **31** 1583 (1985)
188. Avetisyan Yu A et al. *Sov. Phys. JETP* **68** 891 (1989); *Zh. Eksp. Teor. Fiz.* **95** 1541 (1989)
189. Boursey E, Meziane J, Topouzkhanian A *IEEE J. Quantum Electron.* **29** 1038 (1993)
190. Boursey E, Itji H, Meziane J *IEEE J. Quantum Electron.* **30** 2653 (1994)
191. Avetisyan Yu A, Trifonov E D *Opt. Spectrosc.* **86** 753 (1999); *Opt. Spektrosk.* **86** 842 (1999)
192. Prasad S, Glauber R J *Phys. Rev. A* **61** 063814 (2000)
193. Cong K et al. *Phys. Rev. B* **91** 235448 (2015)
194. Egorov V S, Chekhonin I A, Shubin N N *Opt. Spectrosc.* **62** 509 (1987); *Opt. Spektrosk.* **62** 853 (1987)
195. Haake F, Kolobov M I, Steudel H *Opt. Commun.* **92** 385 (1992)
196. Jansen A, Stahl D *Europhys. Lett.* **18** 33 (1992)
197. Kocharovsky Vl V, Kalinin P A, Kocharovskaya E R, Kocharovsky V V, in *Nelineinye Volny 2012* (Nonlinear Waves 2012) (Exec. Eds A G Litvak, V I Nekorkin) (Nizhny Novgorod: IPF RAN, 2013), p. 398
198. Kocharovsky V V, Belyanin A A, Kocharovskaya E R, Kocharovsky Vl V, in *Advanced Lasers*: *Laser Physics and Technology for Applied and Fundamental Science* (Berlin: Springer, 2015) p. 49
199. Kocharovskaya E R, Ginzburg N S, Sergeev A S, Kocharovsky V V, Kocharovsky Vl V *Radiophys. Quantum Electron.* **59** 484 (2016); *Izv. Vyssh. Uchebn. Zaved. Radiofiz.* **59** 535 (2016)
200. Vasil'ev P P, Penty R V, White I H *Light Sci. Appl.* **5** e16086 (2016)
201. Kogelnik H, Shank C V *J. Appl. Phys.* **43** 2327 (1972)
202. Flanders D C et al. *Appl. Phys. Lett.* **24** 194 (1974)
203. Wang S *IEEE J. Quantum Electron.* **10** 413 (1974)
204. Zhu L, Scherer A, Yariv A *IEEE J. Quantum Electron.* **43** 934 (2007)
205. Mock A et al. *IEEE J. Select. Topics Quantum Electron.* **15** 892 (2009)
206. Akiba S *Distributed Feedback Lasers* (Boca Raton: CRC Press, 2010)
207. Turitsyn S K et al. *Phys. Rep.* **542** 133 (2014)
208. Mattar F P, Bowden C M *Phys. Rev. A* **27** 345 (1983)
209. Bowden C M, Sung C C *Phys. Rev. Lett.* **50** 156 (1983)
210. Scherrer D, Kneubehl F *Infrared Phys.* **34** 227 (1993)
211. Nakano Y, Luo Y, Tada K *Appl. Phys. Lett.* **55** 1606 (1989)
212. Luo Y et al. *Appl. Phys. Lett.* **56** 1620 (1990)
213. Jones D J et al. *IEEE J. Quantum Electron.* **31** 1051 (1995)
214. Malcuit M S et al. *Phys. Rev. Lett.* **59** 1189 (1987)
215. Belyanin A A, Kocharovsky V V, Kocharovsky Vl V *Quantum Semiclass. Opt.* **9** (1) 1 (1997)
216. Agranovich V M, Ginzburg V L *Crystal Optics with Spatial Dispersion, and Excitons* (Berlin: Springer-Verlag, 1984); Translated from Russian: *Kristallooptika s Uchetom Prostranstvennoi Dispersii i Teoriya Eksitonov* (Moscow: Nauka, 1979)
217. Haug H, Koch S W *Quantum Theory of the Optical and Electronic Properties of Semiconductors* (Singapore: World Scientific, 2004) p. 453
218. Ivchenko E L *Optical Spectroscopy of Semiconductor Nanostructures* (Harrow: Alpha Science, 2005)
219. Gibbs H M, Khitrova G, Koch S W *Nature Photon.* **5** 273 (2011)
220. Garrison J C, Nathel H, Chiao R Y *J. Opt. Soc. Am. B* **5** 1528 (1988)
221. Maki J J et al. *Phys. Rev. A* **40** 5135 (1989)
222. Kumarakrishnan A, Han X L *Phys. Rev. A* **58** 4153 (1998)
223. Ishikawa A et al. *J. Phys. Soc. Jpn.* **85** 034703 (2016)
224. Mantsyzov B I *Kogerentnaya i Nelineinaya Optika Fotonnykh Kristallov* (Coherent and Nonlinear Optics of Photonic Crystals) (Moscow: Fizmatlit, 2009)
225. Andreev A V, Fedotov M V *Sov. J. Quantum Electron.* **23** 67 (1993); *Kvantovaya Elektron.* **20** 79 (1993)
226. Andreev A V *Sov. J. Quantum Electron.* **23** 500 (1993); *Kvantovaya Elektron.* **20** 581 (1993)
227. Gordon A et al. *Phys. Rev. A* **77** 053804 (2008)
228. Vukovic N et al. *Opt. Express* **24** 26911 (2016)
229. Kaneva E N *Opt. Spectrosc.***70** 94 (1991); *Opt. Spektrosk.* **70** 164 (1991)
230. Burnham D C, Chiao R Y *Phys. Rev.* **188** 667 (1969)
231. Gabitov I, Zakharov V E, Mikhailov A V *Sov. Phys. JETP* **59** 703 (1984); *Zh. Eksp. Teor. Fiz.* **86** 1204 (1984)
232. Gabitov I, Zakharov V E, Mikhailov A V *Theor. Math. Phys.* **63** 328 (1985); *Teor. Mat. Fiz.* **63** (1) 11 (1985)
233. Bonifacio R et al., in *Cooperative Effects in Matter and Radiation* (Eds C M Bowden, D W Howgate, H R Robl) (New York: Plenum Press, 1977) p. 193
234. Karnyukhin A V, Kuz'min R N, Namiot V A *Sov. Phys. JETP* **55** 334 (1982); *Zh. Eksp. Teor. Fiz.* **82** 561 (1982)
235. Karnyukhin A V, Kuz'min R N, Namiot V A *Sov. Phys. JETP* **57** 509 (1983); *Zh. Eksp. Teor. Fiz.* **84** 878 (1983)
236. Bausch R et al. *Europhys. Lett.* **10** 445 (1989)
237. Kocharovsky V, Kocharovsky Vl, Golubyatnikova E *Comput. Math. Appl.* **34** 773 (1997)
238. Bonifacio R, Gronchi M, Lugiato L, in *Optical Coherence and Quantum Optics IV. Proc. of the Fourth Rochester Conf. on Coherence and Quantum Optics, Rochester, June 8–10, 1977* (Eds L Mandel, E Wolf) (New York: Springer, 1978) p. 939
239. Bonifacio R, Farina J, Narducci L *Opt. Commun.* **31** 377 (1979)
240. Meinardi F et al. *Phys. Rev. Lett.* **91** 247401 (2003)
241. Miyajima K et al. *Phys. Status Solidi B* **243** 3795 (2006)
242. Timofeev V B, Gorbunov A V, Larionov A V *J. Phys. Condens. Matter* **19** 295209 (2007)
243. Miyajima K et al. *J. Phys. Condens. Matter* **21** 195802 (2009)
244. Deng H, Haug H, Yamamoto Y *Rev. Mod. Phys.* **82** 1489 (2010)
245. Miyajima K et al. *Phys. Status Solidi C* **8** 209 (2011)
246. High A A et al. *Nano Lett.* **12** 2605 (2012)
247. Vasil'ev P et al. *Europhys. Lett.* **104** 40003 (2013)
248. Timothy Noe G (II) et al. *Nature Phys.* **8** 219 (2012)
249. Ding C R et al. *Appl. Phys. Lett.* **101** 091115 (2012)
250. Khachatryan B et al. *Phys. Rev. B* **86** 195203 (2012)
251. Kyriienko O, Kavokin A V, Shelykh I A *Phys. Rev. Lett.* **111** 176401 (2013)
252. Noe G T et al. *Fortschr. Phys.* **61** 93 (2013)
253. Laurent T et al. *Phys. Rev. Lett.* **115** 187402 (2015)
254. Belyanin A A, Kocharovsky V V, Kocharovsky Vl V *Solid State Commun.* **80** 243 (1991)
255. Belyanin A A, Kocharovsky V V, Kocharovsky Vl V *Laser Phys.* **2** 952 (1992)
256. Belyanin A A, Kocharovsky V V, Kocharovsky Vl V *Quantum Semiclass. Opt. B* **10** L13 (1998)
257. Schmitt-Rink S, Ell C, Haug H *Phys. Rev. B* **33** 1183 (1986)
258. Schuurmans M *Opt. Commun.* **34** 185 (1980)
259. Temnov V V, Woggon U *Phys. Rev. Lett.* **95** 243602 (2005)
260. Stroucken T et al. *Adv. Solid State Phys.* **38** 265 (1999)
261. Kuhl J et al. *Adv. Solid State Phys.* **38** 281 (1999)
262. Ikawa T, Cho K *Phys. Rev. B* **66** 085338 (2002)
263. Ivchenko E L et al. *Phys. Rev. B* **70** 195106 (2004)
264. Ivchenko E L, Poddubny A N *Phys. Solid State* **55** 905 (2013)
265. Chang C H et al. *Opt. Express* **23** 11946 (2015)
266. Baryshev V R, Ginzburg N S *Quantum Electron.* **41** 34 (2011); *Kvantovaya Elektron.* **41** 34 (2011)
267. Chumakov A I, in *Materialy XX Mezhdunarod. Simpoziuma "Nanofizika i Nanoelektronika"* (Proc. of XX Intern. Symp. on Nanophysics and Nanoelectronics) Vol. 1 (Nizhny Novgorod: NNGU, 2016) p. 424
268. MacGillivray J C, Feld M S *Phys. Rev. A* **23** 1334 (1981)
269. Greiner C, Boggs B, Mossberg T W *Phys. Rev. Lett.* **85** 3793 (2000)
270. Julsgaard B, Mølmer K *Phys. Rev. A* **86** 063810 (2012)
271. Asadullina N Ya, Asadullin T Ya, arXiv:1503.07641
272. Inouye S et al. *Science* **285** 571 (1999)
273. Avetisyan Yu A, Trifonov E D *Phys. Usp.* **58** 286 (2015); *Usp. Fiz. Nauk* **185** 307 (2015)
274. Noginov M A et al. *Laser Phys. Lett.* **1** 291 (2004)
275. Wiersma D S *Nature Phys.* **4** 359 (2009)
276. Wiersma D S, Noginov M A *J. Opt.* **12** 020201 (2010)
277. Baudouin Q et al. *Nature Phys.* **9** 357 (2013); arXiv:1301.0522
278. Haake F et al. *Phys. Rev. Lett.* **71** 995 (1993)

279. Kuppens S J M, van Exter M P, Woerdman J P *Phys. Rev. Lett.* **72** 3815 (1994)
280. Drummond P D et al. *Phys. Rev. Lett.* **78** 836 (1997)
281. Meiser D et al. *Phys. Rev. Lett.* **102** 163601 (2009)
282. Kalinin P A, Kocharovsky V V, Kocharovsky Vl V *Solid State Commun.* **152** 1008 (2012)
283. Wang Y-F, Chen J-B *Chin. Phys. Lett.* **29** 073202 (2012)
284. Maier T et al. *Opt. Express* **22** 13269 (2014)
285. Bohnet J G et al. *Nature* **484** 78 (2012)
286. Weiner J M et al. *Phys. Rev. A* **95** 033808 (2017); arXiv:1503.06464
287. Norcia M A, Thompson J K *Phys. Rev. X* **6** 011025 (2016)
288. Norcia M A et al. *Sci. Adv.* **2** e1601231 (2016)
289. Björk G et al. *Phys. Rev. B* **50** 17336 (1994)
290. Khanin Ya I *Fundamentals of Laser Dynamics* (Cambridge: Cambridge Intern. Science Publ., 2006); Translated from Russian: *Osnovy Dinamiki Lazerov* (Moscow: Nauka, 1999)
291. Arecchi F T, Harrison R G (Eds) *Instabilities and Chaos in Quantum Optics* (Berlin: Springer, 2011)
292. Weiss C O et al. *Appl. Phys. B* **61** 223 (1995)
293. Chenkosol P, Casperson L W *J. Opt. Soc. Am. B* **20** 2539 (2003)
294. Font J et al. *Opt. Commun.* **261** 336 (2006)
295. Chenkosol P, Casperson L W *J. Opt. Soc. Am. B* **24** 1199 (2007)
296. Jahanpanah J, Eslami H *Opt. Commun.* **293** 102 (2013)
297. Germann T D et al. *Appl. Phys. Lett.* **92** 101123 (2008)
298. Kalinin P A, Kocharovskaya E R, Kocharovsky Vl V, Kukushkin V A, in *Trudy III Simpoziuma po Kogerentnomu Opticheskomu Izlucheniyu Poluprovodnikovykh Soedinenii i Struktur 2011* (Proc. of III Symp. on Coherent Optical Radiation of Semiconductor Compounds and Structures 2011) (Moscow: FIAN, 2012) p. 71
299. Qiao P et al. *Opt. Express* **21** 30336 (2013)
300. Kocharovskaya E R et al. *J. Phys. Conf. Ser.* **740** 012007 (2016)
301. Kocharovskaya E R, Ginzburg N S, Sergeev A S *Quantum Electron.* **41** 733 (2011); *Kvantovaya Elektron.* **41** 733 (2011)
302. Kocharovsky Vl V, Garasev M A, Kalinin P A, Kocharovskaya E R, in *Trudy II Simpoziuma po Kogerentnomu Opticheskomu Izlucheniyu Poluprovodnikovykh Soedinenii i Struktur 2009* (Proc. of II Symp. on Coherent Optical Radiation of Semiconductor Compounds and Structures 2009) (Moscow: FIAN, 2010) p. 68
303. Miyamoto Y et al. *Prog. Theor. Exp. Phys.* **2014** 113C01 (2014)
304. Goban A et al. *Phys. Rev. Lett.* **115** 063601 (2015)
305. Tighineanu P et al. *Phys. Rev. Lett.* **116** 163604 (2016)
306. Guerin W, Araújo M O, Kaiser R *Phys. Rev. Lett.* **116** 083601 (2016)
307. Nagy D, Szirmai G, Domokos P *Eur. Phys. J. D* **48** 127 (2008)
308. Nagy D et al. *Phys. Rev. Lett.* **104** 130401 (2010)
309. Liu C, Di Falco A, Fratalocchi A *Phys. Rev. X* **4** 021048 (2014)
310. Keeling J, Bhaseen M J, Simons B D *Phys. Rev. Lett.* **112** 143002 (2014)
311. Chen Y, Yu Z, Zhai H *Phys. Rev. Lett.* **112** 143004 (2014)
312. Bakhtiari M R et al. *Phys. Rev. Lett.* **114** 123601 (2015)
313. Longo P, Keitel C H, Evers J *Sci. Rep.* **6** 23628 (2016)
314. Hayn M, Emary C, Brandes T *Phys. Rev. A* **84** 053856 (2011)
315. Ryzhov I V et al. *JETP* **124** (5) (2017) in press; *Zh. Eksp. Teor. Fiz.* **151** 803 (2017)